NACA

RESEARCH MEMORANDUM

EFFECTS OF SWEEP AND THICKNESS ON THE

STATIC LONGITUDINAL AERODYNAMIC CHARACTERISTICS OF A

SERIES OF THIN, LOW-ASPECT-RATIO, HIGHLY TAPERED WINGS

AT TRANSONIC SPEEDS

TRANSONIC-BUMP METHOD

By Albert G. Few, Jr., and Paul G. Fournier

Langley Aeronautical Laboratory
Langley Field, Va.

NATIONAL ADVISORY COMMITTEE
FOR AERONAUTICS
WASHINGTON
April 8, 1954

NATIONAL ADVISORY COMMITTEE FOR AERONAUTICS

RESEARCH MEMORANDUM

EFFECTS OF SWEEP AND THICKNESS ON THE

STATIC LONGITUDINAL AERODYNAMIC CHARACTERISTICS OF A

SERIES OF THIN, LOW-ASPECT-RATIO, HIGHLY TAPERED WINGS

AT TRANSONIC SPEEDS

TRANSONIC-BUMP METHOD

By Albert G. Few, Jr., and Paul G. Fournier

SUMMARY

An investigation by the transonic-bump technique of the static longi-tudinal aerodynamic characteristics of a series of thin, low-aspect-ratio, highly tapered wings has been made in the Langley high-speed 7- by 10-foot tunnel. The Mach number range extended from about 0.60 to 1.18, with corresponding Reynolds numbers ranging from about 0.75×10^6 to 0.95×10^6. The angle-of-attack range was from $-10°$ to approximately $32°$.

The effects on drag and lift-drag ratio of a variation in sweep angle from $-14.03°$ to $45°$ with respect to the quarter-chord line for wings of 3-percent-chord thickness was found to be small in comparison to the effects of a variation in thickness from 2 percent chord to 4.5 percent chord for wings with $14.03°$ sweepback.

For the range of variables considered, variations in plan form were considerably more important with regard to longitudinal stability char-acteristics than the variations in thickness. For the series of basic wings having an aspect ratio of 4, the most nearly linear pitching-moment characteristics were obtained with $26.57°$ of sweepback of the quarter-chord line. However, for the modified series of wings (obtained by clip-ping the tips of the original wings parallel to the plane of symmetry to give an aspect ratio of 3 and a taper ratio of 0.143), the most nearly linear pitching-moment characteristics were obtained with $36.87°$ of sweep-back. By decreasing the thickness-to-chord ratios from 0.03 to 0.02, a large increase in lift-curve slope was obtained for both the basic and modified wings. All of the wings of both series had fairly large inward shifts of the lateral center-of-pressure location (indicative of tip stalling) with increasing lift coefficient, except those wings having minimum sweepback angles.

INTRODUCTION

Investigations such as those reported in references 1 and 2 have
established that, regardless of wing sweep angle, it is important to
utilize the thinnest airfoil sections that can be tolerated from struc-
tural considerations in order to achieve maximum performance, particu-
larly at transonic and supersonic speeds. It is also well known that
highly tapered plan forms offer certain structural advantages over wings
of less taper and therefore the airfoil-section thickness ratio normally
can be reduced somewhat as the ratio of tip chord to root chord is
decreased. An important problem which still exists concerns the choice
of sweep angle of thin, highly tapered wings in order to achieve satis-
factory longitudinal stability characteristics.

The present investigation was conducted primarily for the purpose
of exploring at transonic speeds the longitudinal stability character-
istics of thin, highly tapered wings having quarter-chord sweep angles
varying from -14.03° to 45° and also to provide information on wing
performance characteristics. The basic series of six wings had NACA
65A003 airfoil sections, an aspect ratio of 4, and a taper ratio of 0.
A modified series of wings was formed from the basic series by clipping
the wing tips parallel to the plane of symmetry to give an aspect ratio
of 3 and a taper ratio of 0.143. The effect of thickness on the longi-
tudinal stability of one of the basic and one of the modified plan forms
having 14.03° quarter-chord sweep was determined by testing additional
wings having NACA 65A002 and 65A004.5 airfoil sections.

The investigation utilized reflection-plane wing models mounted on
a transonic bump in the Langley high-speed 7- by 10-foot tunnel. The
Mach number range extended from 0.60 to approximately 1.18 with corre-
sponding Reynolds numbers varying from about 0.75×10^6 to 0.95×10^6.
The results presented herein were derived from measurements of lift,
drag, pitching moment, and root bending moment due to lift.

COEFFICIENTS AND SYMBOLS

C_L lift coefficient, $\dfrac{\text{Twice semispan lift}}{qS}$

C_D drag coefficient, $\dfrac{\text{Twice semispan drag}}{qS}$

ΔC_{D_p} pressure-drag rise (maximum zero-lift drag coefficient
             minus zero-lift drag coefficient at $M = 0.60$)

C_m pitching-moment coefficient referred to $0.25\bar{c}$,
$$\frac{\text{Twice semispan pitching moment}}{qS\bar{c}}$$

C_B bending-moment coefficient due to lift about longitudinal-
stability axis, $\dfrac{\text{Bending moment}}{q\frac{S}{2}\frac{b}{2}}$

q effective dynamic pressure over span of wing, $\dfrac{\rho V^2}{2}$,
lb/sq ft

q_a average chordwise local dynamic pressure, lb/sq ft

S twice area of semispan wing model, sq ft

A aspect ratio, b^2/S

$\bar{c}$ mean aerodynamic chord of wing, based on relationship

$$\frac{2}{S}\int_0^{b/2} c^2 dy, \text{ ft}$$

c local wing chord, ft

λ taper ratio

b twice span of semispan model, ft

ρ air density, slugs/cu ft

V free-stream velocity, ft/sec

M effective Mach number over span of wing

M_a average chordwise local Mach number

M_l local Mach number

R Reynolds number based on $\bar{c}$

α angle of attack, deg

Λ_{LE} wing sweep angle with respect to the leading edge, deg

$\Lambda_{c/4}$ wing sweep angle with respect to quarter-chord line, deg

$\Lambda_{c/2}$ wing sweep angle with respect to half-chord line, deg

y_{cp} lateral center-of-pressure location, percent wing semi-
span, $100 \dfrac{C_B}{C_L}$

x_{cp} longitudinal center-of-pressure location, $100 \left(0.25 - \dfrac{C_m}{C_L}\right)$,
percent wing mean aerodynamic chord

x_{ac} longitudinal aerodynamic-center location, percent wing
mean aerodynamic chord

$\left(\dfrac{L}{D}\right)_{max}$ maximum lift-drag ratio

t/c airfoil-section thickness ratio

MODELS AND APPARATUS

The semispan-wing models used in the investigation were constructed
of steel. Sketches of the wing plan forms and a tabulation of pertinent
geometric parameters are given in table I. The models included a basic
series of six wings all having an aspect ratio of 4, a taper ratio of 0,
and NACA 65A003 airfoil sections parallel to the plane of symmetry with
quarter-chord sweep angles varying from -14.03° to 45°. A modified
series was formed from the basic series by clipping the tips of each of
the wings parallel to the plane of symmetry to give an aspect ratio of 3
and a taper ratio of 0.143. In addition to the models having NACA
65A003 airfoil sections, models having NACA 65A002 and 65A004.5 airfoil
sections were provided for one sweep angle (14.03°, or c/2 line per-
pendicular to plane of symmetry). The thickness series was investigated
for both the basic wing of aspect ratio 4 and the modified wing of aspect
ratio 3. A detailed drawing of representative models used in the inves-
tigation is given in figure 1. A photograph of one of the models mounted
on the bump in the Langley high-speed 7- by 10-foot tunnel is shown as
figure 2. The wings were mounted on an electrical strain-gage balance
which was enclosed in the bump and measured the lift, drag, pitching
moment, and root bending moment due to lift. A small gap existed between
the wing-root section and the balance cover plate; however, use of a
sponge rubber seal at the base of the models minimized air leakage from
the balance chamber.

TESTS AND CORRECTIONS

The tests were made in the Langley high-speed 7- by 10-foot tunnel, employing an adaptation of the NACA wing-flow technique for obtaining transonic speeds. The technique used in the present investigation involves the mounting of the wings in a high-velocity flow field (generated over the curved surface of a bump located on the tunnel floor) and is similar to that used in reference 3.

Typical contours of local Mach number in the vicinity of the model location on the bump (obtained from surveys with no model in position), are shown in figure 3. It can be seen that a Mach number variation of about 0.02 exists over the model semispan at the lowest Mach numbers and about 0.04 at the highest Mach numbers. The chordwise Mach number variation is generally less than 0.02. No attempt has been made to evaluate the effects of the chordwise and spanwise Mach number variations. The effective test Mach number was obtained from contour charts similar to those presented in figure 3, by using the relationship

$$M = \frac{2}{S} \int_0^{b/2} cM_a \; dy$$

Similarly, the effective dynamic pressure has been obtained from contour charts using the relationship

$$q = \frac{2}{S} \int_0^{b/2} cq_a \; dy$$

Figure 4 shows the variation of mean test Reynolds number with Mach number.

Force and moment data were obtained for the wing-alone configurations through a Mach number range from 0.60 to approximately 1.18 and an angle-of-attack range from approximately -10° to 32°.

Jet-boundary corrections have not been evaluated, since the boundary conditions to be satisfied are not rigorously defined. However, inasmuch as the effective flow field is large compared with the span and chord of the wings, the corrections are believed to be small.

RESULTS AND DISCUSSION

Presentation of Results

Aerodynamic characteristics of a series of thin, low-aspect-ratio, highly tapered wings are presented as follows:

In order to expedite publication of these data, only a brief discussion, based primarily on the summary curves of figures 21 to 27, is presented herein. The slopes presented in the summary figures have been averaged over a lift-coefficient range of ±0.10.

Lift and Drag Characteristics

The summary data presented in figure 21 indicate that, with regard to lift-curve slopes, the variation in thickness was more significant than the variation in sweep. By decreasing the thickness-to-chord ratios from 0.03 to 0.02, a large increase in lift-curve slope was obtained for both the basic wings of aspect ratio 4 and the modified wings of aspect ratio 3 and taper ratio 0.143. Similar results are indicated by the data presented in references 4 and 5. The large values of lift-curve slope obtained for the 2-percent-thick wings were not due to aeroelastic distortion, since a check on the flexibility of this wing indicated that aeroelastic effects should be very small.

The lift coefficient at an angle of attack of $20°$, $(C_L)_{\alpha=20°}$, was selected as being representative of the maximum lift coefficient inasmuch as the lift values in the high angle range were erratic. Indicated in figure 21 is the same pronounced rise in $(C_L)_{\alpha=20°}$ at transonic speeds as has been noted in other investigations (ref. 6). The basic and modified wings having the least sweep experienced the largest change in $(C_L)_{\alpha=20°}$ at transonic speeds, as would be expected on the basis of previous experience.

Figure 22 shows a comparison of the experimental pressure-drag-rise increment ΔC_{D_p} for the present wings with results predicted by the method presented in reference 1. Sweep of the half-chord line was used as a reference since the minimum pressure occurs somewhere in the vicinity of the half-chord line in the subsonic-speed range of these airfoil sections. At the lower sweep angles, the experimental and predicted results are in good agreement; however, at the higher sweep angles the measured drag-rise increments were larger than the predicted values, with the result that the reduction of ΔC_{D_p} with sweep was smaller than would be expected from reference 1. However, the results of reference 1 were based on wings of little taper while the wings of the present investigation were highly tapered. It is known that relatively little favorable sweep effect is realized near the plane of symmetry (see ref. 7, for example) and since a large portion of the wing area is concentrated near the root of highly tapered wings, little sweep effect would be expected.

The effect of sweep on $(L/D)_{max}$ is shown in figure 21 to be less significant than the effect of thickness. The data obtained indicate slightly higher values of $(L/D)_{max}$ for the wings with modified tips than for the basic wings through the transonic range, although it would be expected that the wings of greater aspect ratio would provide the higher values of $(L/D)_{max}$. It is also noted that the greater values of $(L/D)_{max}$ for the modified wings are traceable to somewhat lower values of $(C_D)_{C_L=0}$. This unexpected result probably is due to the fact that the tests of the modified wings were made with a somewhat different end-seal condition than that used for the basic wings. This discrepancy is not believed to affect the validity of comparisons of the effects of plan form or thickness for either the basic wing or the modified wing series, or to influence the indicated effect of clipping the wing tips for characteristics not dependent on zero-lift drag.

The effects of sweep angle and of the wing-tip modification on the drag-due-to-lift parameter $\dfrac{\partial C_D}{\partial C_L^2}$ is indicated in figure 23 at Mach numbers of 0.9 and 1.1. With the exception of the modified wing series at Mach number 1.1, the results show about a 15-percent increase in $\dfrac{\partial C_D}{\partial C_L^2}$ as the sweep angle is increased from $0°$ to $45°$. As would be expected, values of $\dfrac{\partial C_D}{\partial C_L^2}$ generally were somewhat higher for the modified wings than for the basic wings.

The effect of thickness and of the wing-tip modification on the drag-due-to-lift parameter $\dfrac{\partial C_D}{\partial C_L{}^2}$ is indicated in figure 24 through the Mach number range. Lower values of drag due to lift were obtained for the 4.5-percent-thick wings at the subsonic Mach numbers whereas the 2-percent-thick wings indicated lower values above Mach number 0.95. Similar results also are indicated by the data presented in reference 4. The decrease in $\dfrac{\partial C_D}{\partial C_L{}^2}$ with decreasing thickness at supersonic speeds appears to be due to the increase in lift-curve slope mentioned previously (figs. 21(a) and 21(b)), inasmuch as little, if any, leading-edge suction would be expected for these wings at supersonic speeds.

Comparisons of lift-drag ratios plotted against lift coefficient are shown in figure 25 for selected sweep angles and Mach numbers. At a Mach number of 0.9, the -14.03° swept wing provided the highest values of L/D over most of the lift-coefficient range; however, at M = 1.1, no very definite advantage was indicated for any of the sweep angles.

Longitudinal-Stability Characteristics

The effects of sweep on $\dfrac{\partial C_m}{\partial C_L}$ are shown in figure 21 to be generally consistent with past results and of more significance for these tests than the effect of thickness. The effect of sweep on the aerodynamic-center location for Mach numbers of 0.60 and 1.10 and a comparison of these results with those obtained from references 8 and 9 are presented in figure 26. The experimental results at low sweep indicate a more forward aerodynamic center than that predicted by theory; however, fair agreement is attained as the sweep angle is increased. The maximum rearward shift of the aerodynamic center from subsonic to supersonic speeds for the basic-series wings was about 22 percent for the low sweep angles and about 12 percent for the high sweep angles. The modified-series wings showed little effect of sweep on the rearward shift of the aerodynamic center, which averaged approximately 17 percent.

One of the primary objectives of the present investigation was to determine the relation of the plan-form variations to the shape of the pitching-moment curves, particularly at high lift coefficients. For airplanes having tails, the wing-alone characteristics are not necessarily indicative of the characteristics of the complete airplane; nevertheless, it is believed to be of interest to point out certain aspects of the wing-alone stability characteristics. Inspection of the pitching-moment curves of the basic data (figs. 5 to 20) indicates that, for the basic-wing

series of aspect ratio 4, the most nearly linear pitching-moment curves
were obtained with the wing having 26.57° of sweepback (fig. 8(b));
whereas, for the modified wings of aspect ratio 3, the pitching-moment
curves for the 36.87° sweptback wing (fig. 17(b)) were most nearly linear.
The pitching-moment curves of wings having sweep angles less than the
values mentioned are characterized by increasing stability with increasing
lift and the opposite is true of wings having larger sweep angles.

In order to illustrate some interesting trends in longitudinal and
lateral changes in center-of-pressure location with lift coefficient at
$M = 0.9$ and $M = 1.1$, three wings of each series were selected
$\left(\Lambda_{c/4} = -14.03^\circ,\ 26.57^\circ,\ \text{and}\ 45^\circ\right)$ and the data are presented in fig-
ure 27. It is evident that the changes with lift coefficient of the
longitudinal center-of-pressure location x_{cp} at a Mach number of 1.1
are considerably smaller for either wing series than the changes at a
Mach number of 0.9. However, appreciable changes in the lateral center-
of-pressure location y_{cp} with lift coefficient occurred at both Mach
numbers. It is of interest to point out that, for either series of wings
or for either Mach number, the wing plan form which gives the least
change in longitudinal center-of-pressure location with lift coefficient
experiences an appreciable inward shift in the lateral center-of-pressure
location with lift coefficient. Such inward shifts are associated with
tip separation and a resulting reduction in the effective span of the
trailing vortex sheet. The wing plan form (-14.03° sweepback) which gave
the least inward shift in lateral center-of-pressure location, experi-
enced an increase in stability with lift coefficient.

CONCLUSIONS

Results of an investigation, by the transonic-bump technique, of the
longitudinal characteristics of a basic and modified series of thin, low-
aspect-ratio, highly tapered wings with varying degrees of sweep and
thickness, indicate the following conclusions:

1. A decrease in the thickness-to-chord ratio from 0.03 to 0.02
caused an appreciable increase in lift-curve slope throughout the test
range of Mach numbers for both the basic and modified wings. The
increased lift-curve slope resulted in reduced drag due to lift for the
2-percent-thick wings at supersonic speeds.

2. The effects on drag and lift-drag ratio of a variation in sweep
angle from -14.03° to 45° for wings of 3-percent-chord thickness was
small in comparison to the effects of a variation in thickness from 2
to 4.5 percent chord for wings with 14.03° sweepback.

3. For the scope of these tests, variations in plan form were considerably more important with regard to longitudinal stability characteristics than variations in thickness.

4. For the series of basic wings of aspect ratio 4, the most nearly linear pitching-moment characteristics were obtained with a wing having 26.57° sweepback of the quarter-chord line, and for a modified series of wings (obtained by clipping the tips of the original wings to give an aspect ratio of 3), the most nearly linear pitching-moment characteristics were obtained with a wing having 36.87° sweepback of the quarter-chord line.

5. Inward shifts of the lateral center-of-pressure location (indicative of tip stalling) were fairly large at the higher lift coefficients and were more pronounced for wings of greater sweepback angle.
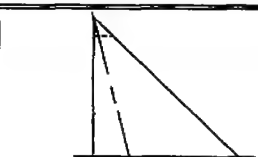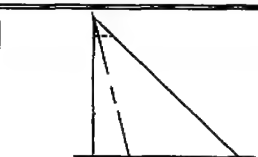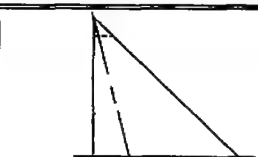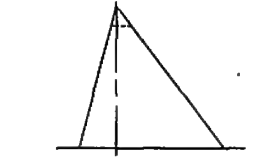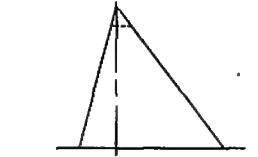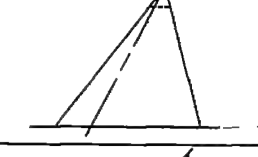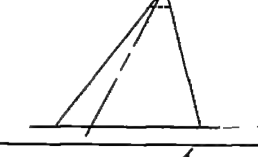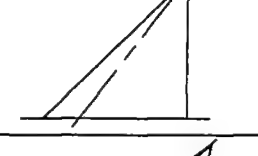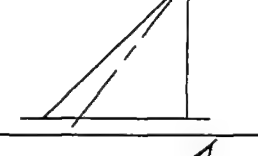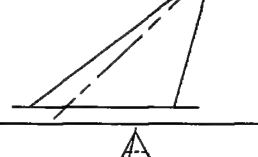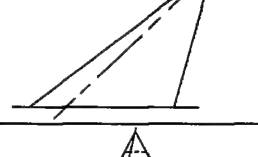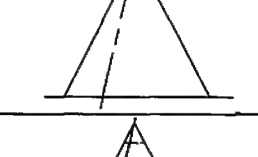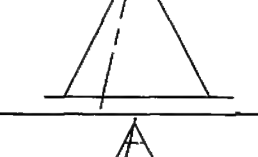
Langley Aeronautical Laboratory,
    National Advisory Committee for Aeronautics,
        Langley Field, Va., February 11, 1954.

REFERENCES

1. Polhamus, Edward C.: Summary of Results Obtained by Transonic-Bump
   Method on Effects of Plan Form and Thickness on Lift and Drag Char-
   acteristics of Wings at Transonic Speeds. NACA RM L51H30, 1951.

2. Bielat, Ralph P., Harrison, Daniel E., and Coppolino, Domenic A.: An
   Investigation at Transonic Speeds of the Effects of Thickness Ratio
   and of Thickened Root Sections on the Aerodynamic Characteristics
   of Wings With 47° Sweepback, Aspect Ratio 3.5, and Taper Ratio 0.2,
   in the Slotted Test Section of the Langley 8-Foot High-Speed Tunnel.
   NACA RM L51I04a, 1951.

3. Donlan, Charles J., Myers, Boyd C., II, and Mattson, Axel T.: A Com-
   parison of the Aerodynamic Characteristics at Transonic Speeds of
   Four Wing-Fuselage Configurations As Determined From Different Test
   Techniques. NACA RM L50H02, 1950.

4. Nelson, Warren H., Allen, Edwin C., and Krumm, Walter J.: The Tran-
   sonic Characteristics of 36 Symmetrical Wings of Varying Taper,
   Aspect Ratio, and Thickness as Determined by the Transonic-Bump
   Technique. NACA RM A53I29, 1953.

5. Nelson, Warren H., and McDevitt, John B.: The Transonic Characteris-
   tics of 17 Rectangular, Symmetrical Wing Models of Varying Aspect
   Ratio and Thickness. NACA RM A51A12, 1951.

6. Lowry, John G., and Cahill, Jones F.: Review of the Maximum-Lift
   Characteristics of Thin and Swept Wings. NACA RM L51E03, 1951.

7. Jones, Robert T.: Subsonic Flow Over Thin Oblique Airfoils at Zero
   Lift. NACA Rep. 902, 1948.

8. DeYoung, John, and Harper, Charles W.: Theoretical Symmetric Span
   Loading at Subsonic Speeds for Wings Having Arbitrary Plan Form.
   NACA Rep. 921, 1948.

9. Falkner, V. M.: Calculated Loadings Due to Incidence of a Number of
   Straight and Swept-Back Wings. Rep. No. 11,542, British A.R.C.,
   June 5, 1948.

Table I

Summary of Wing Geometry

	S, ft^2 (twice semispan)	A	λ	$\Lambda_{c/4}$, deg	Λ_{LE}, deg	NACA Section
	0.1250	4	0	-14.03	0	65A003
	0.1224	3	0.143	-14.03	0	65A003
	0.1250	4	0	0	14.03	65A003
	0.1224	3	0.143	0	14.03	65A003
	0.1250	4	0	14.03	26.57	65A003
	0.1224	3	0.143	14.03	26.57	65A003
	0.1250	4	0	26.57	36.87	65A003
	0.1224	3	0.143	26.57	36.87	65A003
	0.1250	4	0	36.87	45	65A003
	0.1224	3	0.143	36.87	45	65A003
	0.1250	4	0	45	51.33	65A003
	0.1224	3	0.143	45	51.33	65A003
	0.1250	4	0	14.03	26.57	65A004.5
	0.1224	3	0.143	14.03	26.57	65A004.5
	0.1250	4	0	14.03	26.57	65A002
	0.1224	3	0.143	14.03	26.57	65A002
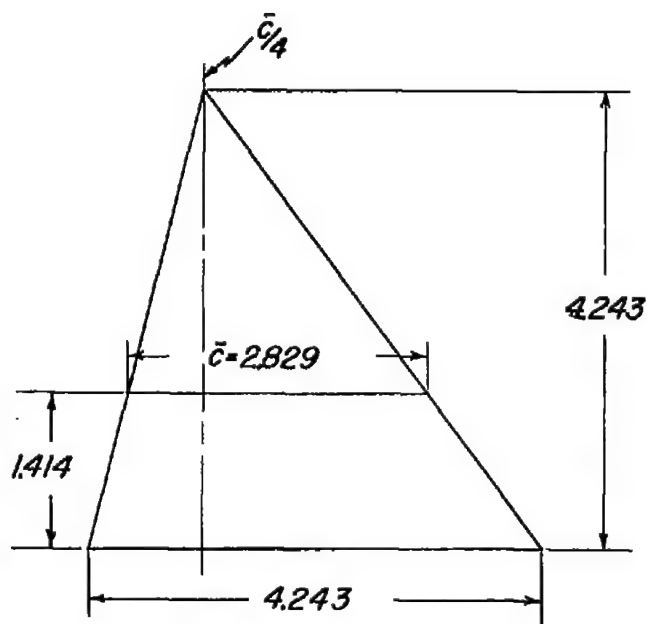
Basic series

$A = 4$
$\Lambda_{c/4} = 0°$
$\lambda = 0°$

Modified series

$A = 3$
$\Lambda_{c/4} = 0°$
$\lambda = 0.143$
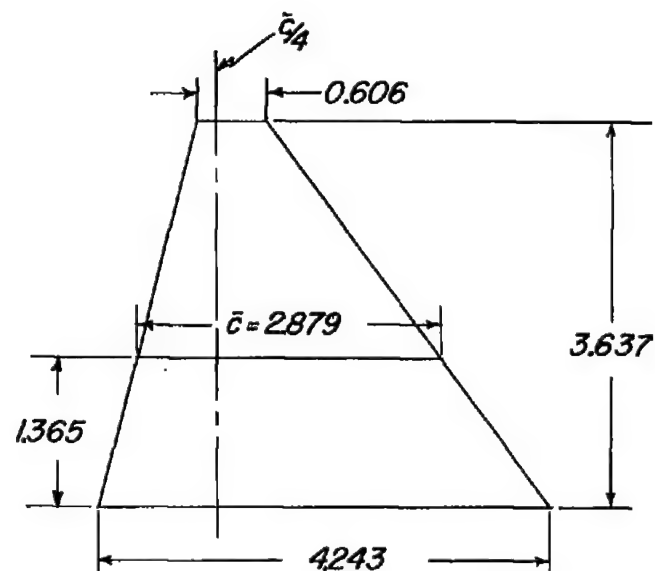
Figure 1.- Geometric characteristics of a wing representative of the series
used in the present investigation. (All dimensions are in inches.)

L-76833.1

Figure 2.- Photograph of wing mounted on transonic bump in the Langley
high-speed 7- by 10-foot tunnel.
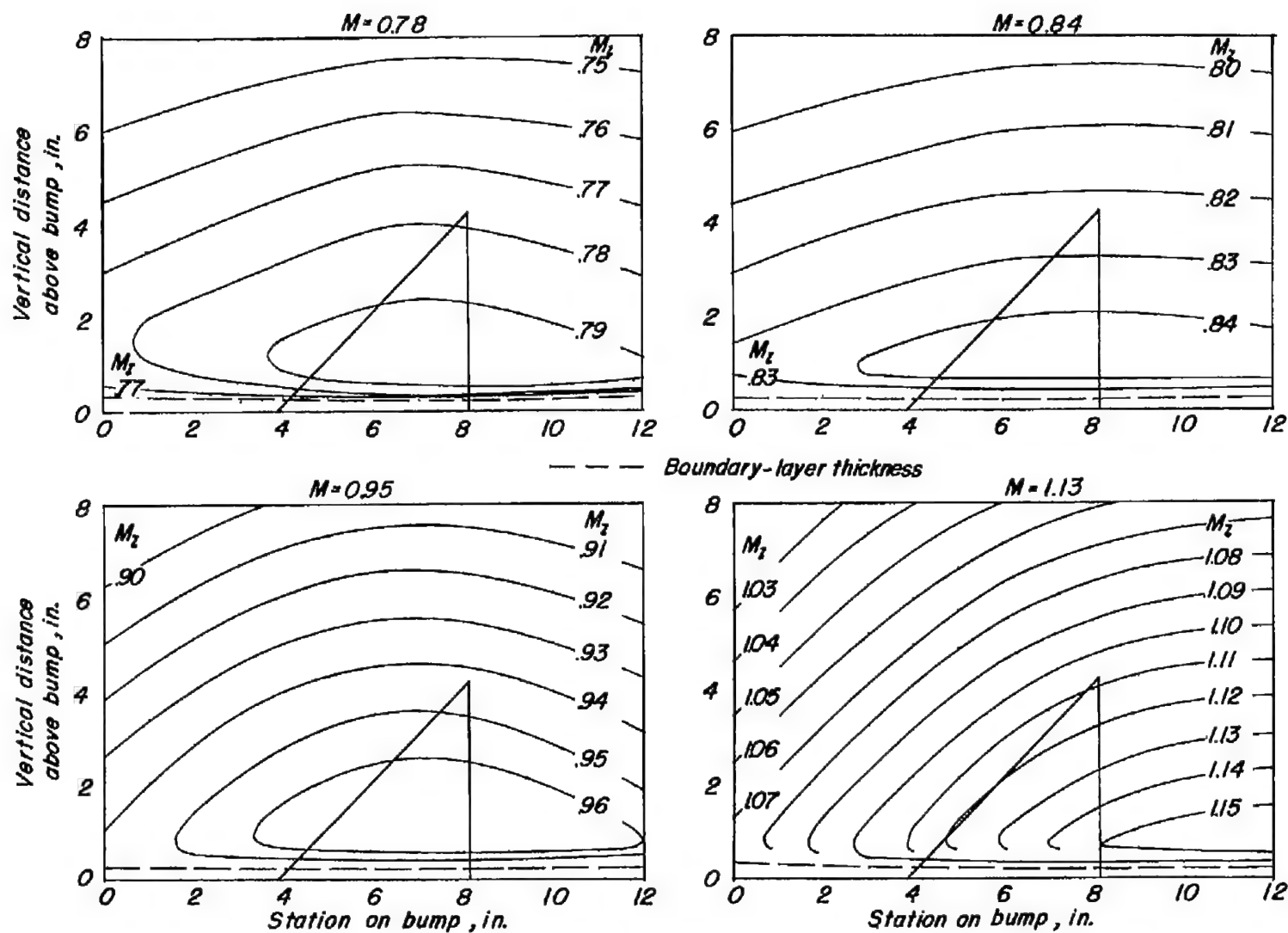
Figure 3.- Typical Mach number contours over transonic bump in region of model location.
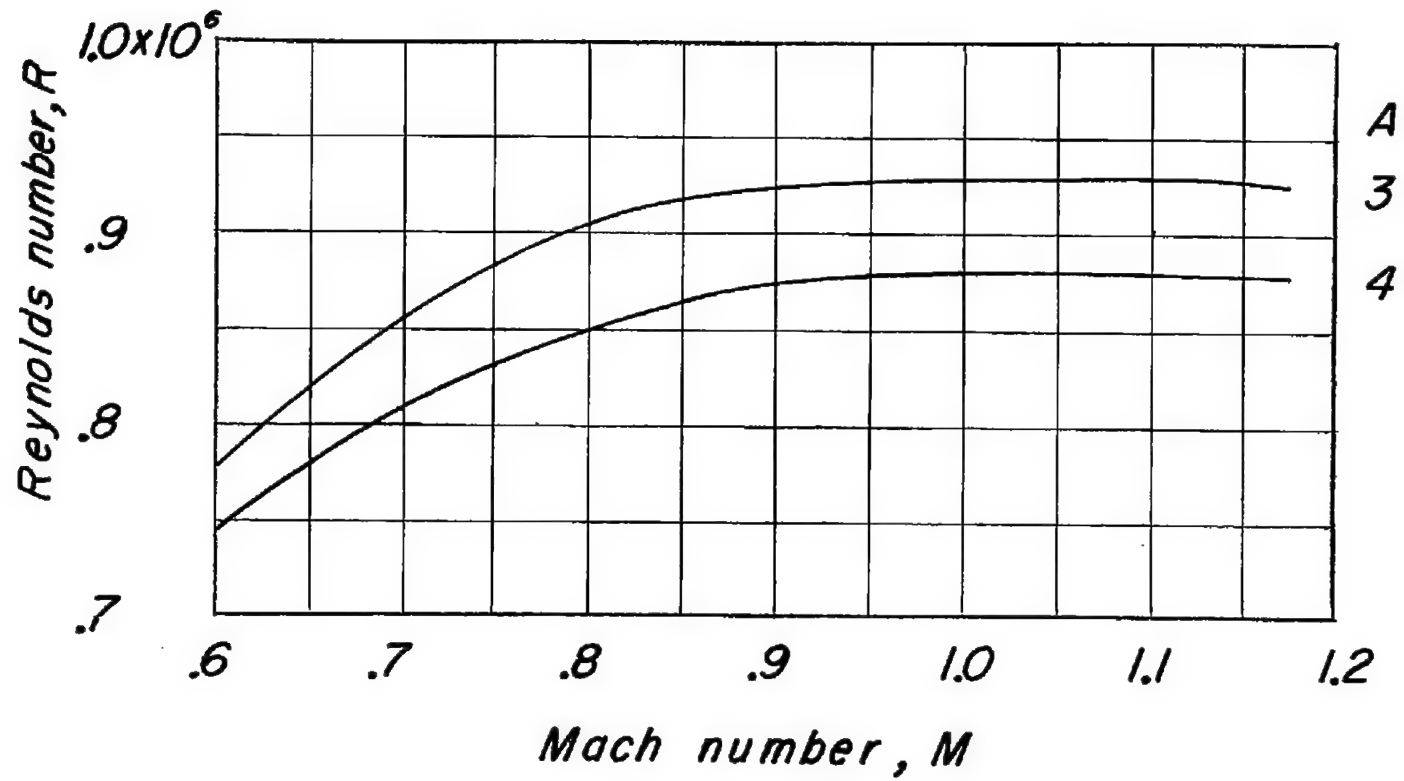
Figure 4.- Variation of mean test Reynolds number with Mach number.
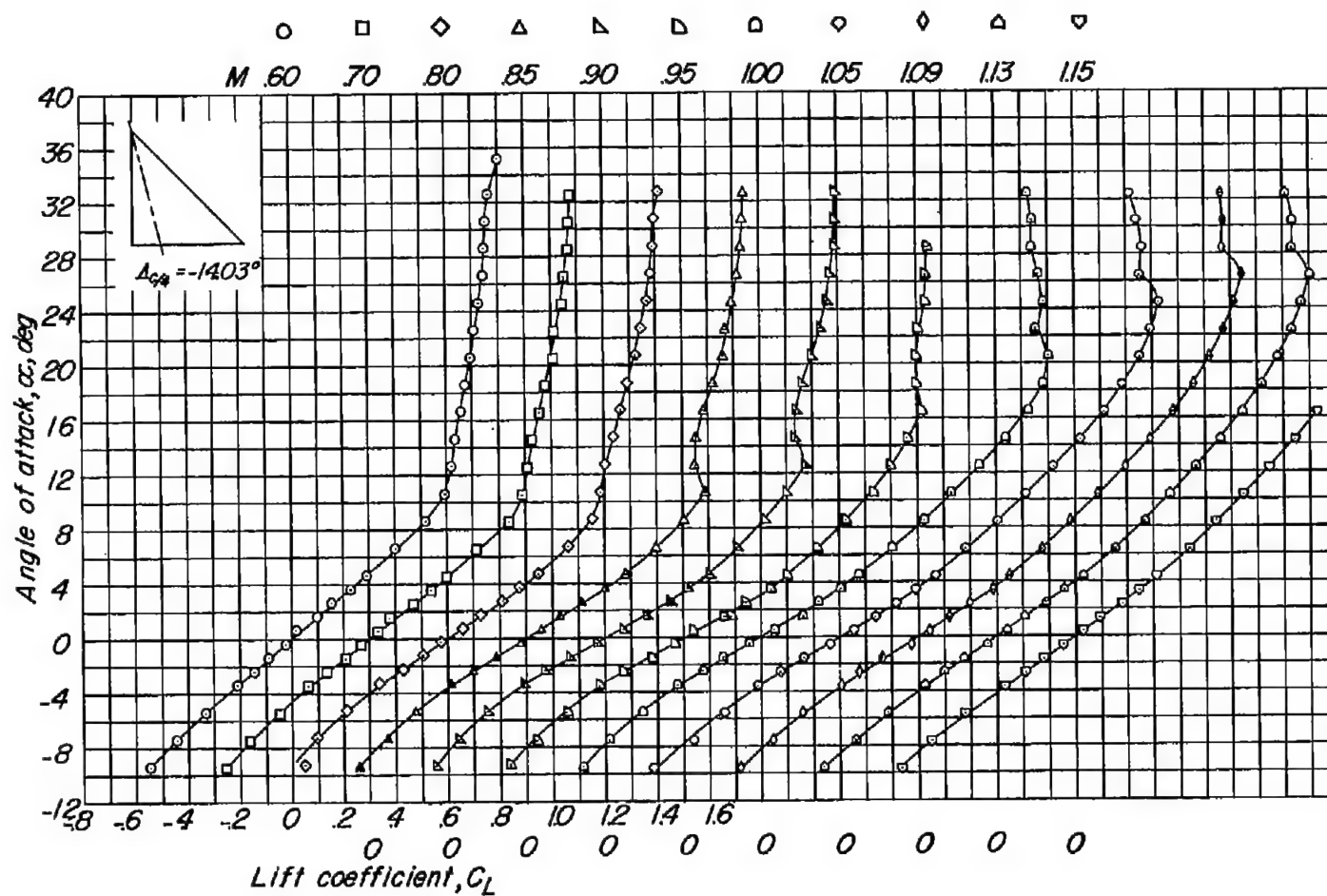
(a) Variation of α with C_L.

Figure 5.- Aerodynamic characteristics of a wing with -14.03° quarter-chord sweep; aspect ratio 4; taper ratio 0; and an NACA 65A003 airfoil section.
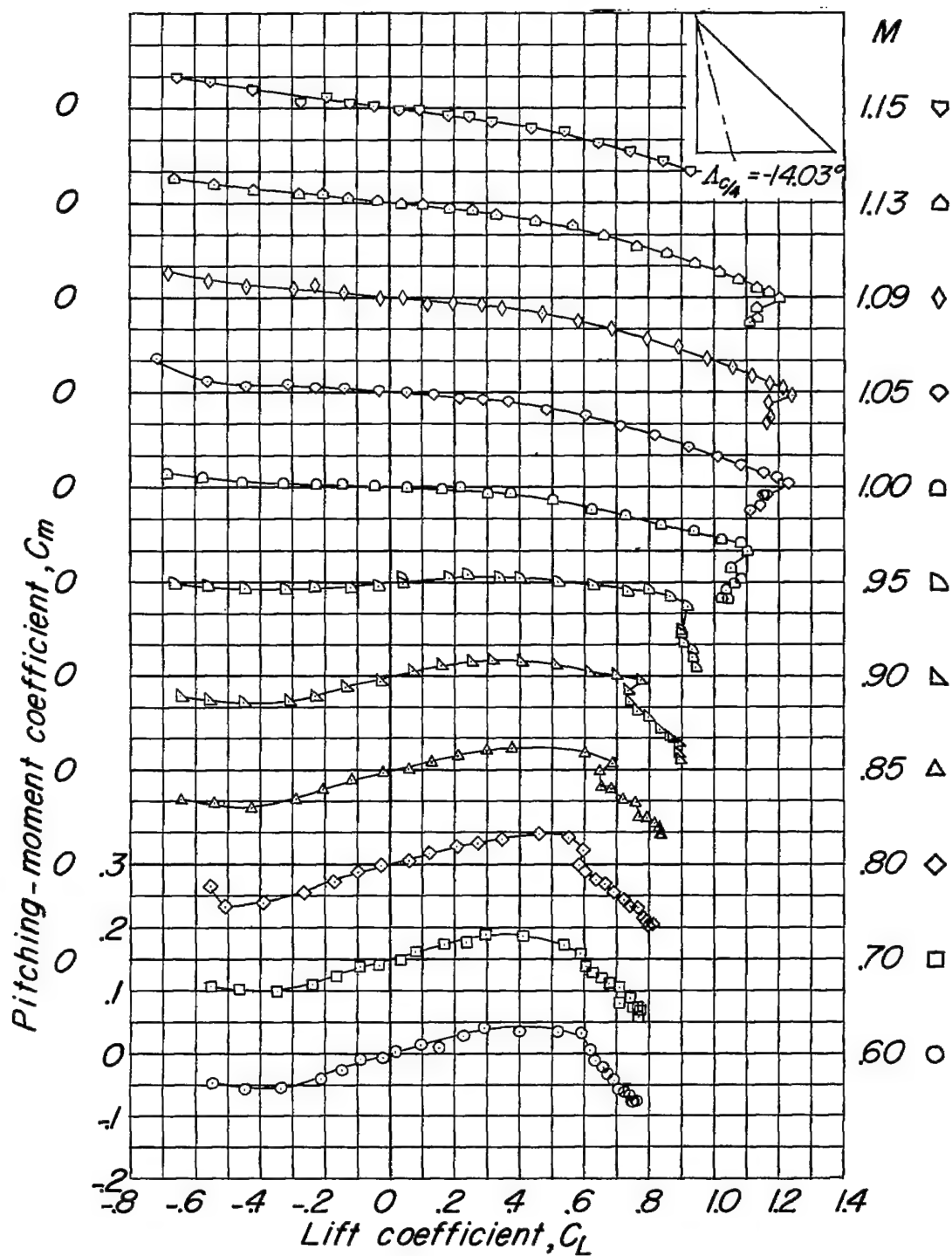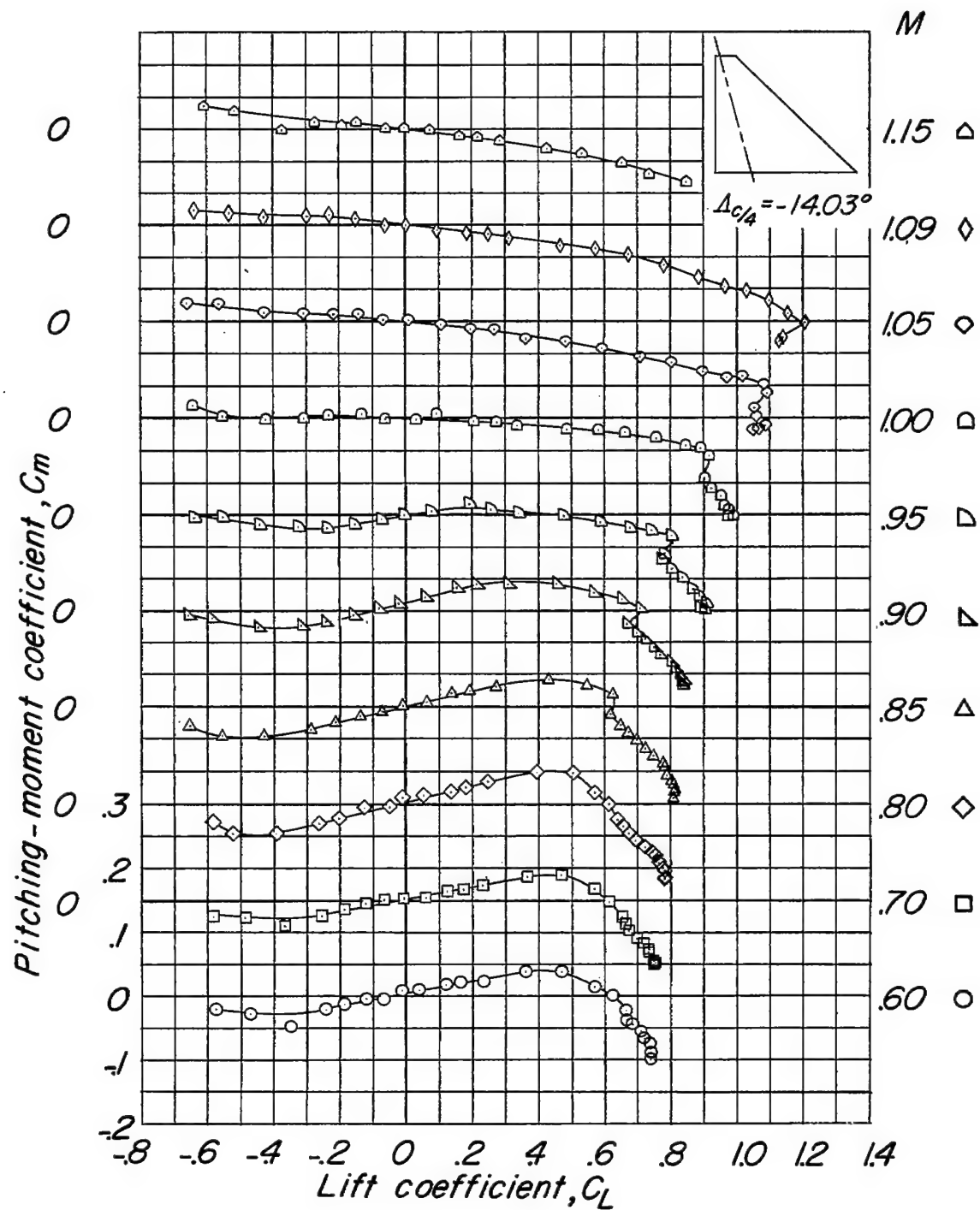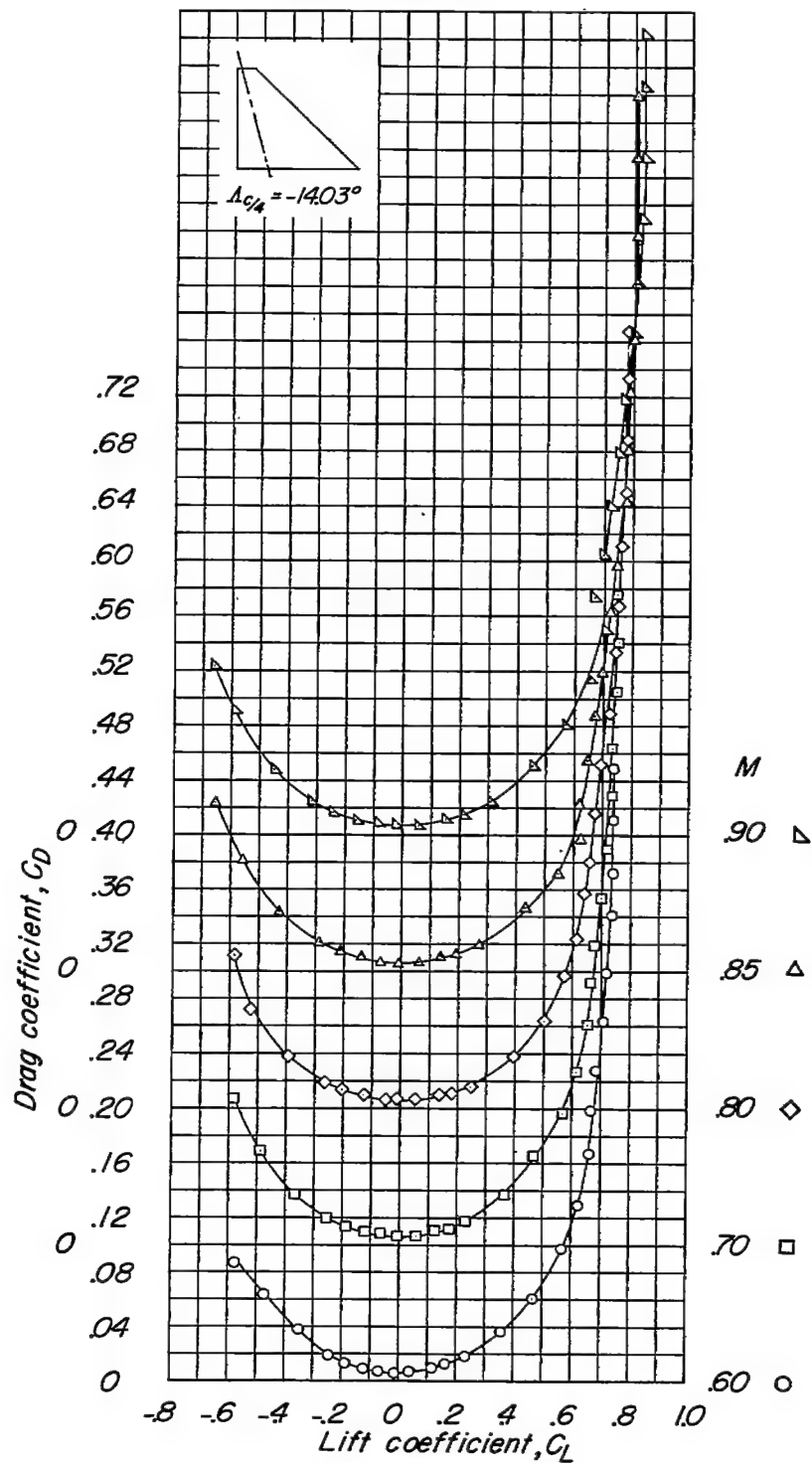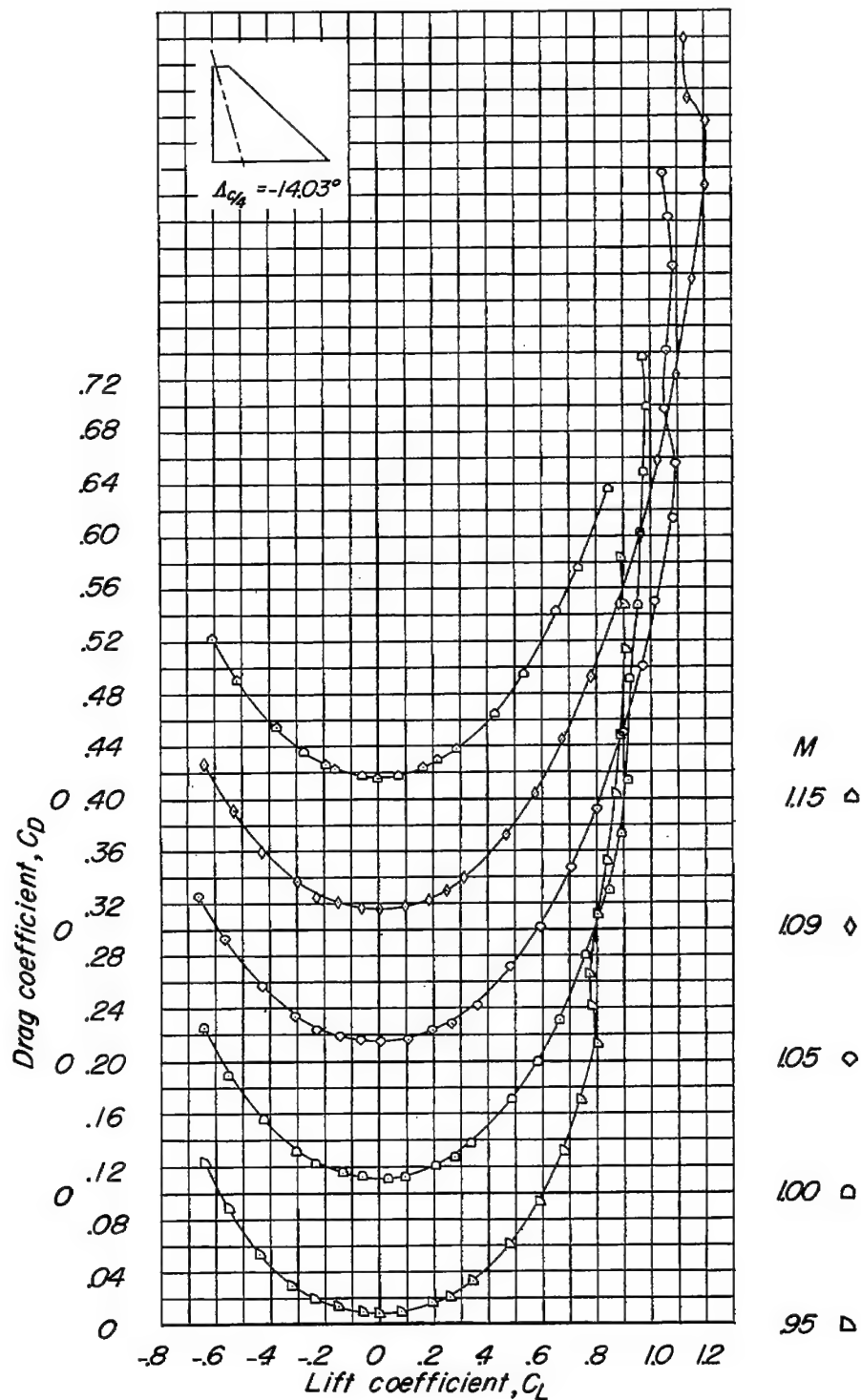
(b) Variation of C_m with C_L.

Figure 5.- Continued.
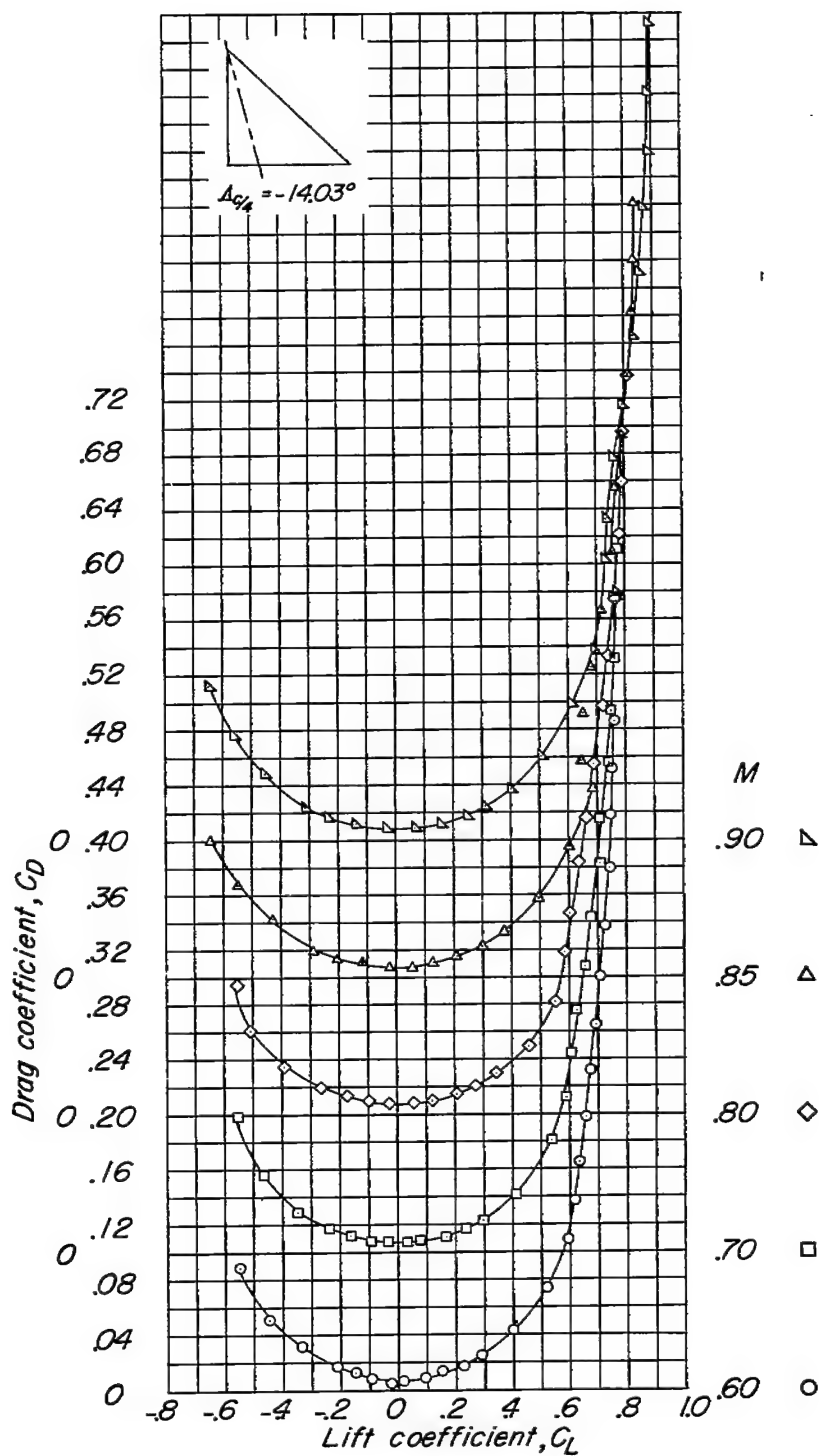
(c) Variation of C_D with C_L.

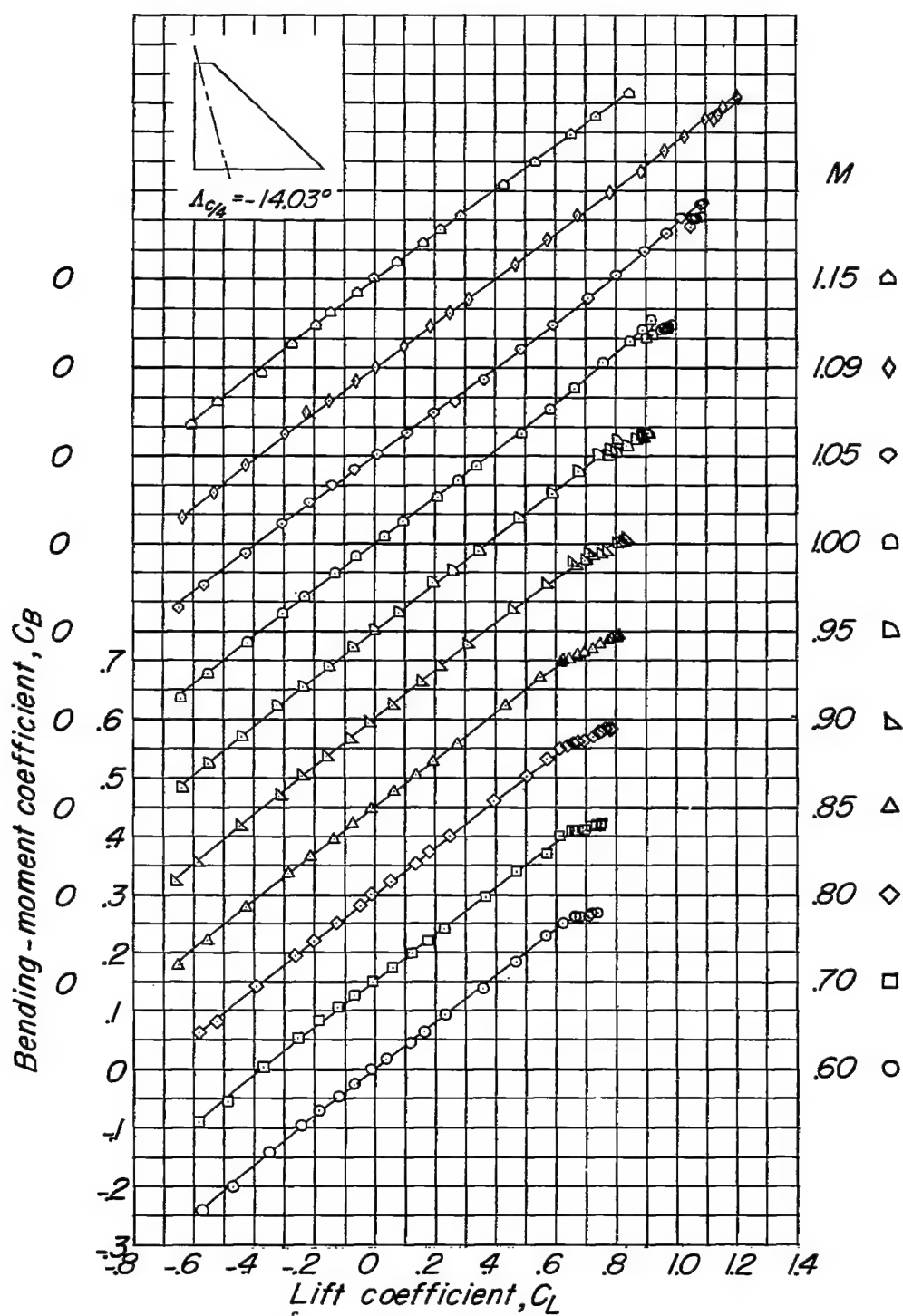Figure 5.- Continued.
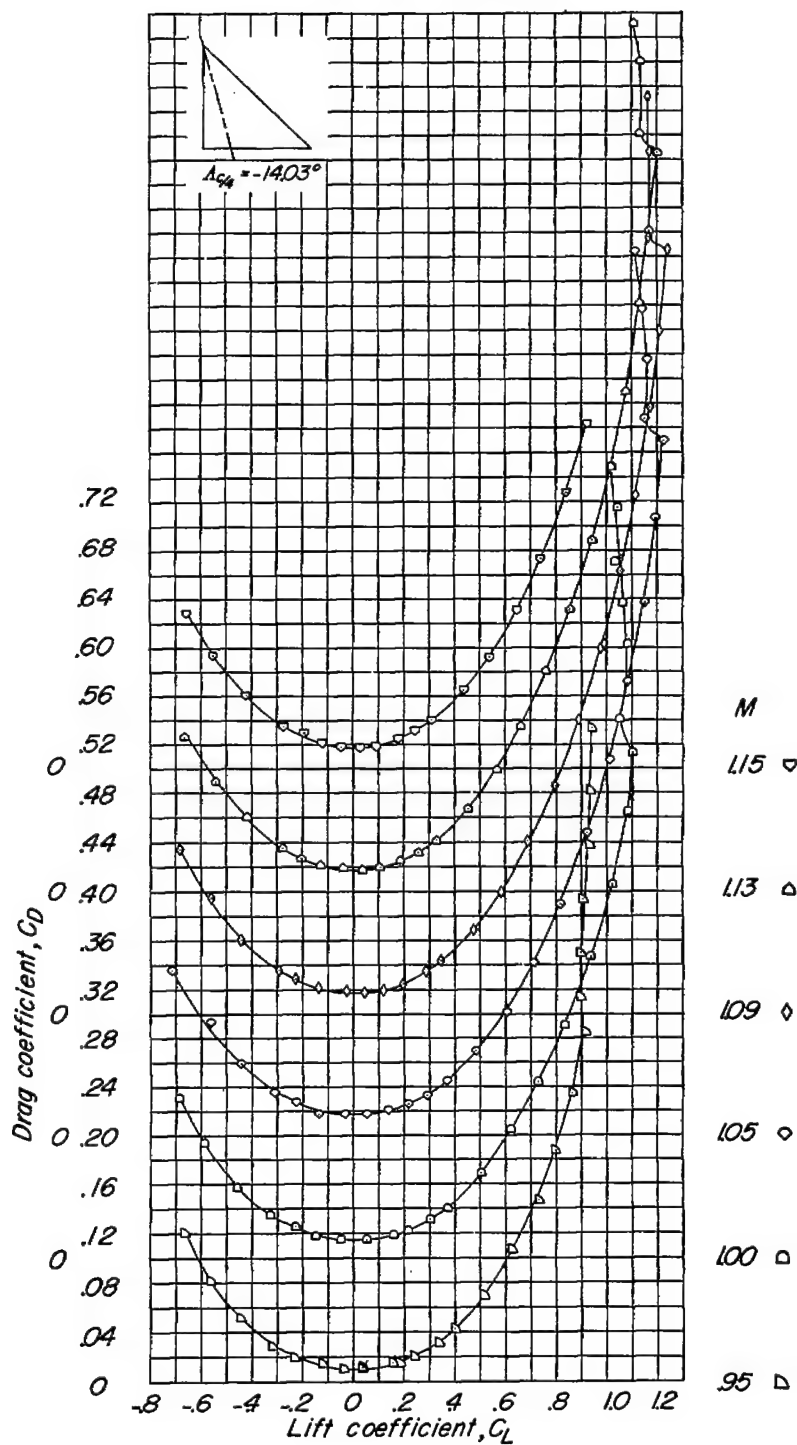
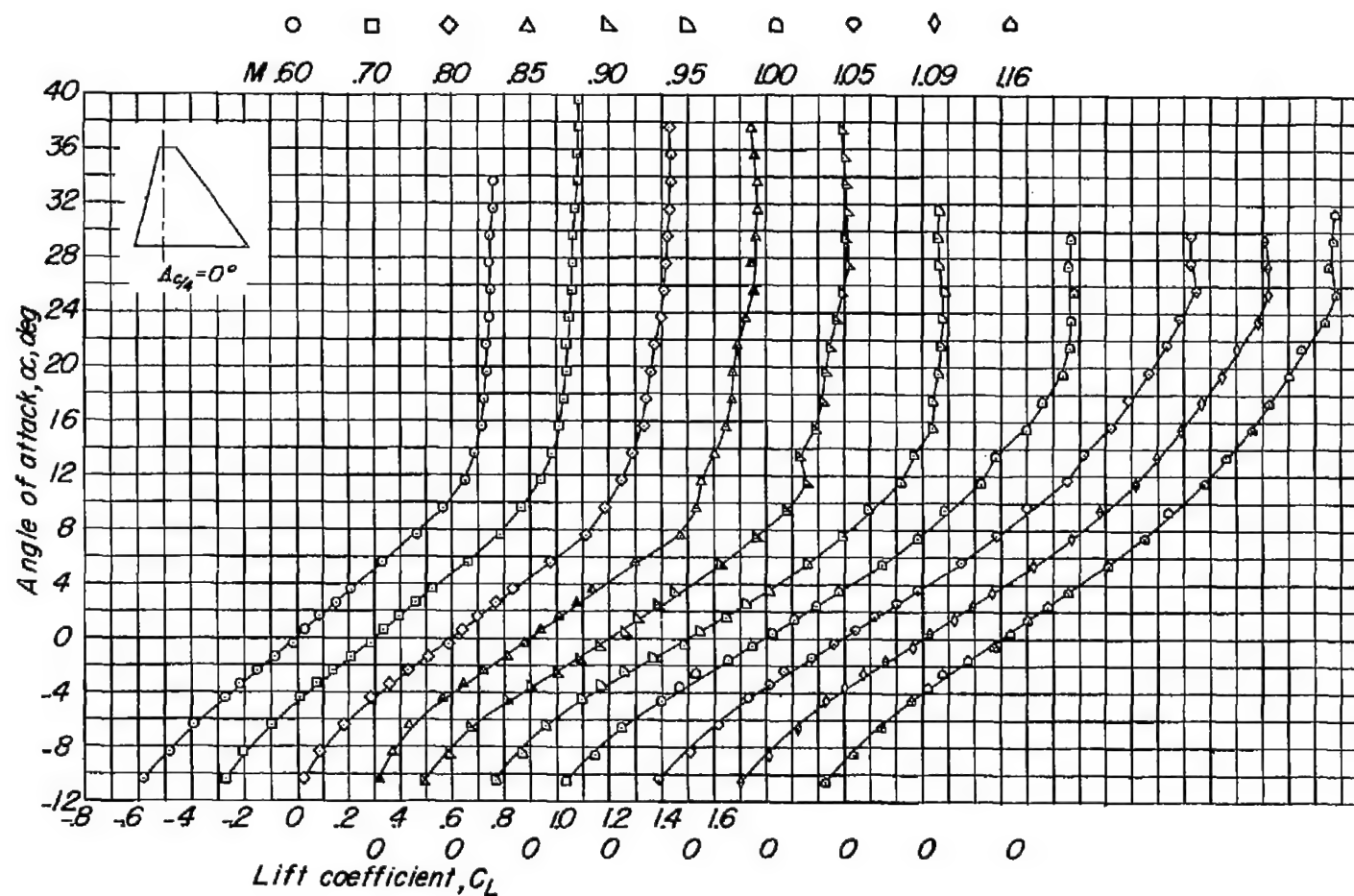(c) Concluded.

Figure 5.- Continued.
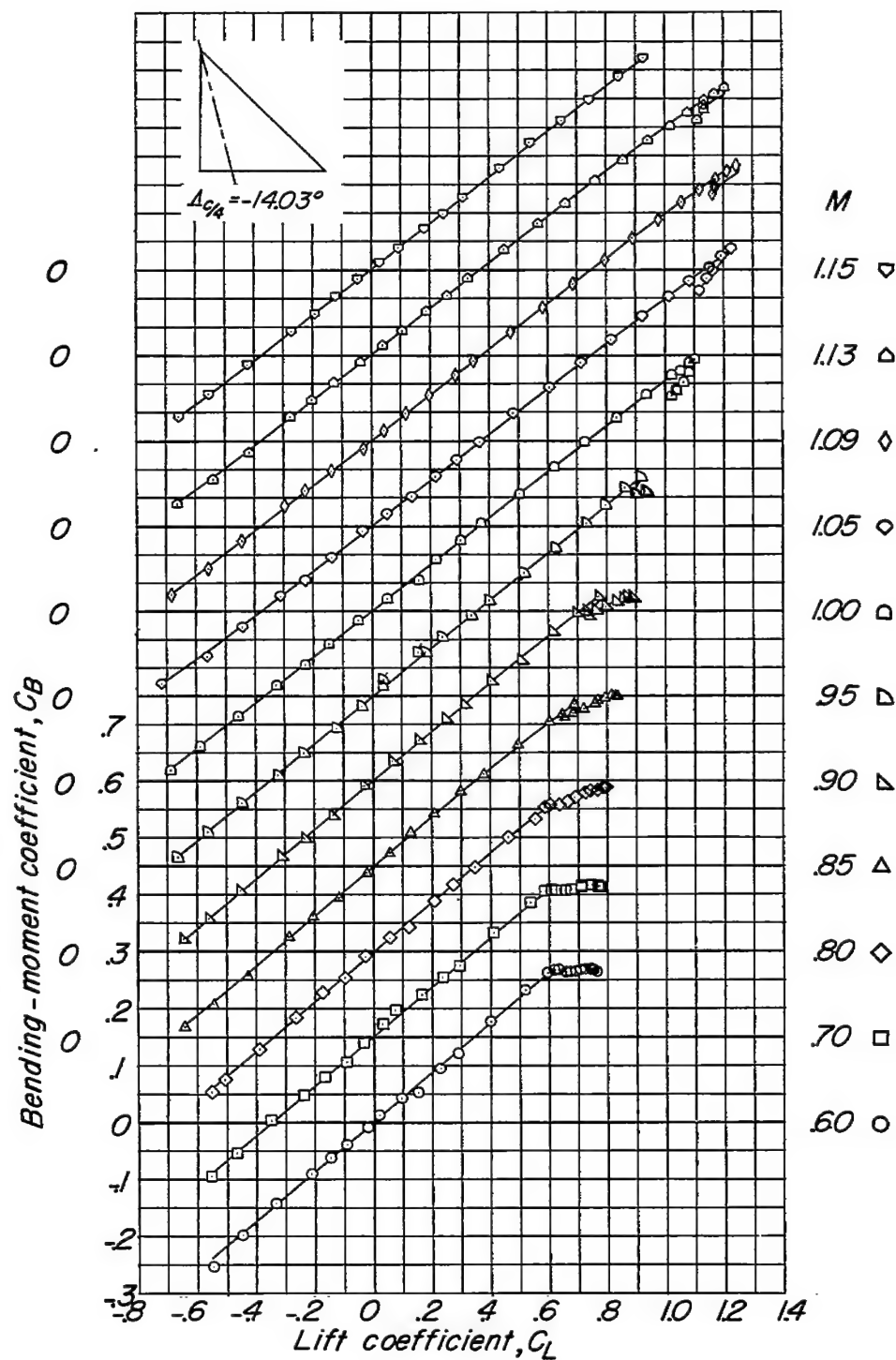
(d) Variation of C_B with C_L.

Figure 5.- Concluded.
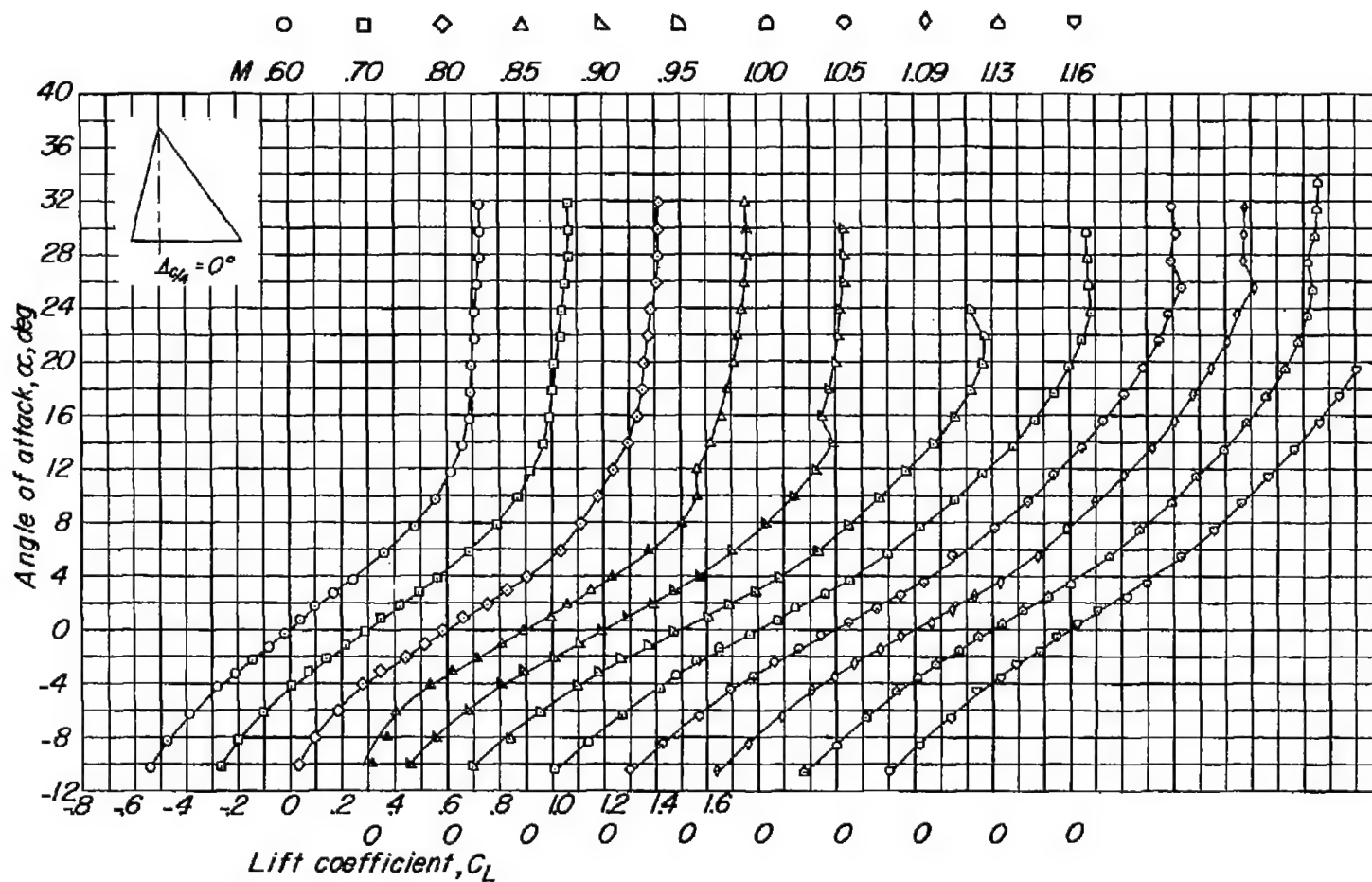
(a) Variation of α with C_L.

Figure 6.- Aerodynamic characteristics of a wing with $0°$ quarter-chord sweep; aspect ratio 4; taper ratio 0; and an NACA 65A003 airfoil section.
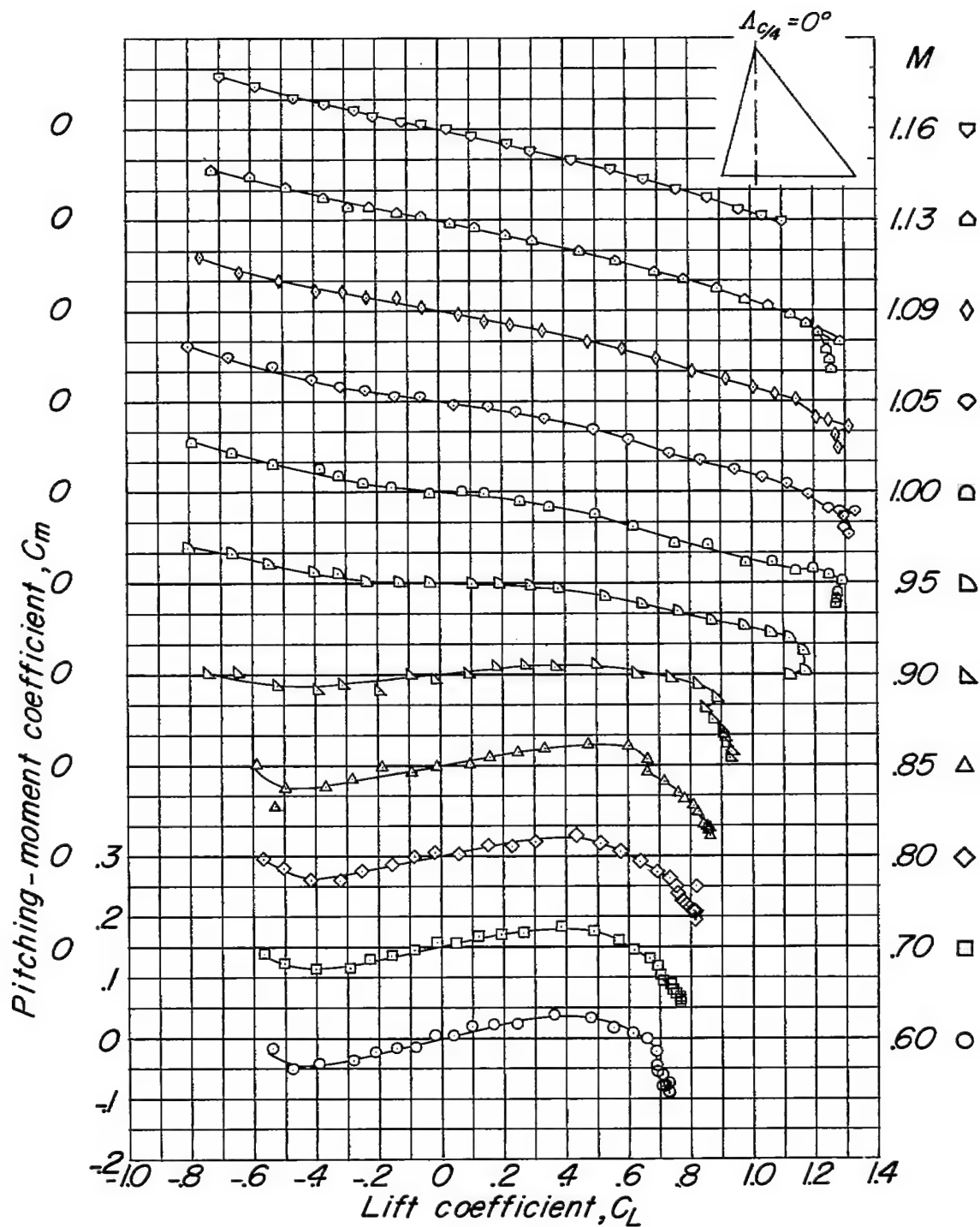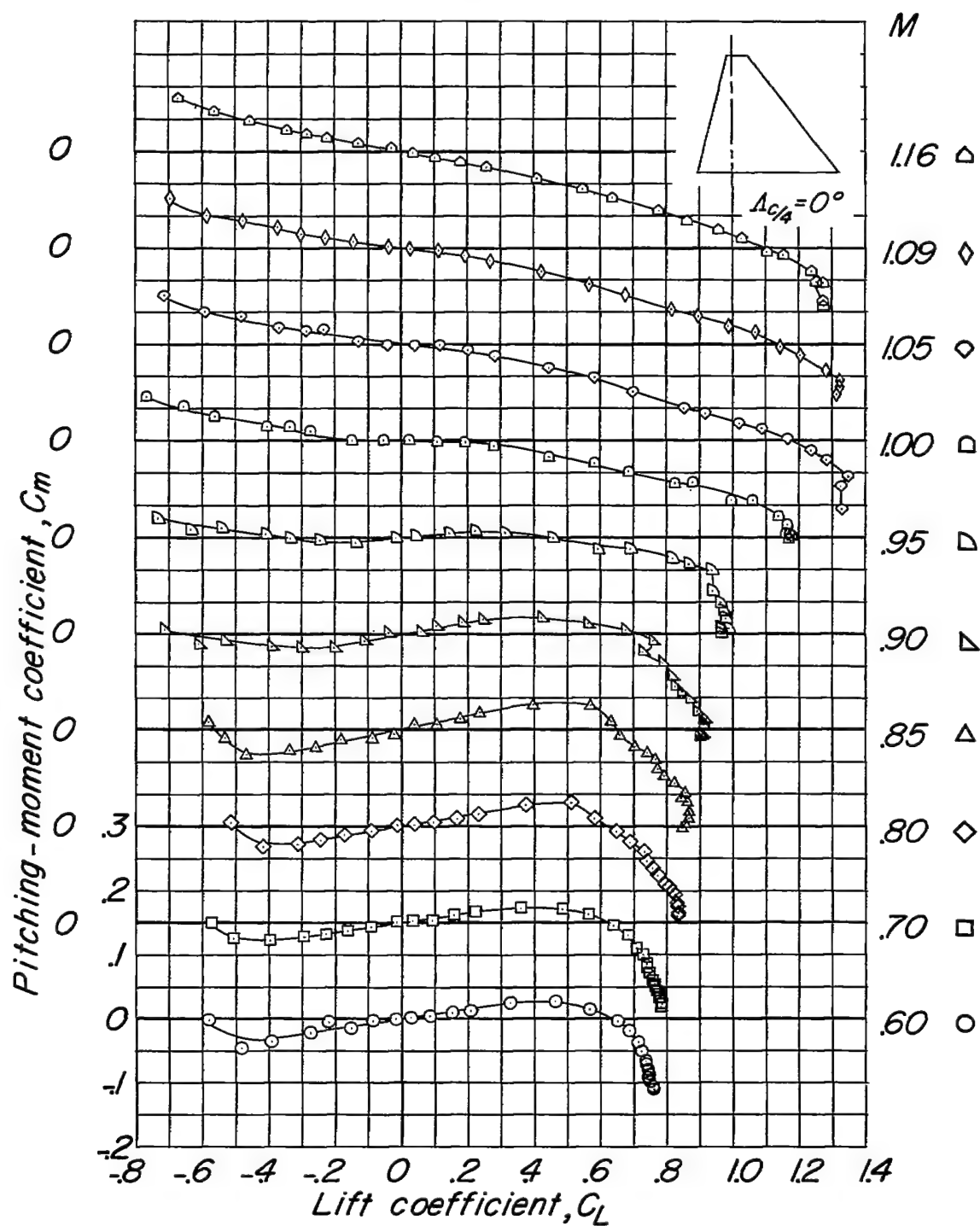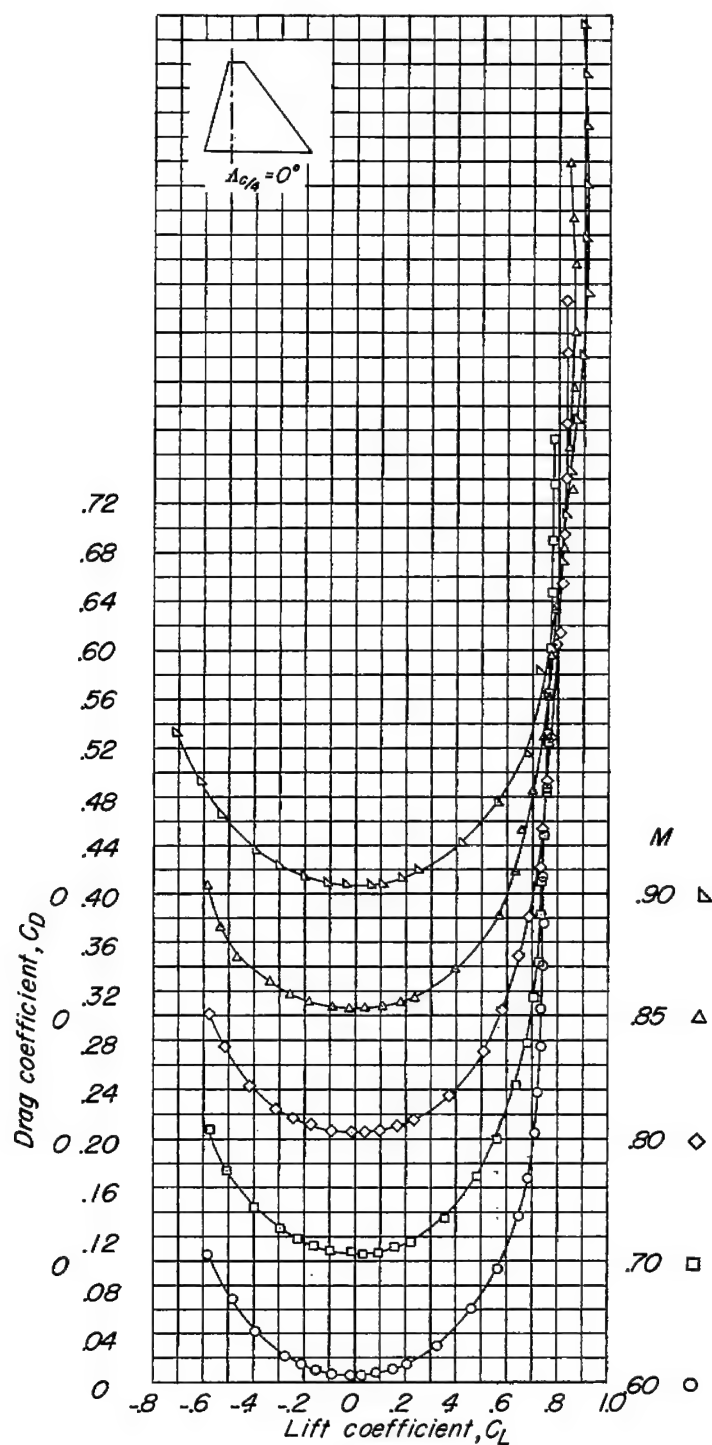
(b) Variation of C_m with C_L.

Figure 6.- Continued.
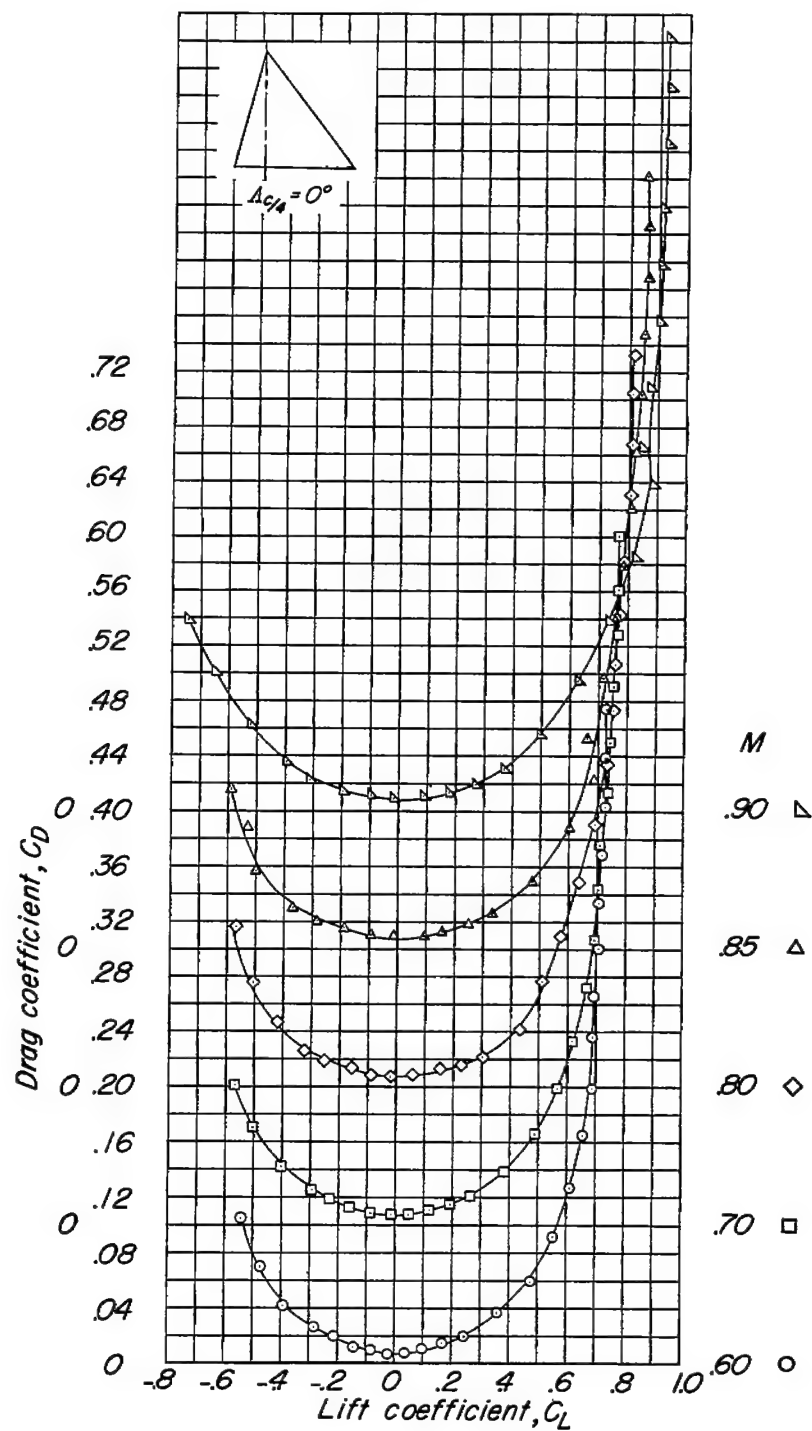
(c) Variation of C_D with C_L.

Figure 6.- Continued.
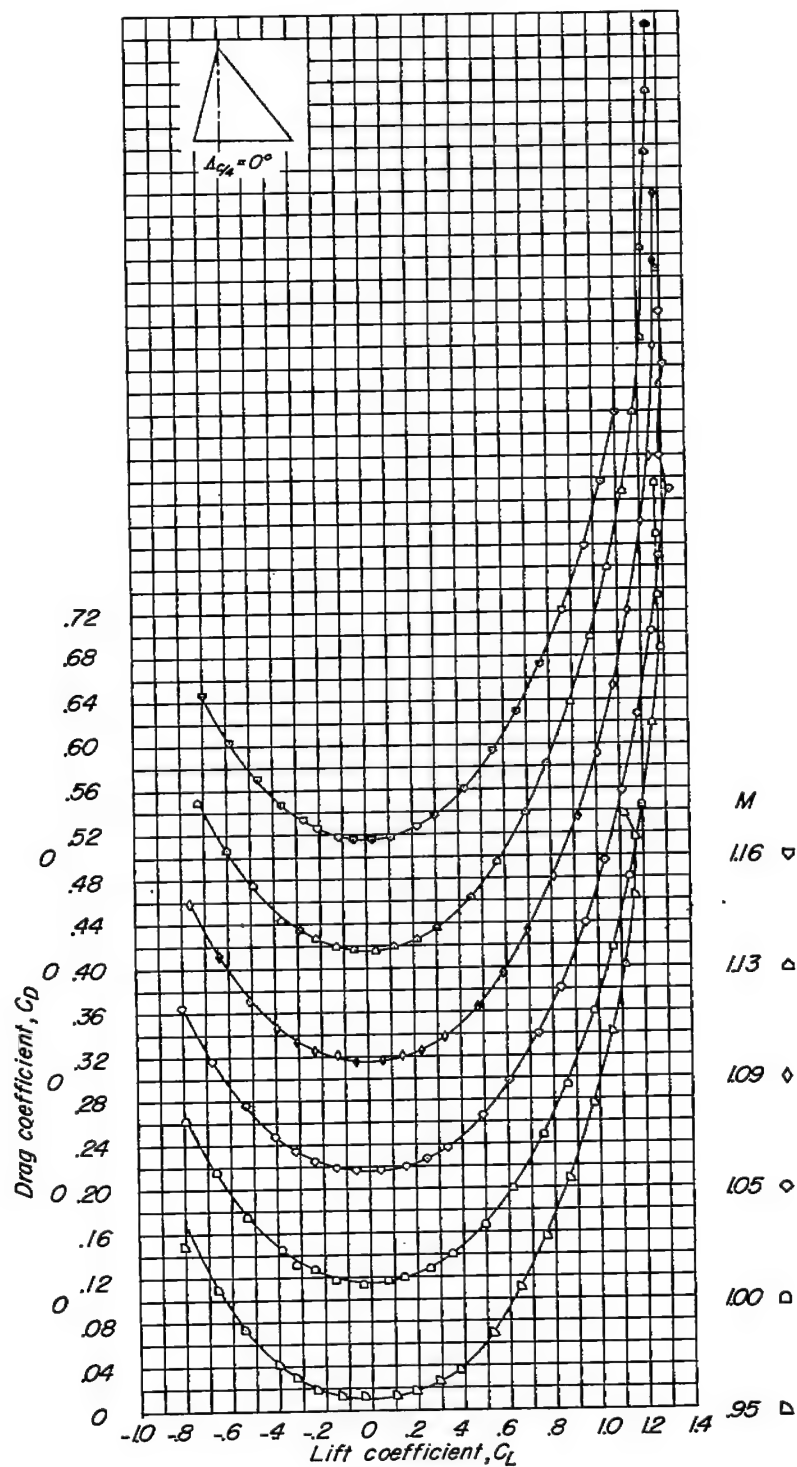
(c) Concluded.

Figure 6.- Continued.
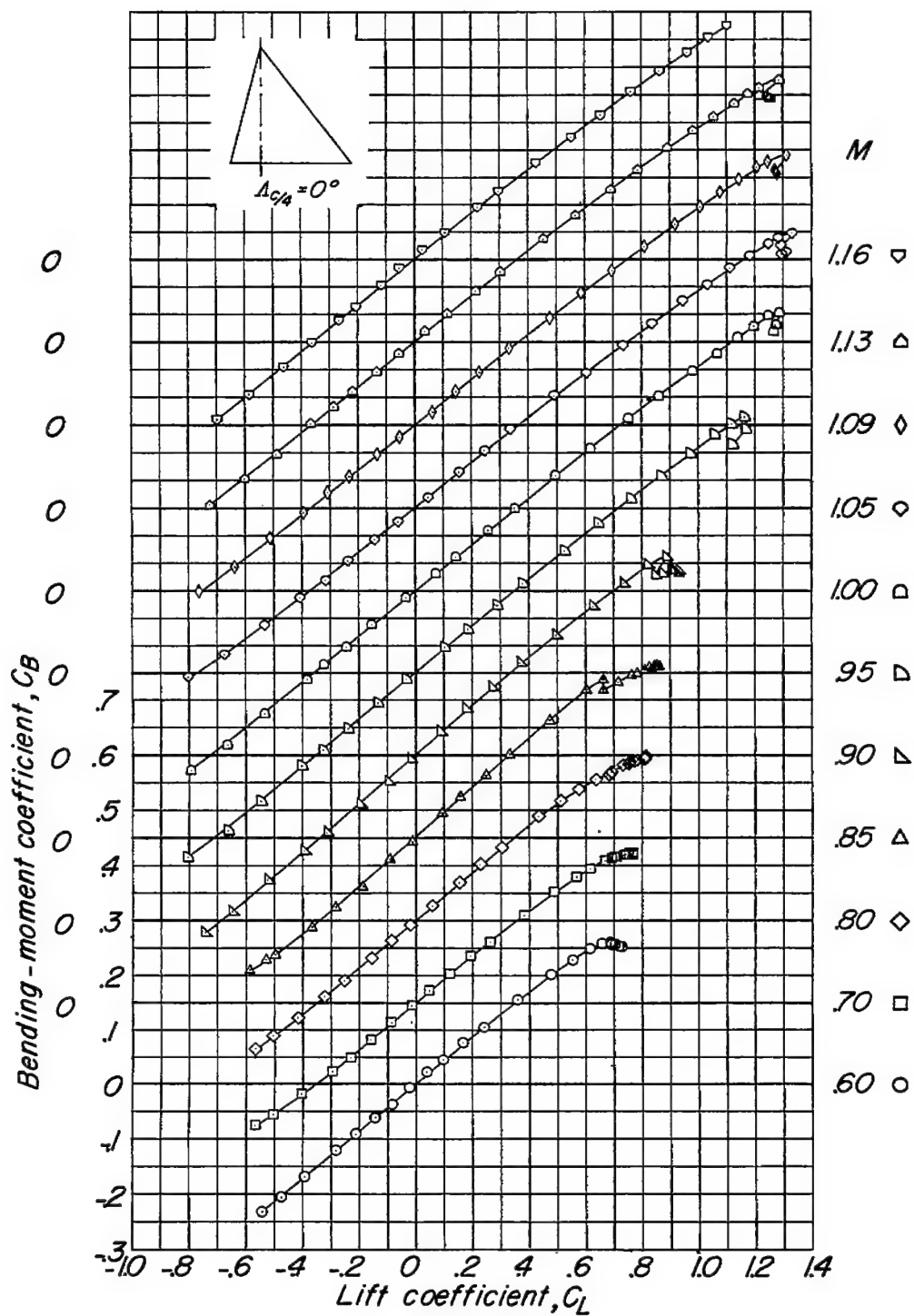
(d) Variation of C_B with C_L.

Figure 6.- Concluded.
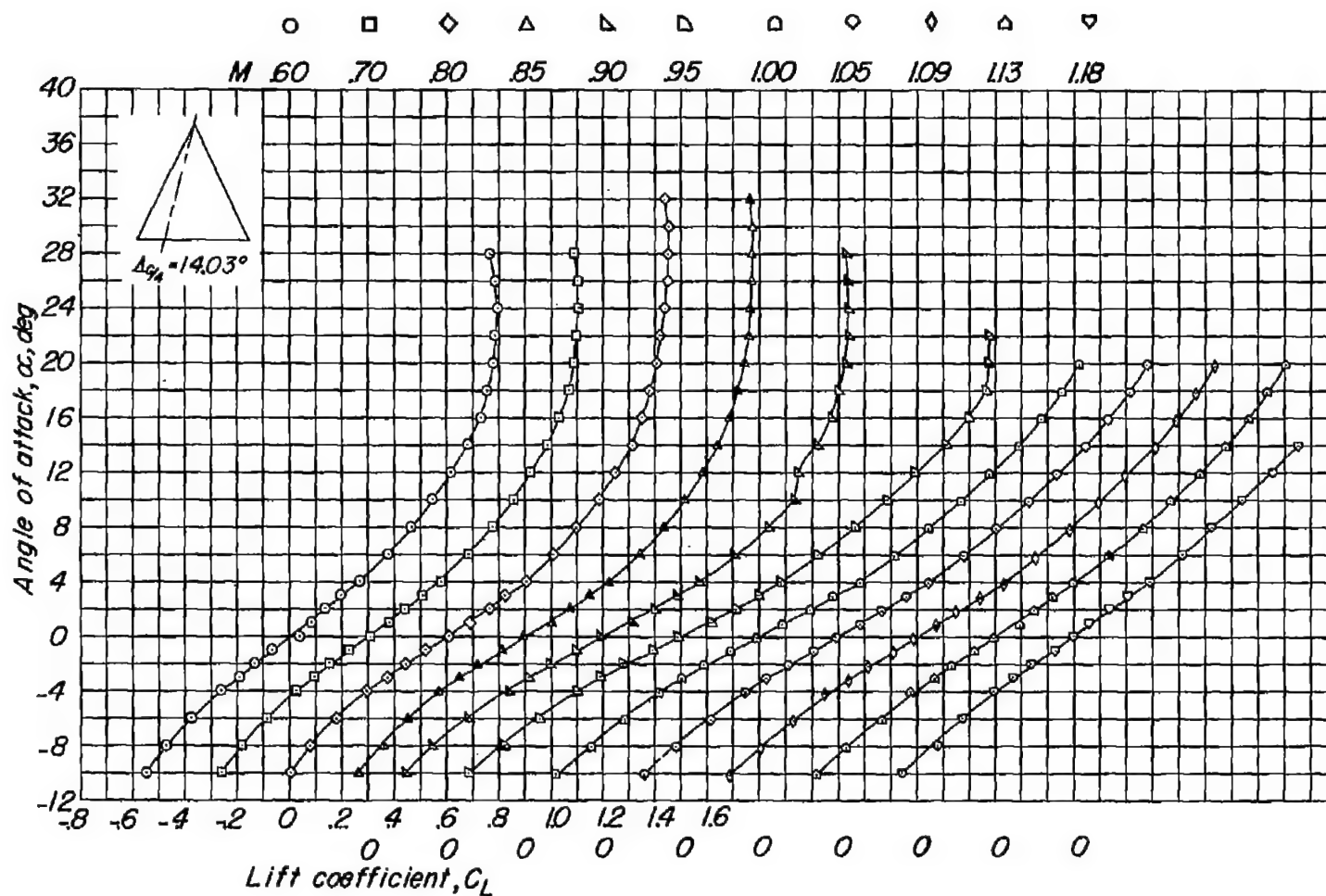
(a) Variation of α with C_L.

Figure 7.- Aerodynamic characteristics of a wing with 14.03° quarter-chord sweep; aspect ratio 4; taper ratio 0; and an NACA 65A003 airfoil section.
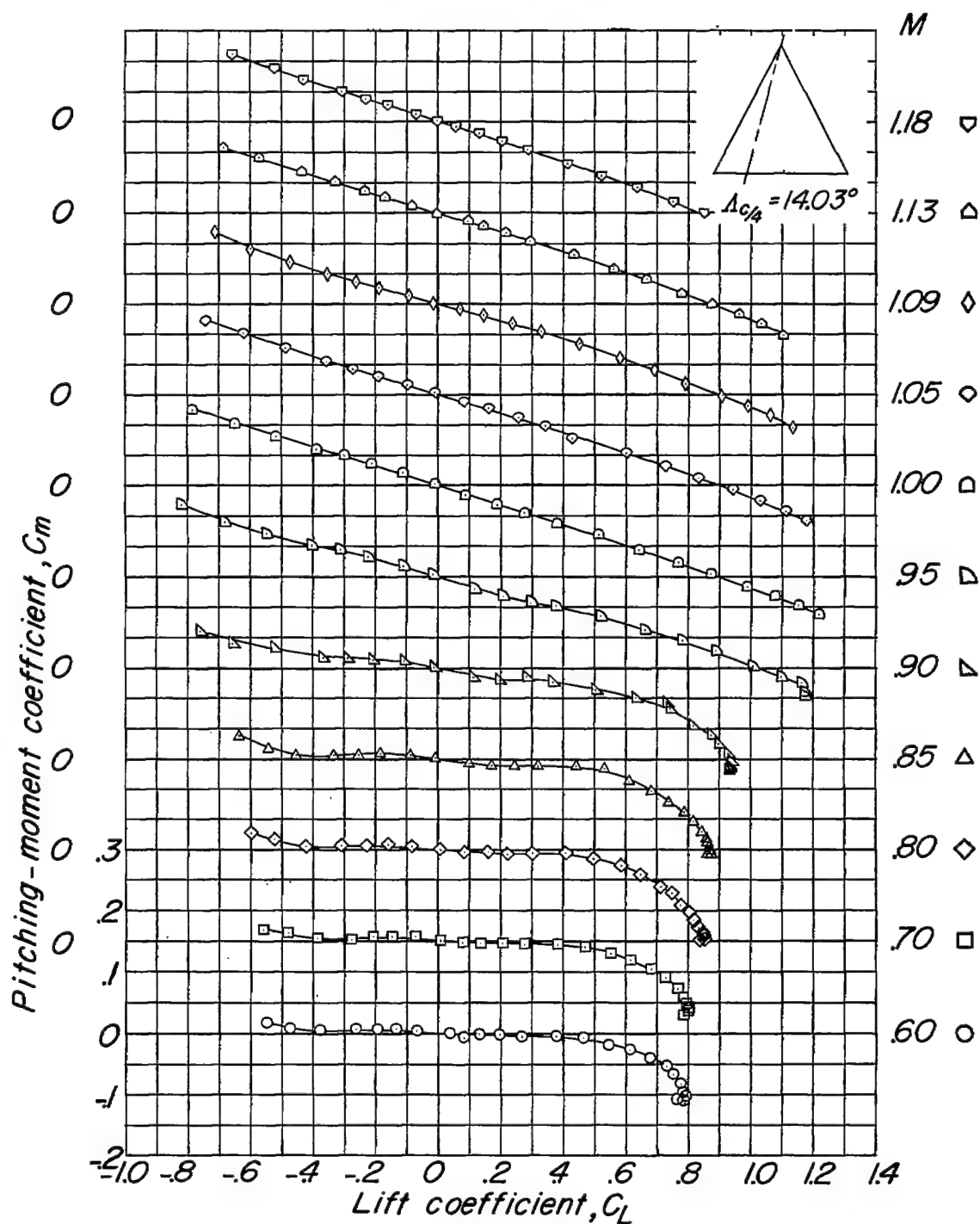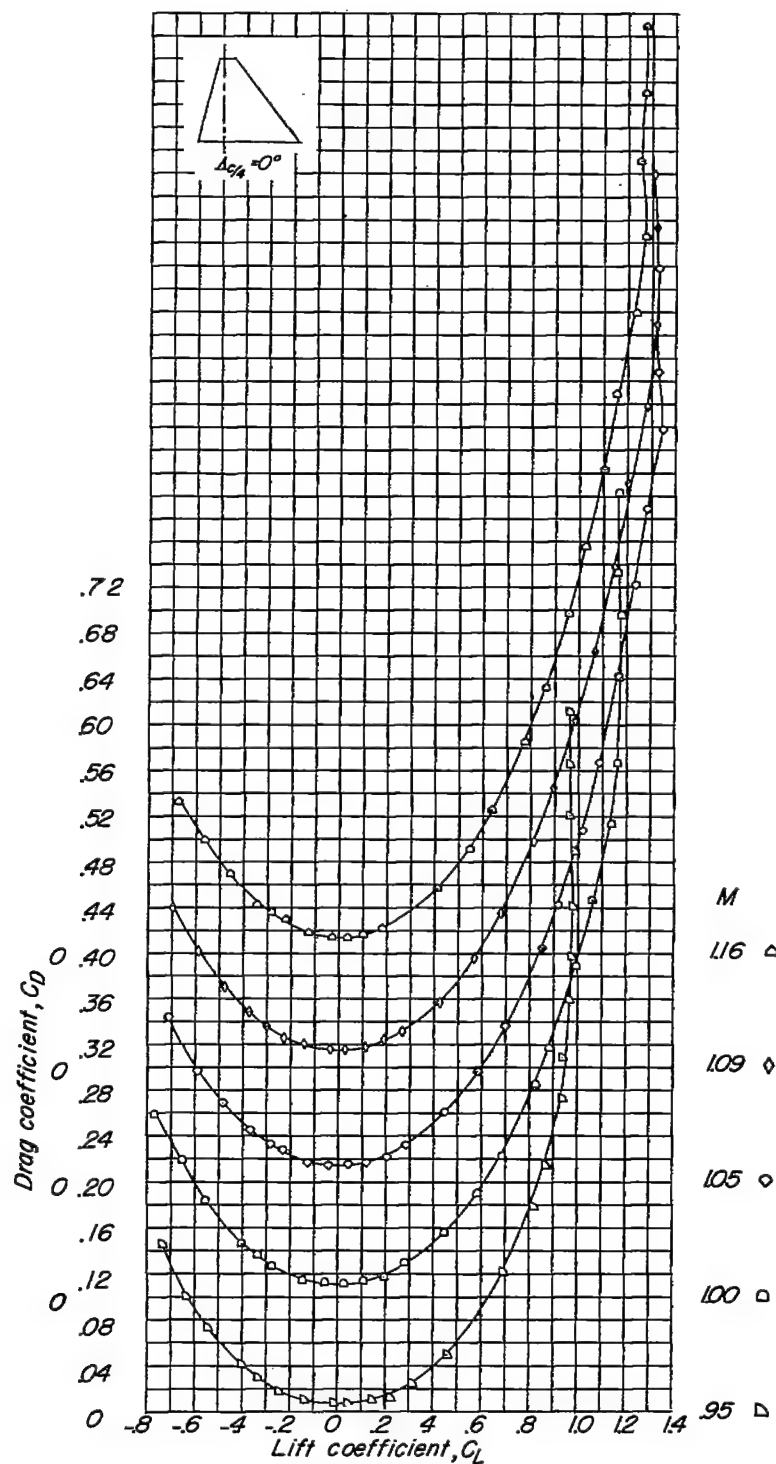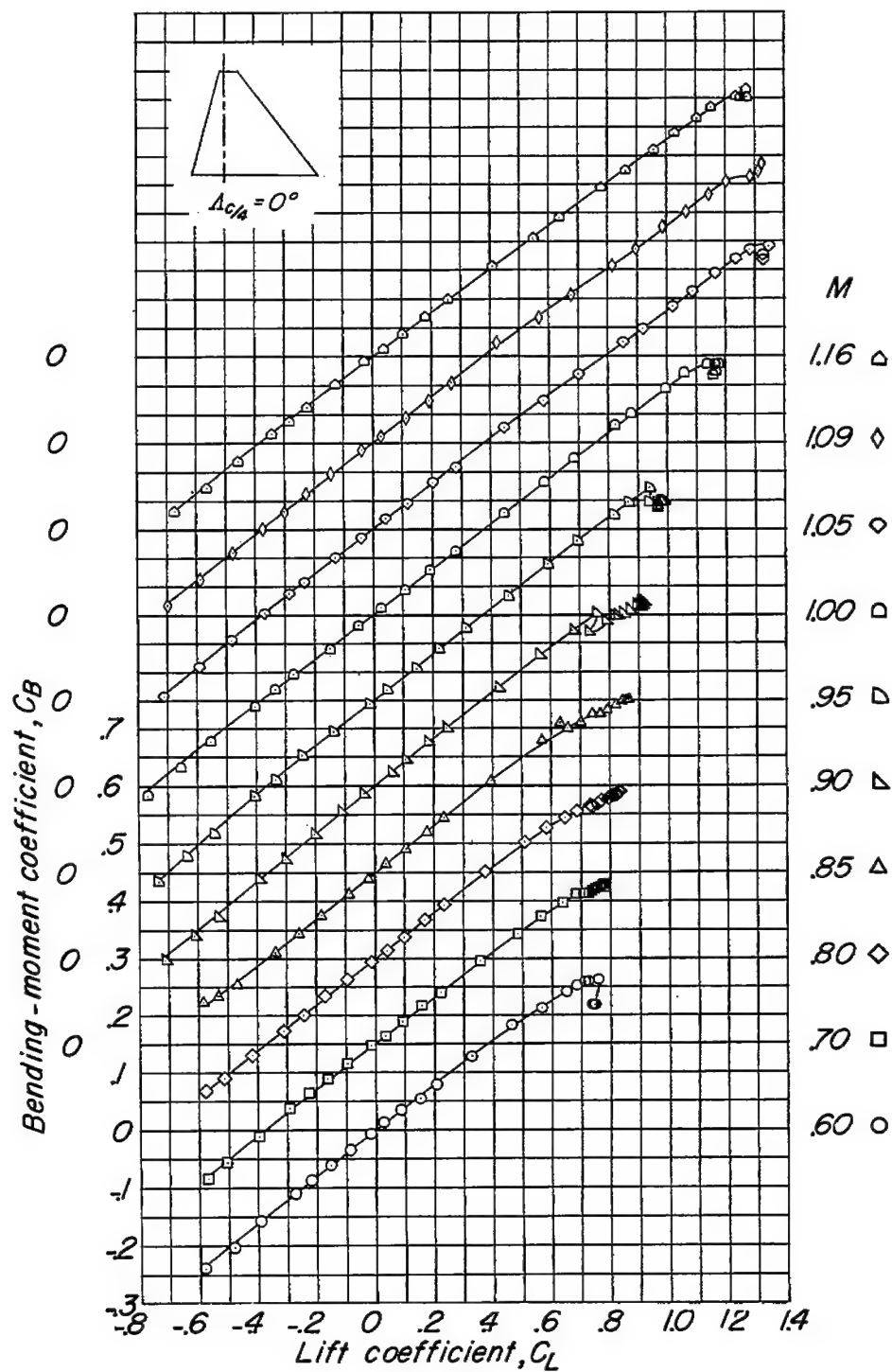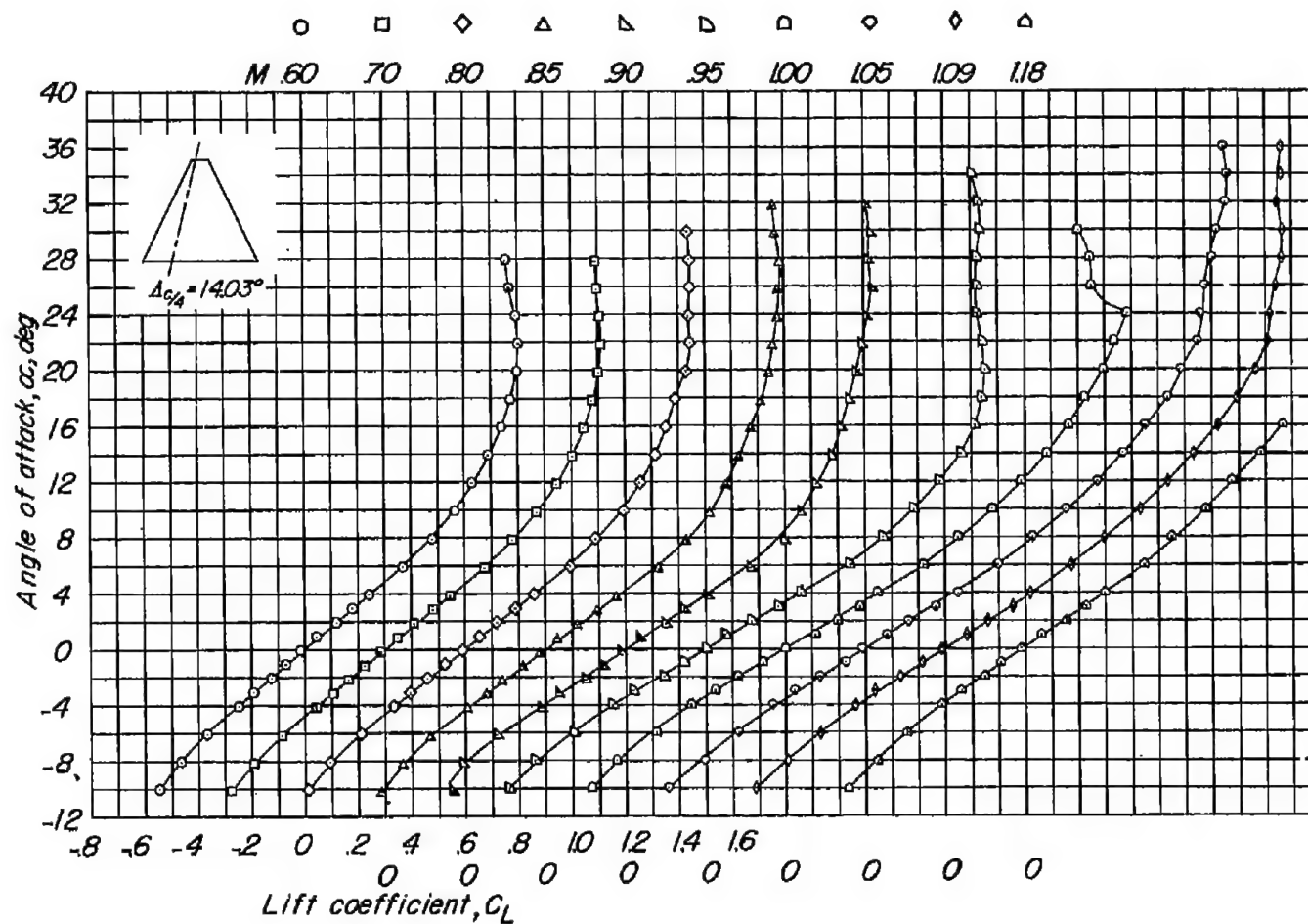
(b) Variation of C_m with C_L.

Figure 7.- Continued.
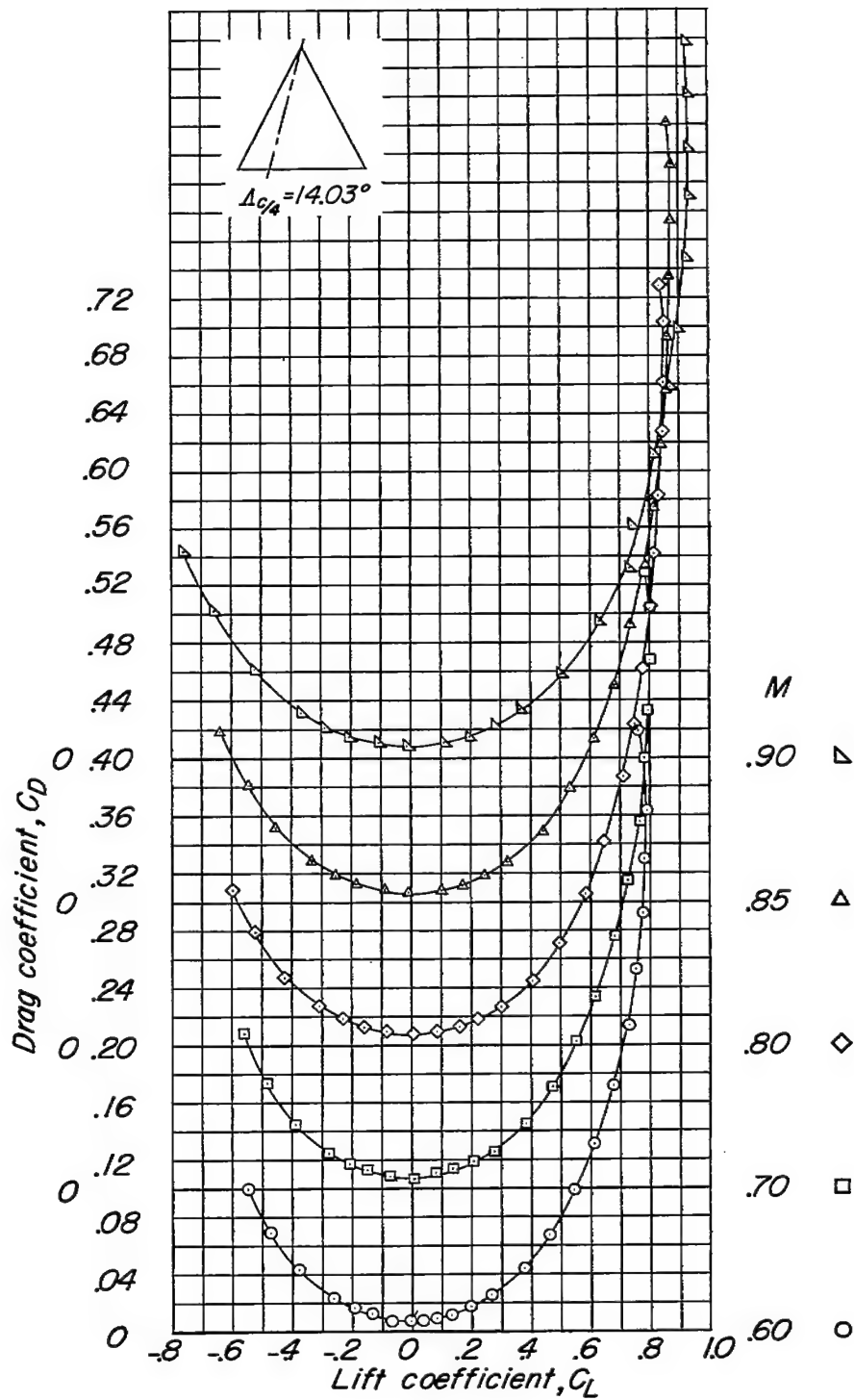
(c) Variation of C_D with C_L.

Figure 7.- Continued.
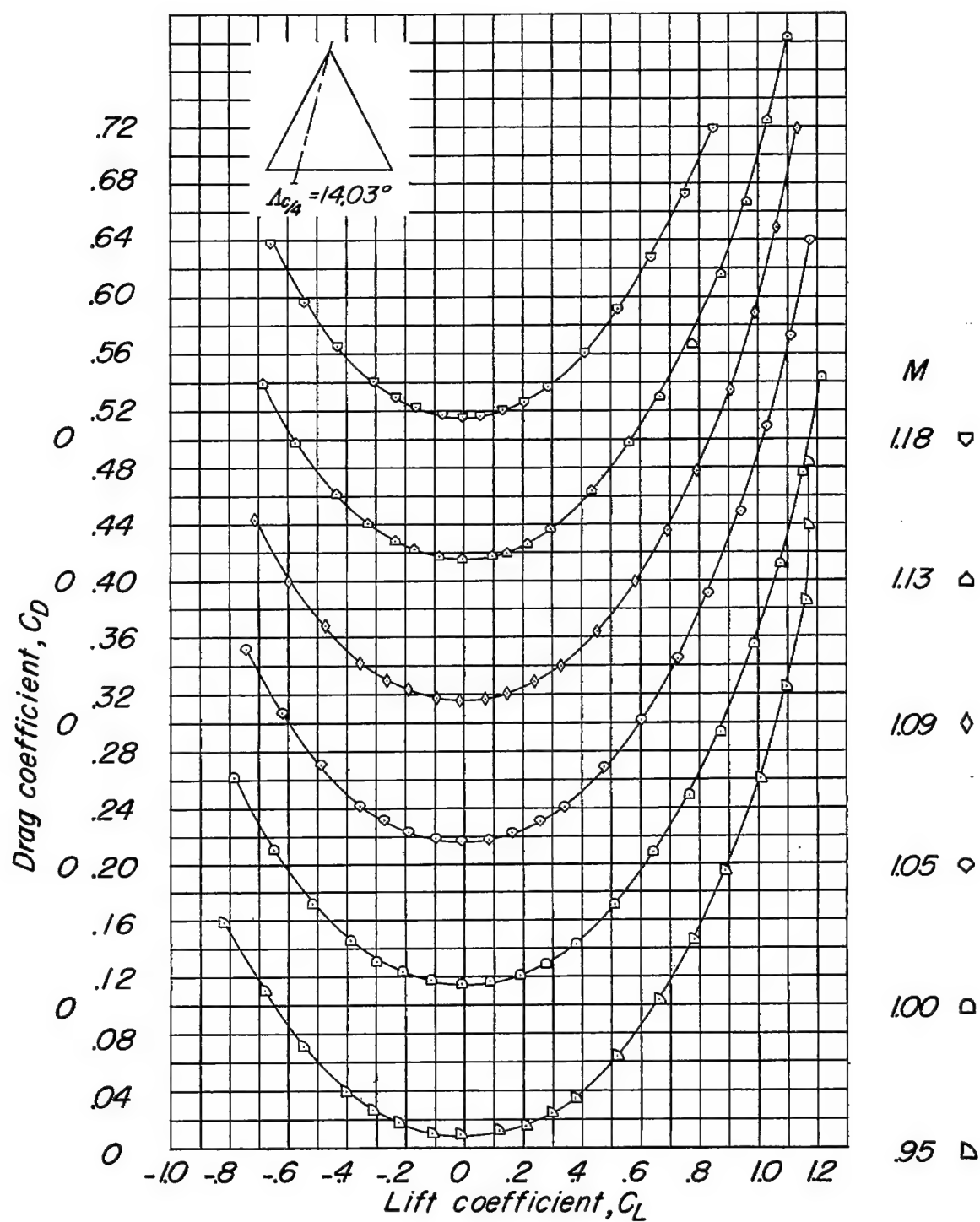
(c) Concluded.

Figure 7.- Continued.
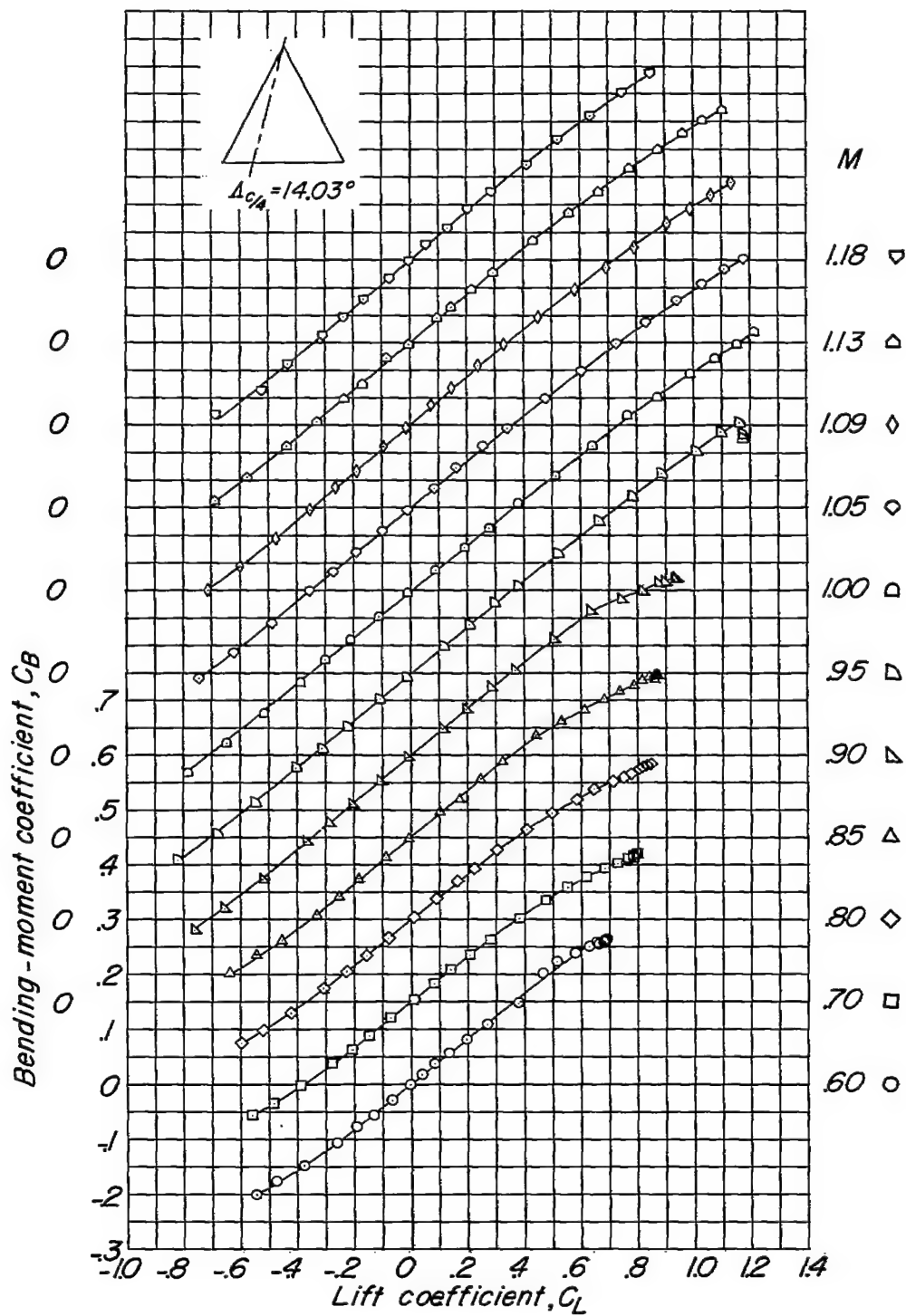
(d) Variation of C_B with C_L.

Figure 7.- Concluded.
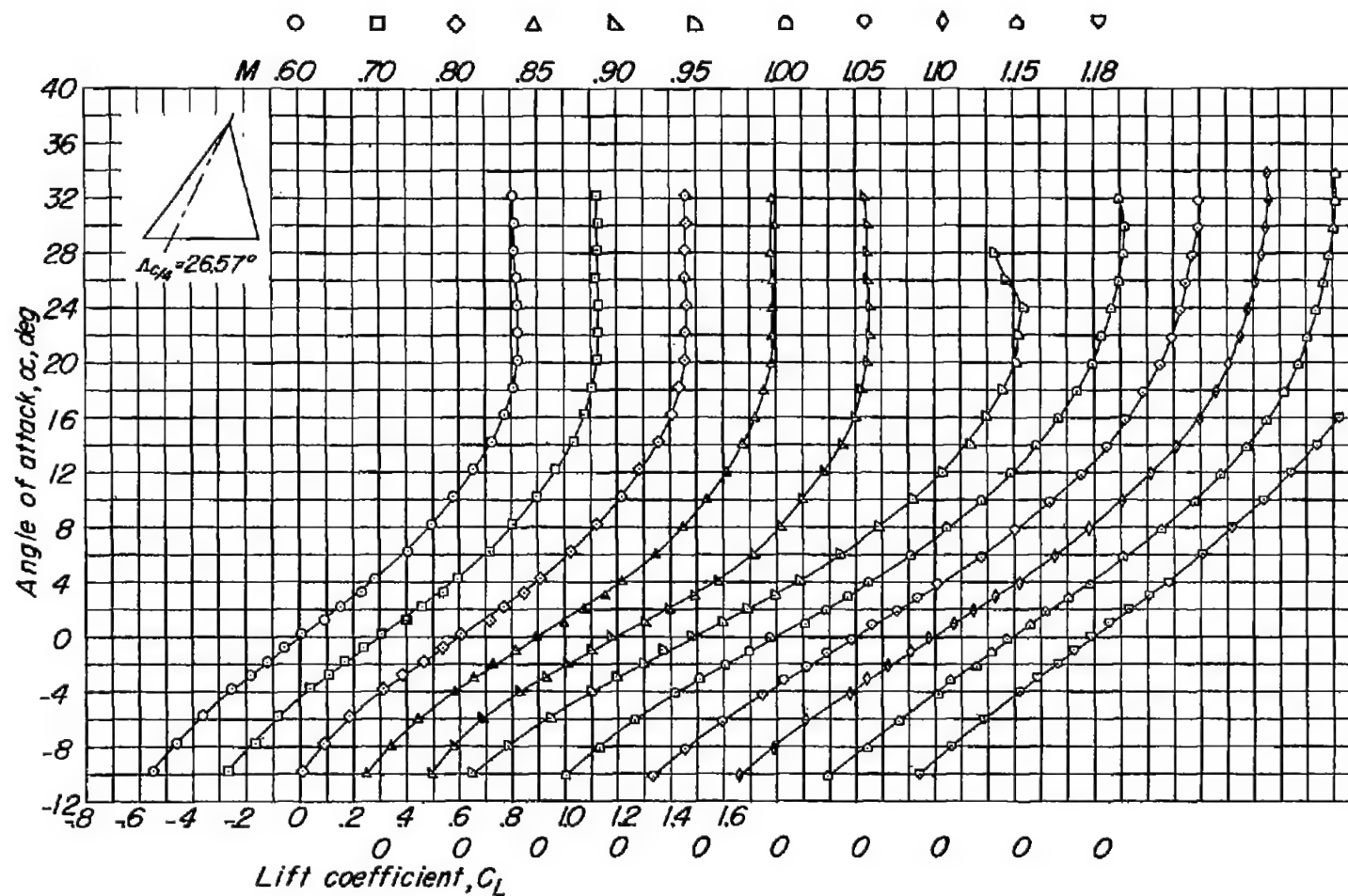
(a) Variation of α with C_L.

Figure 8.- Aerodynamic characteristics of a wing with 26.57° quarter-chord sweep; aspect ratio 4; taper ratio 0; and an NACA 65A003 airfoil section.
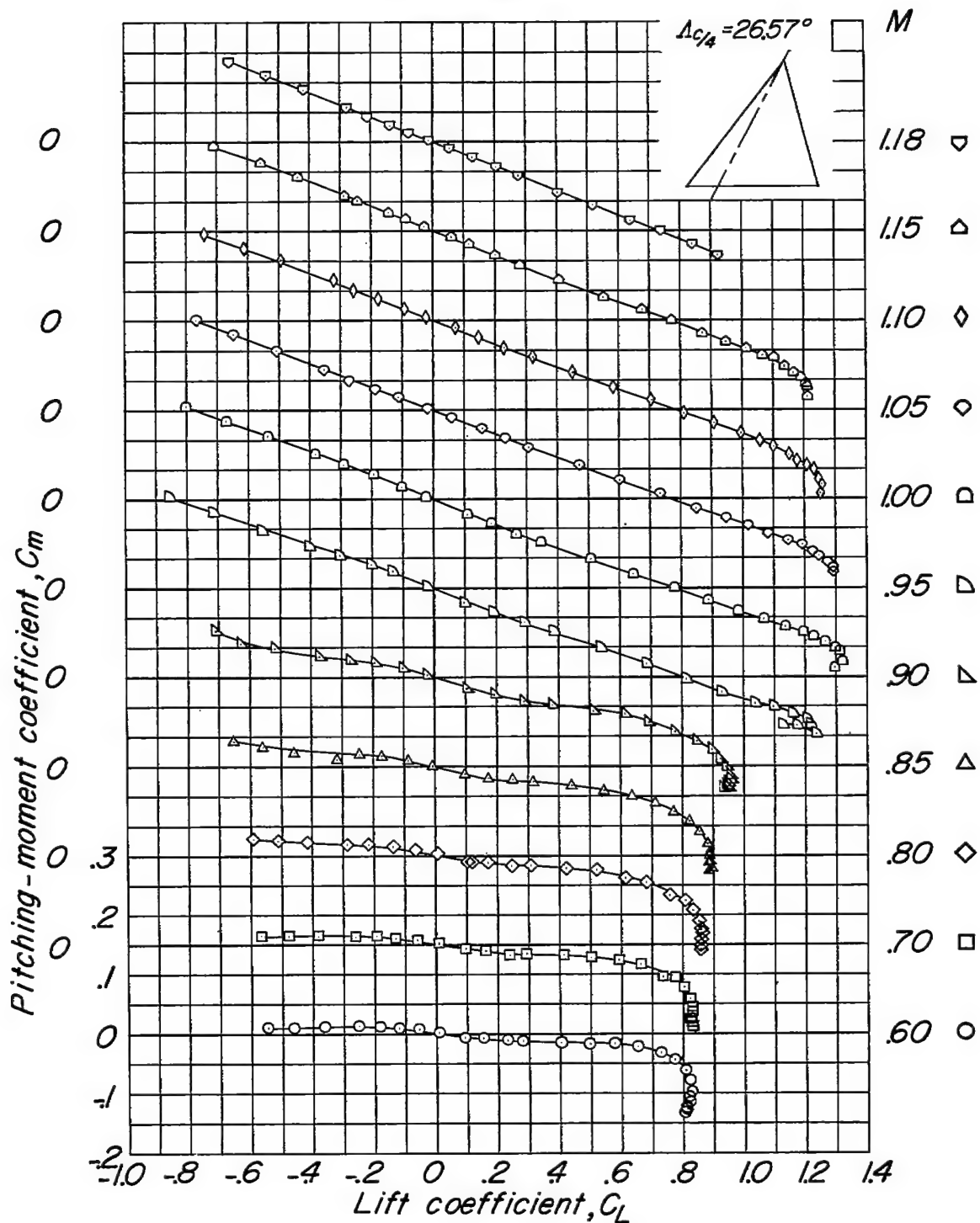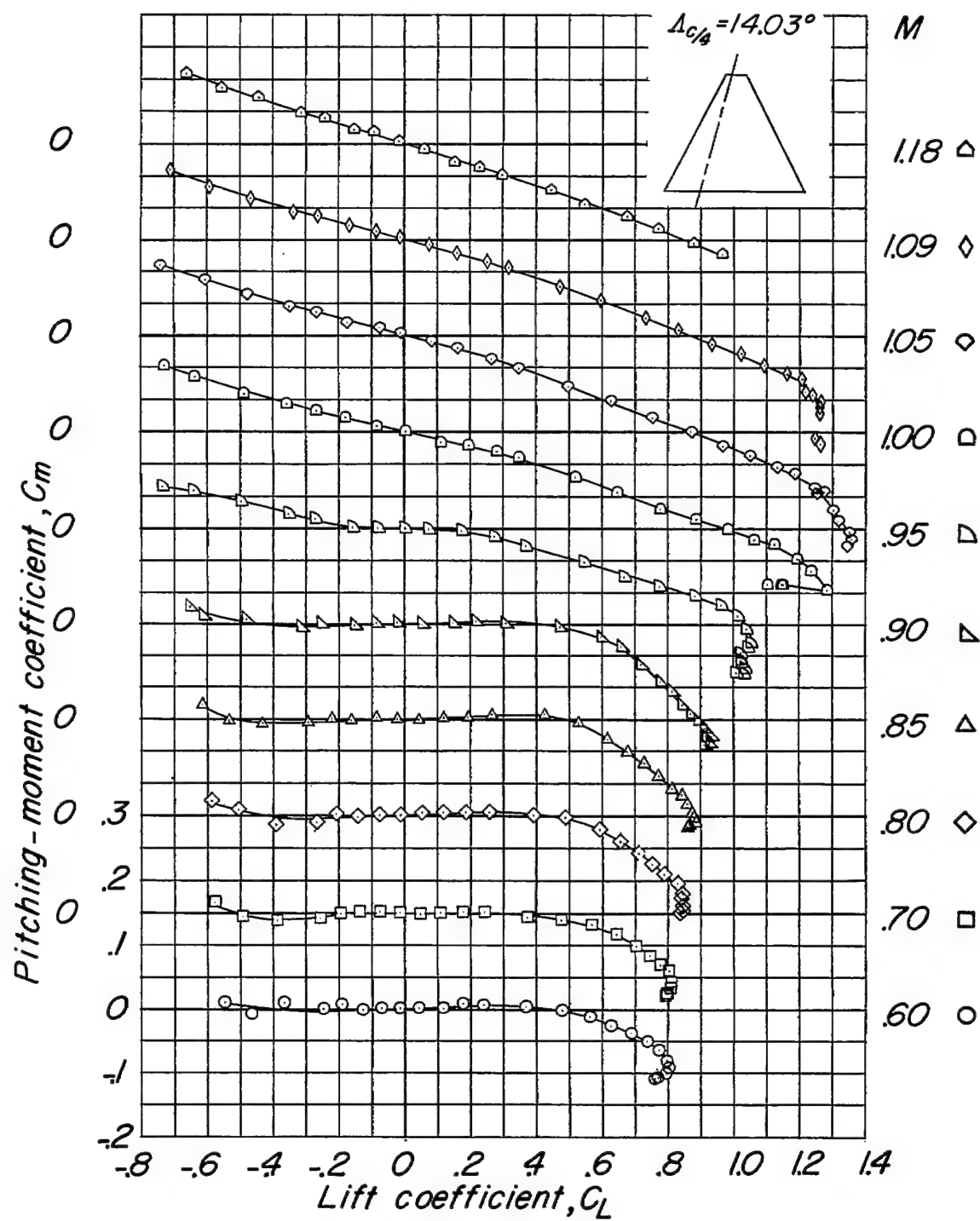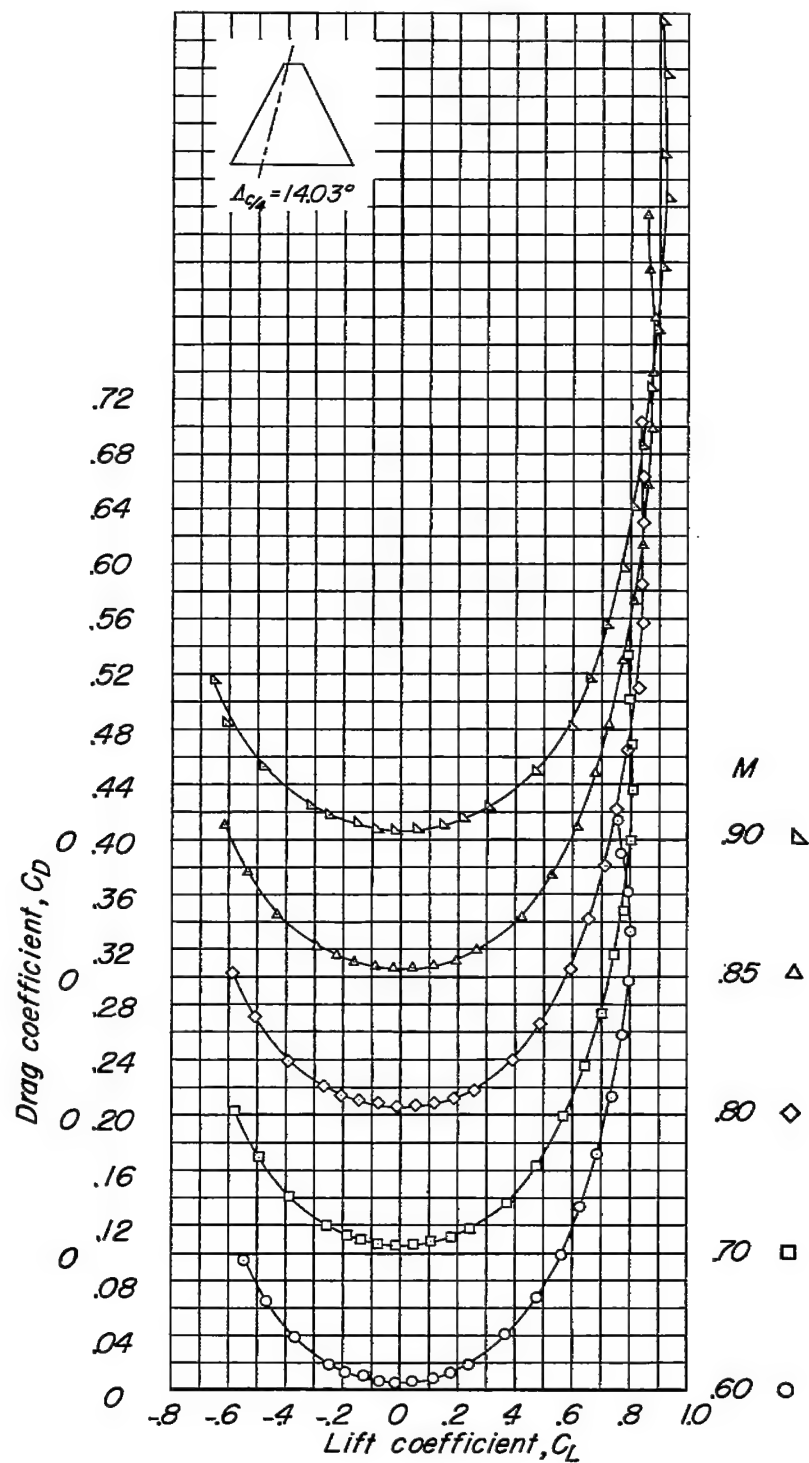
(b) Variation of C_m with C_L.

Figure 8.- Continued.
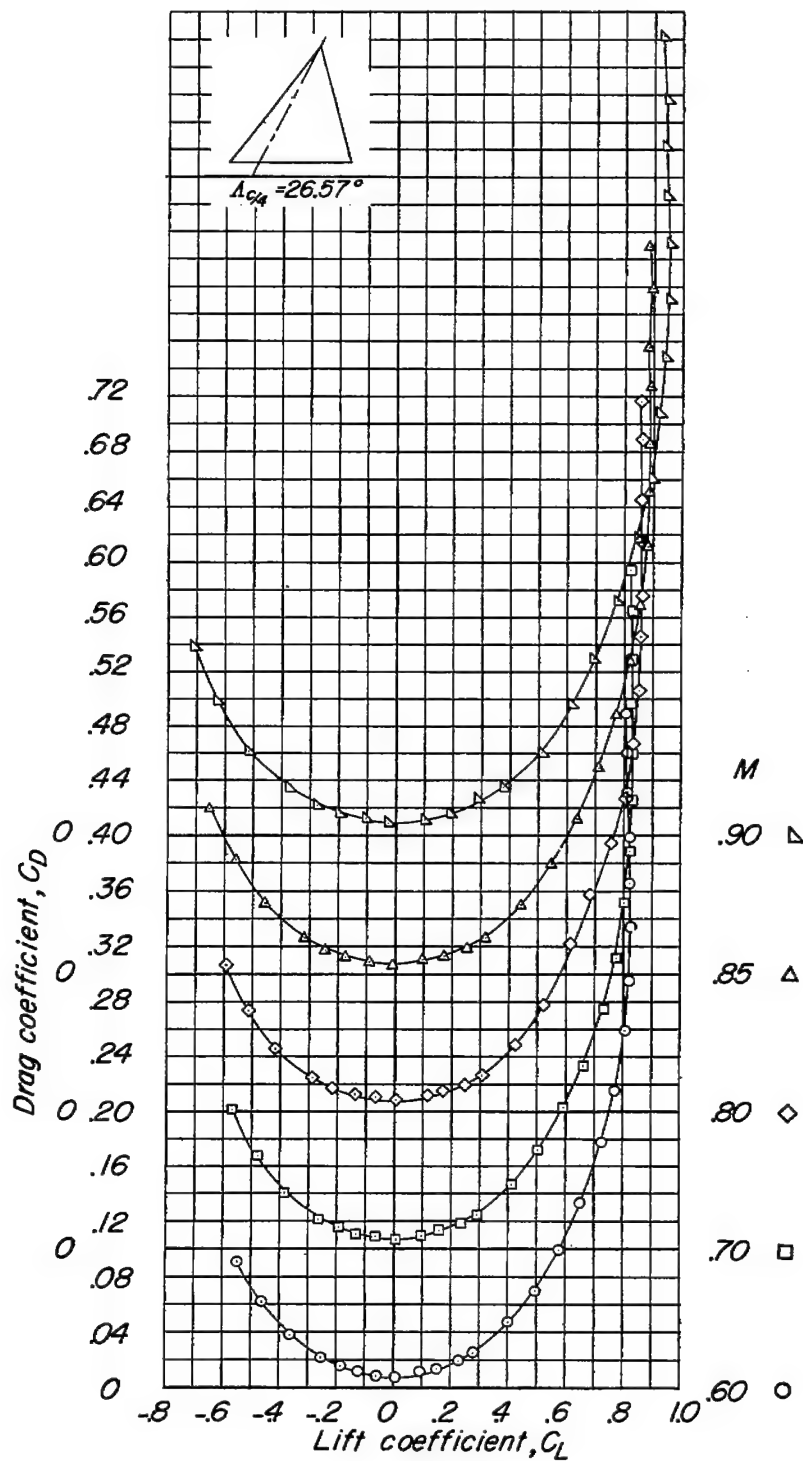
(c) Variation of C_D with C_L.

Figure 8.- Continued.
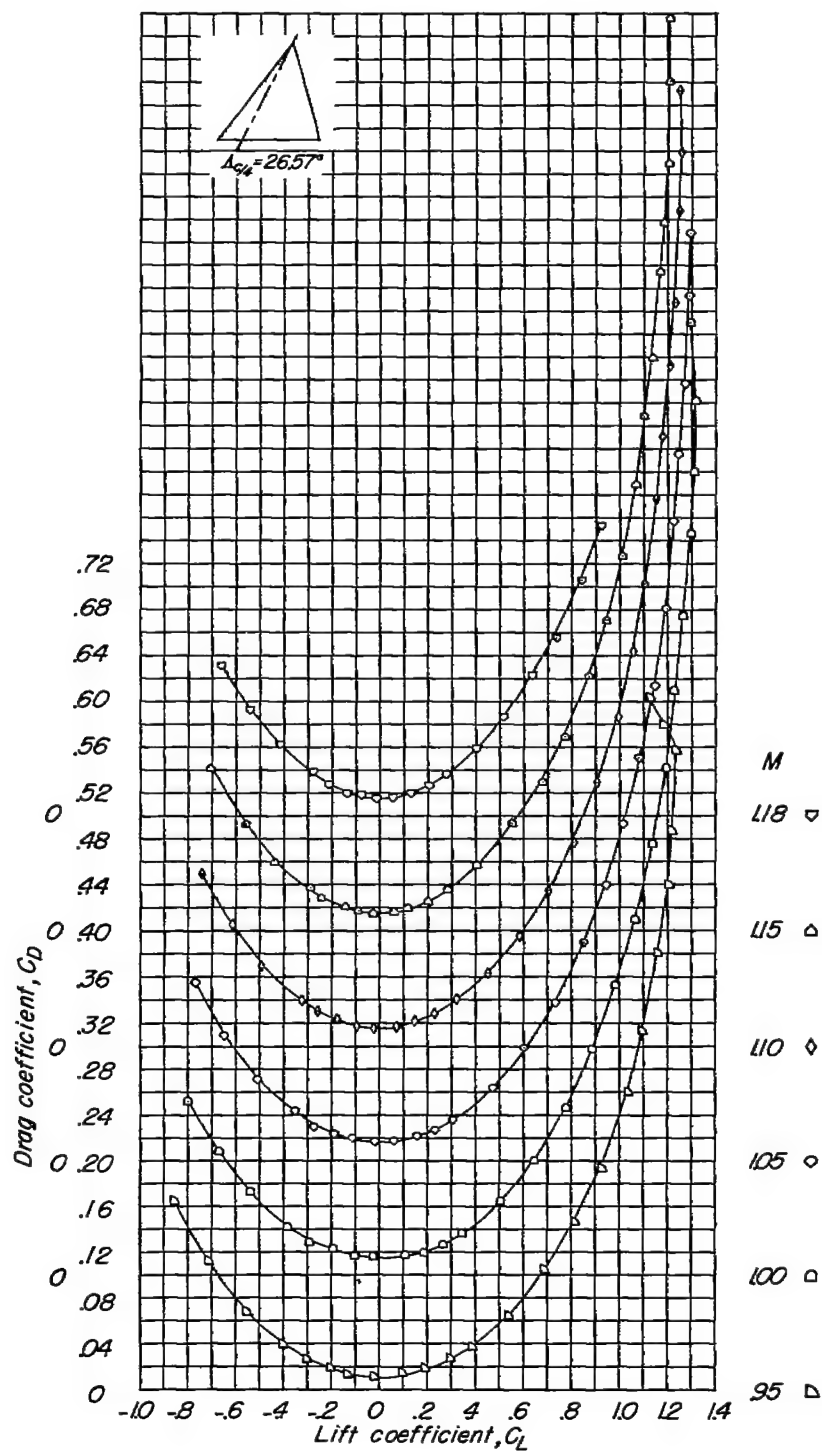
(c) Concluded.

Figure 8.- Continued.
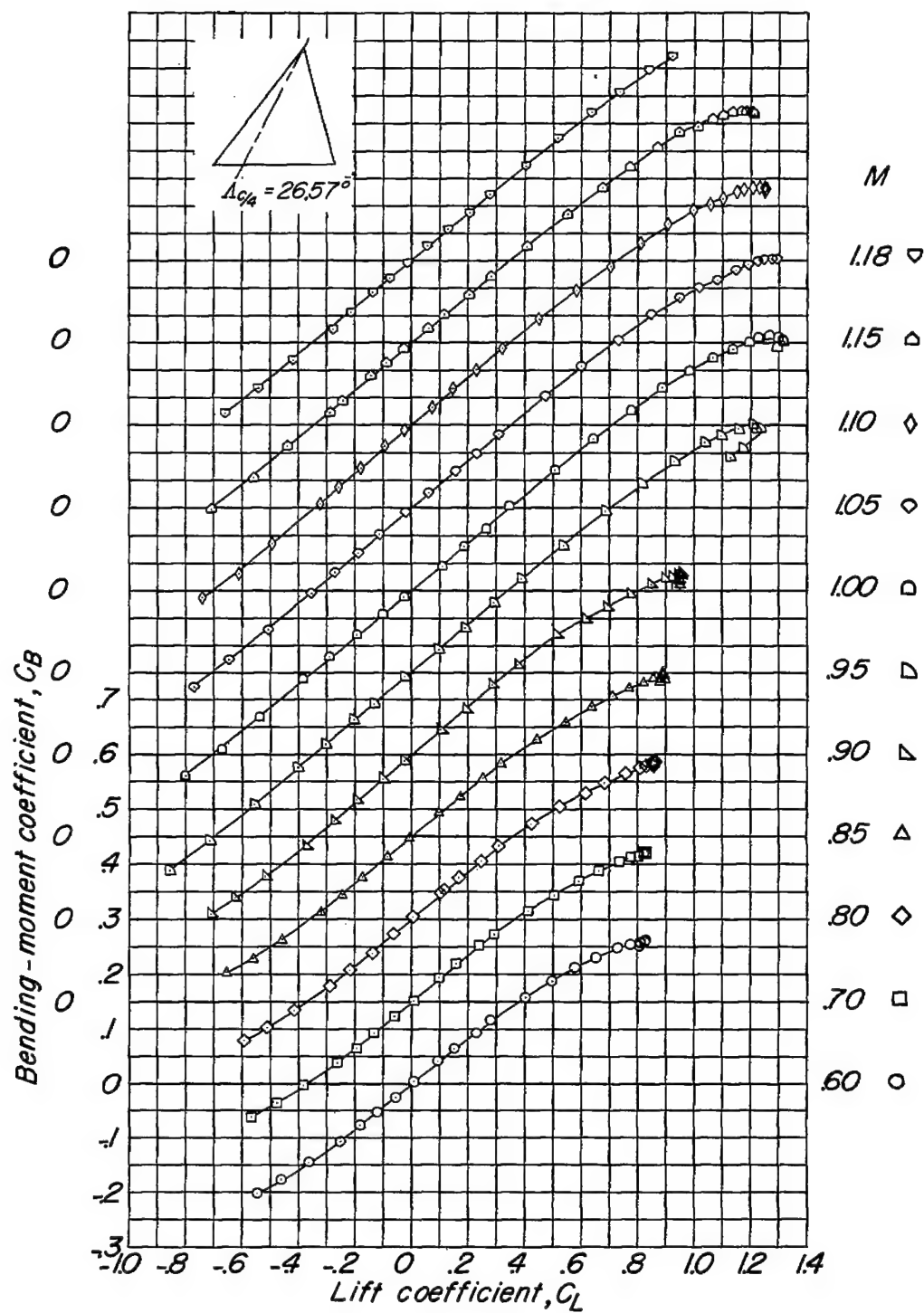
(d) Variation of C_B with C_L.

Figure 8.- Concluded.
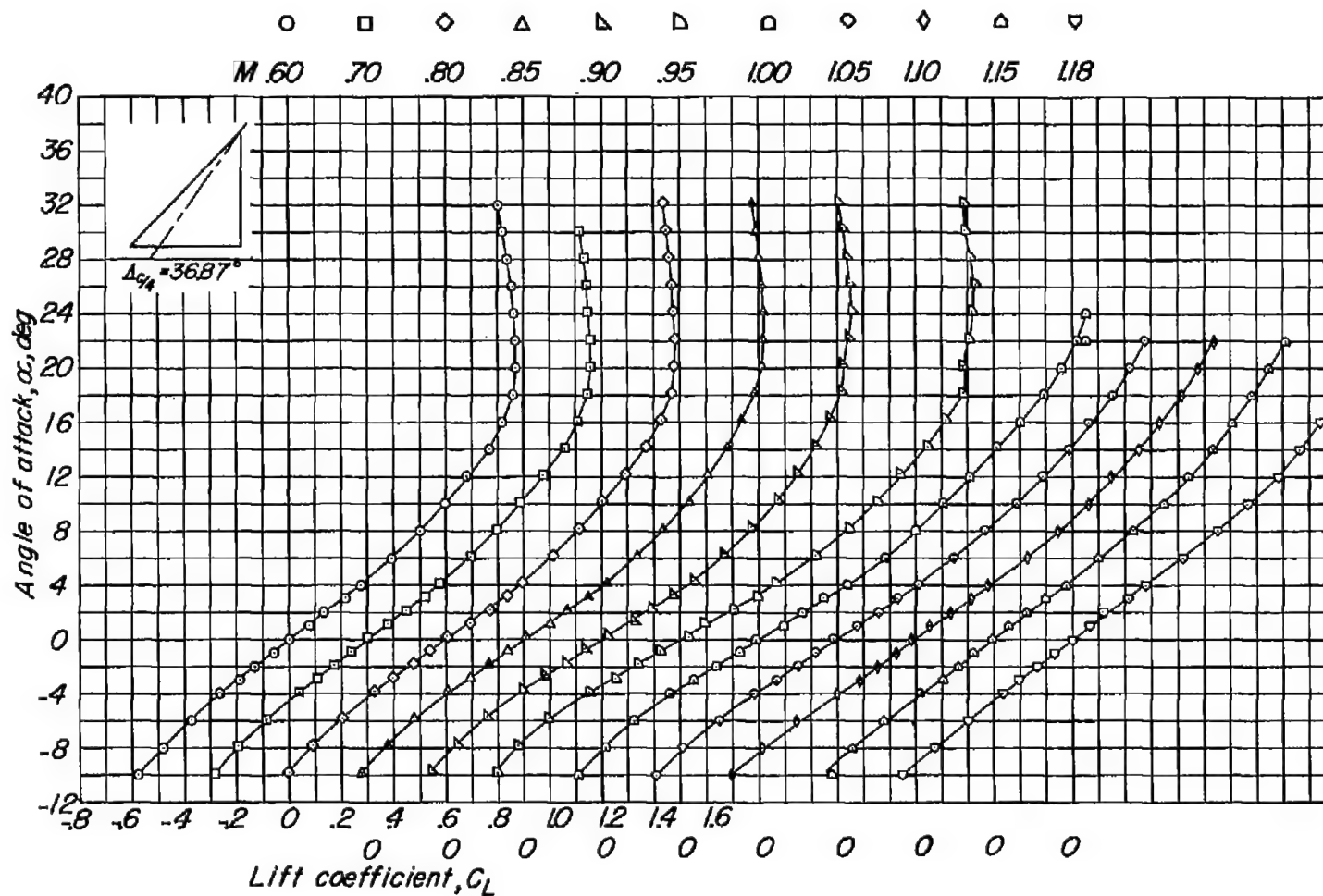
(a) Variation of α with C_L.

Figure 9.- Aerodynamic characteristics of a wing with 36.87° quarter-chord sweep; aspect ratio 4; taper ratio 0; and an NACA 65A003 airfoil section.
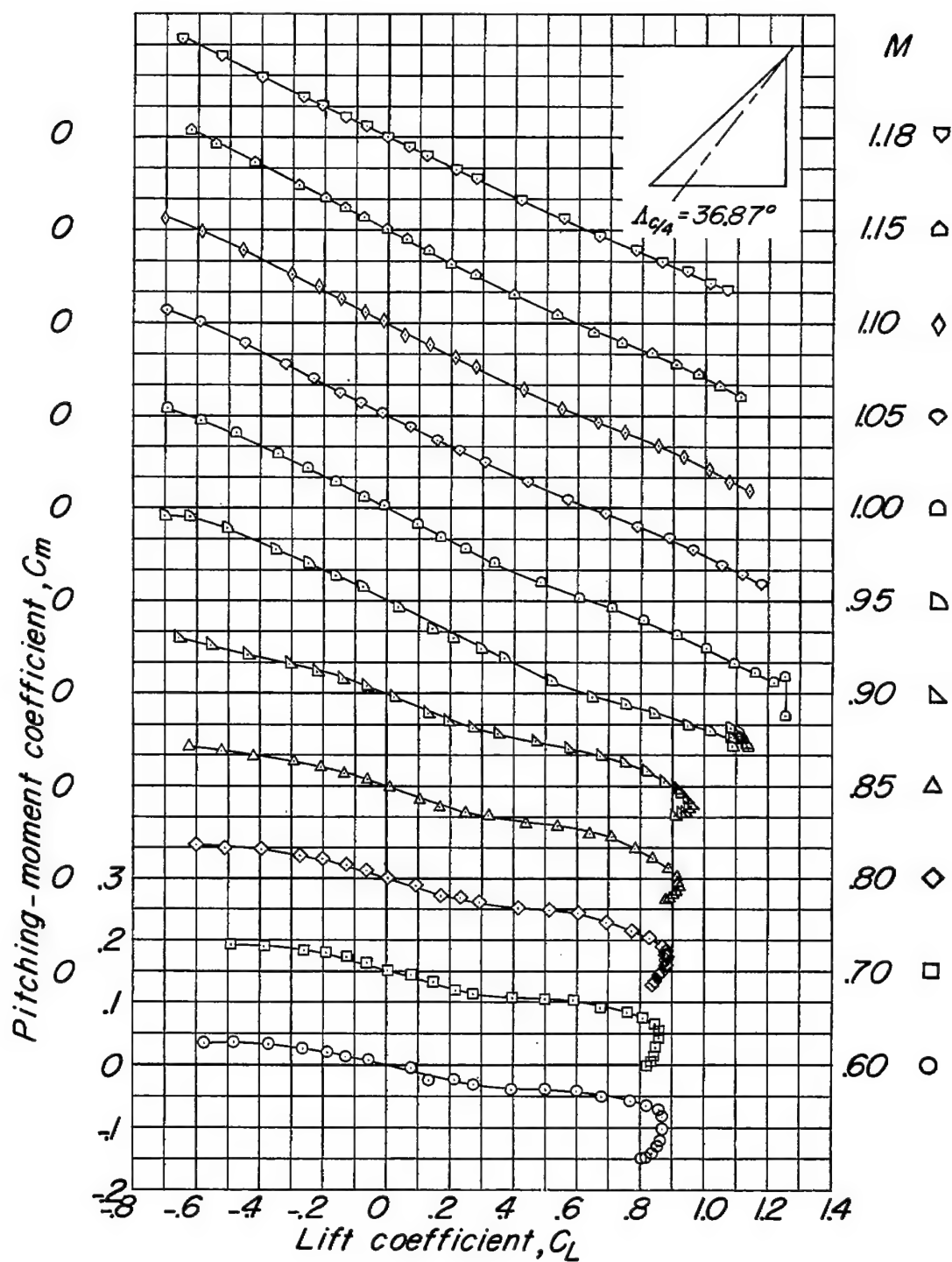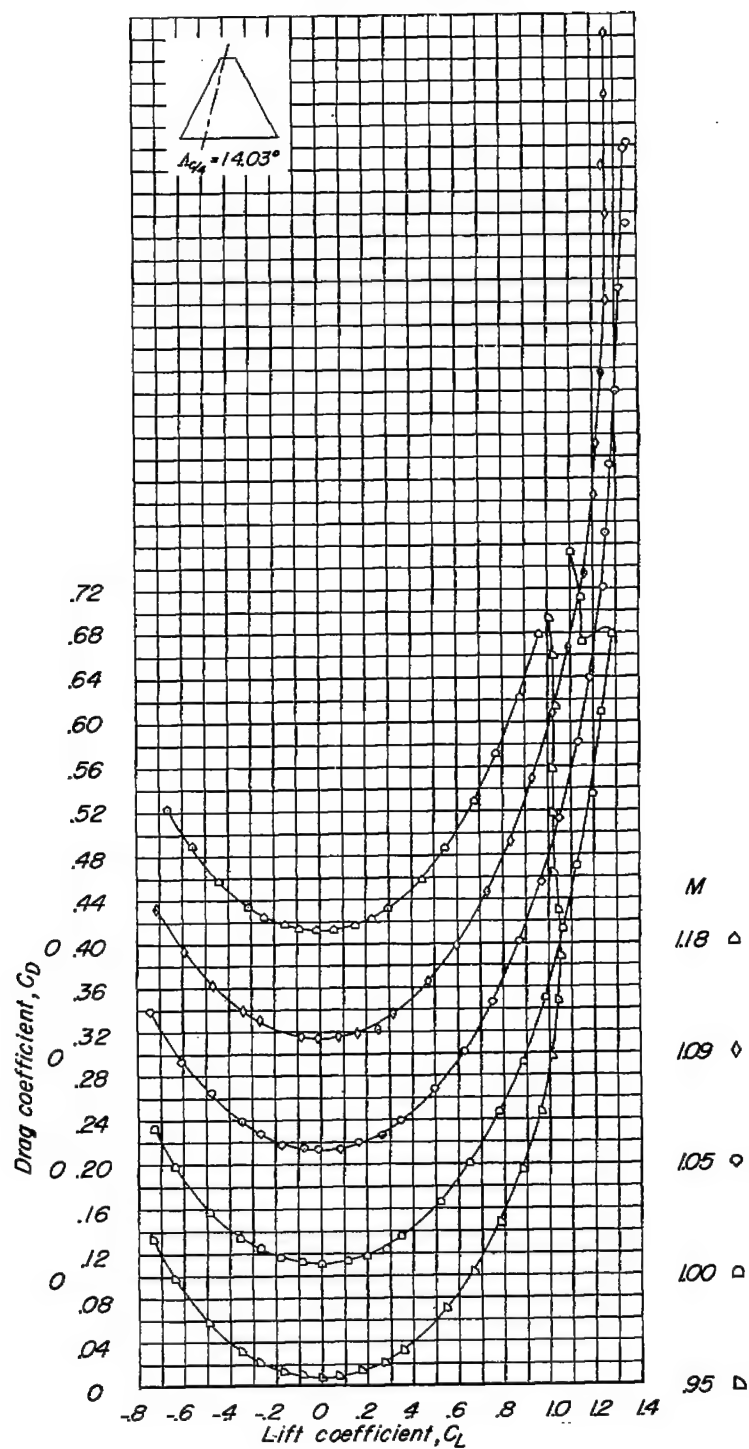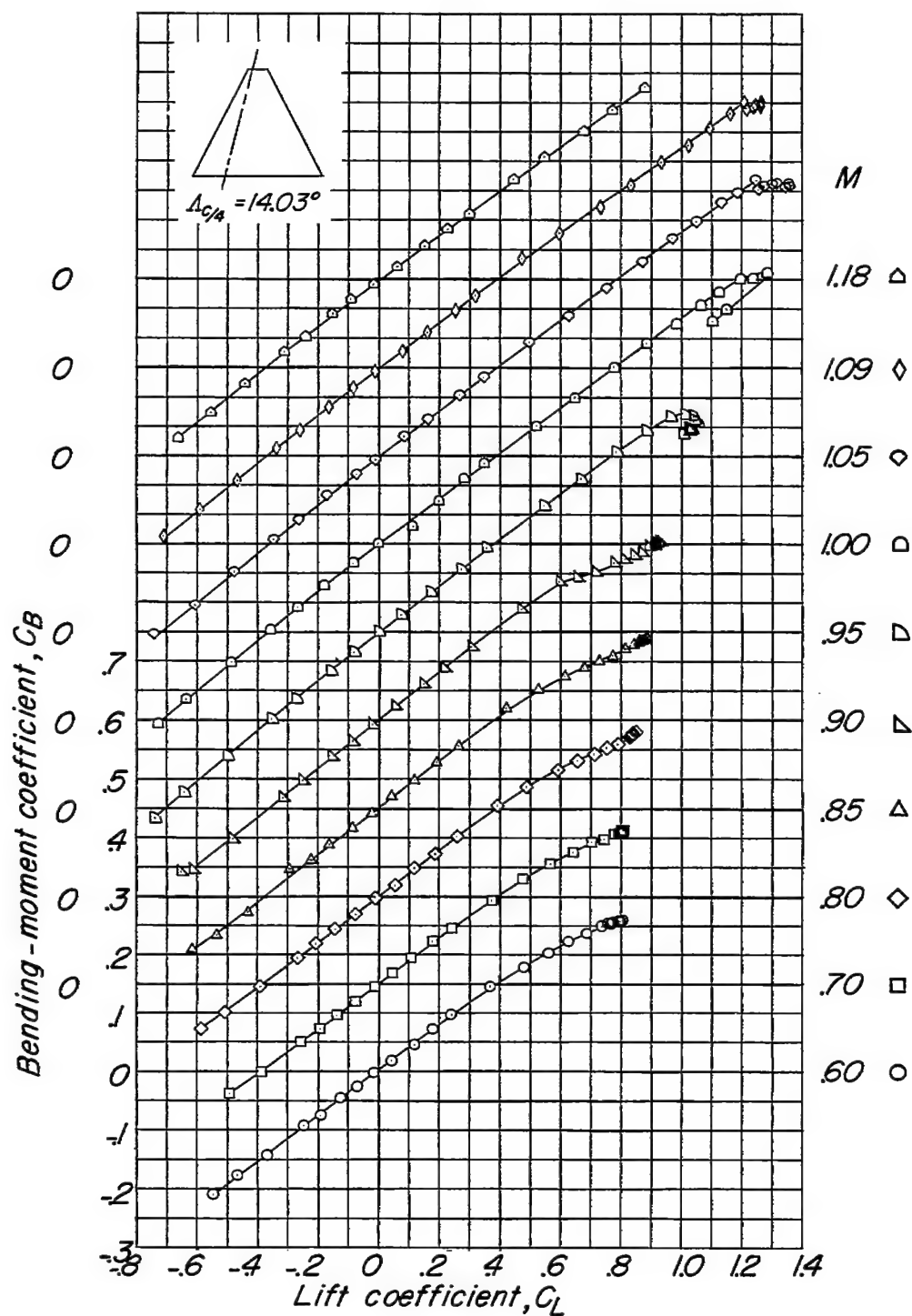
(b) Variation of C_m with C_L.

Figure 9.- Continued.
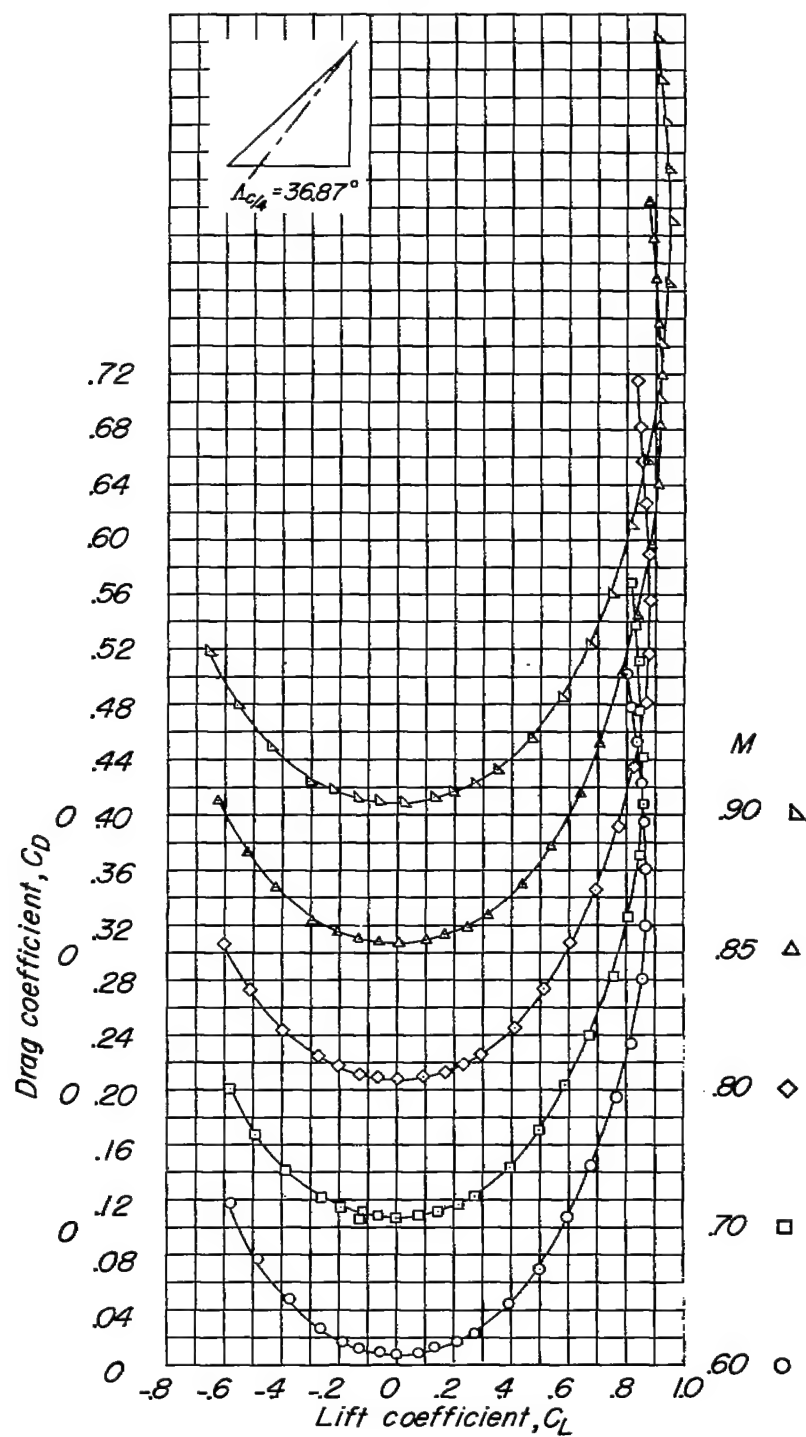
(c) Variation of C_D with C_L.

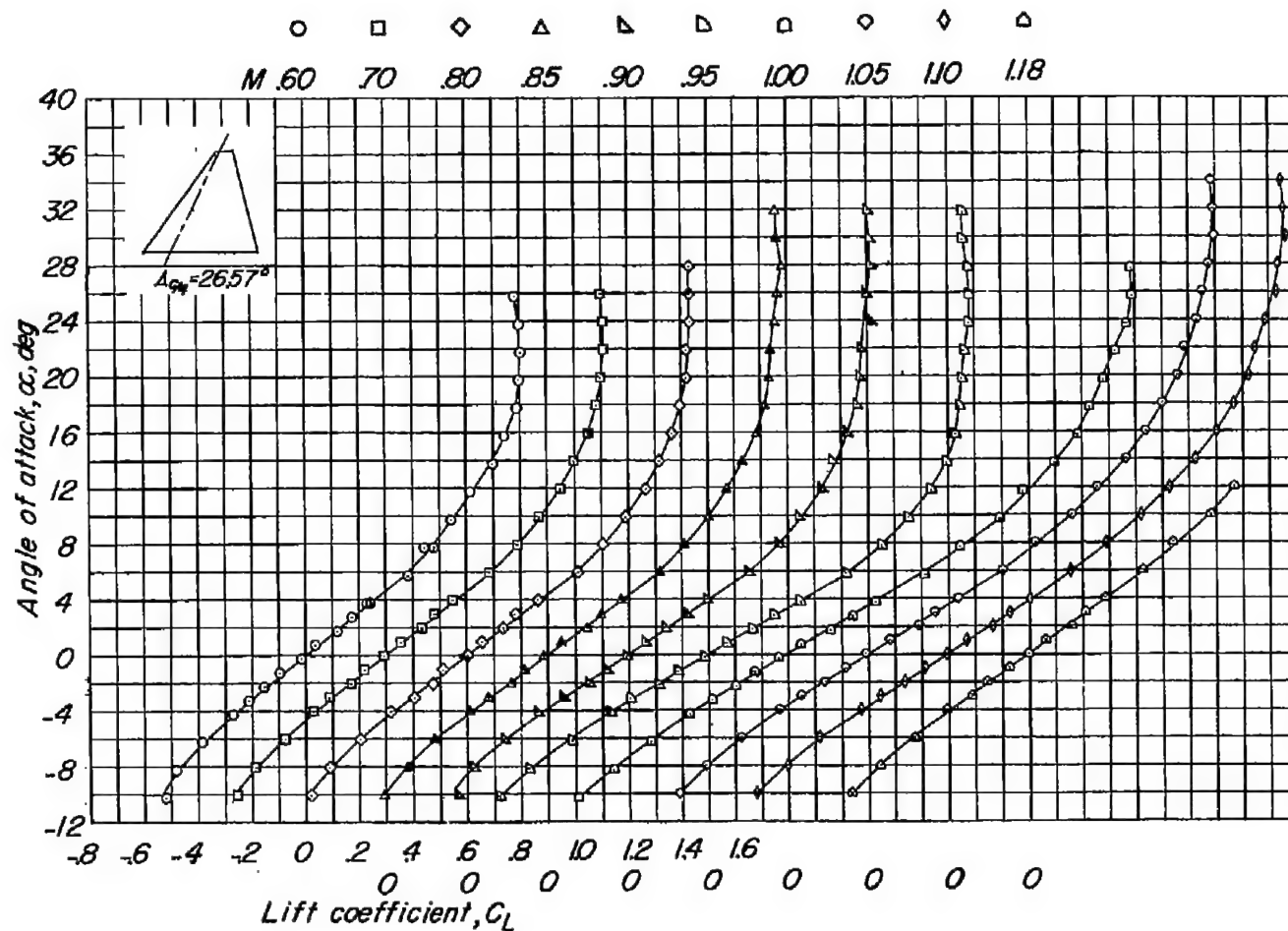Figure 9.- Continued.
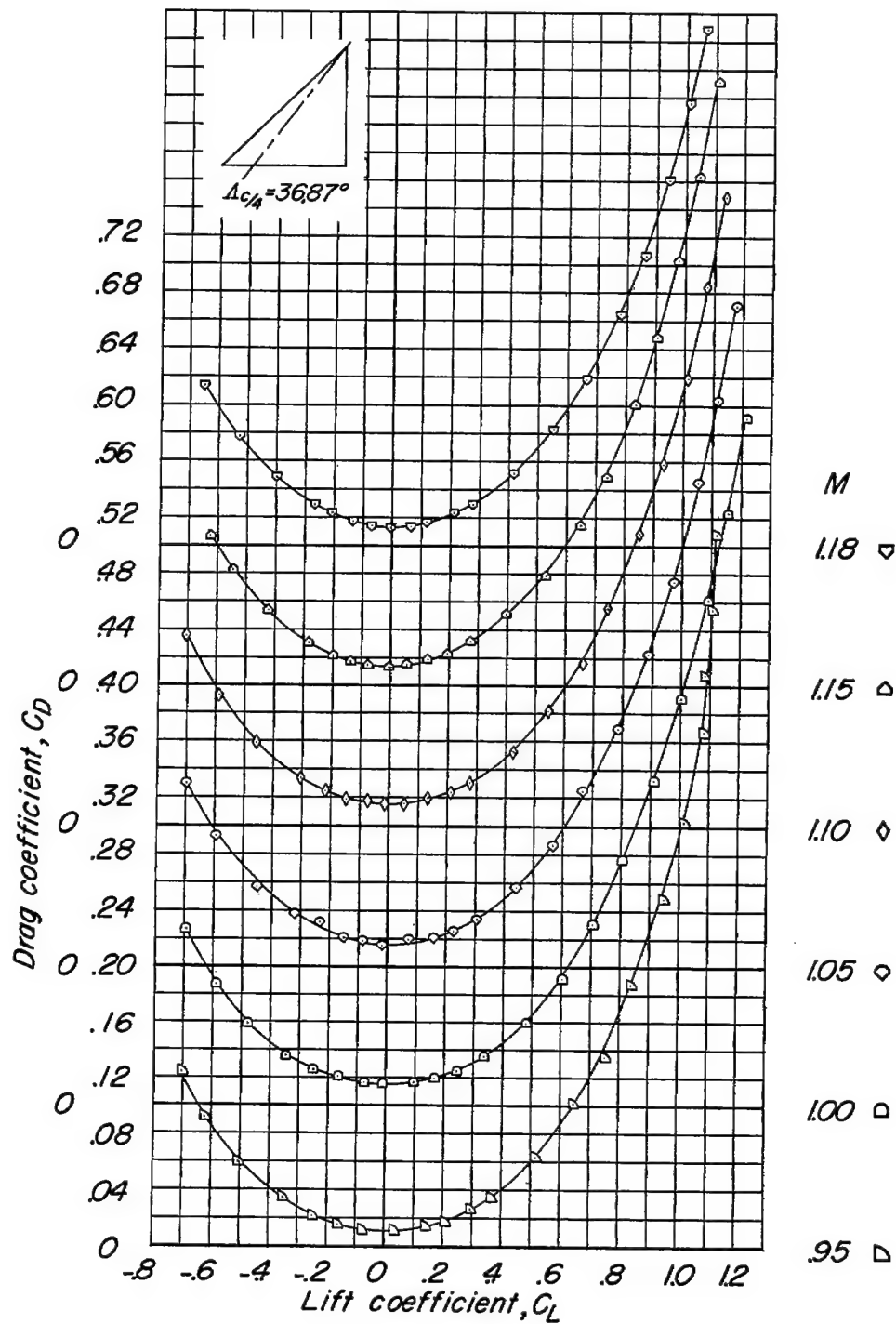
(c) Concluded.

Figure 9.- Continued.
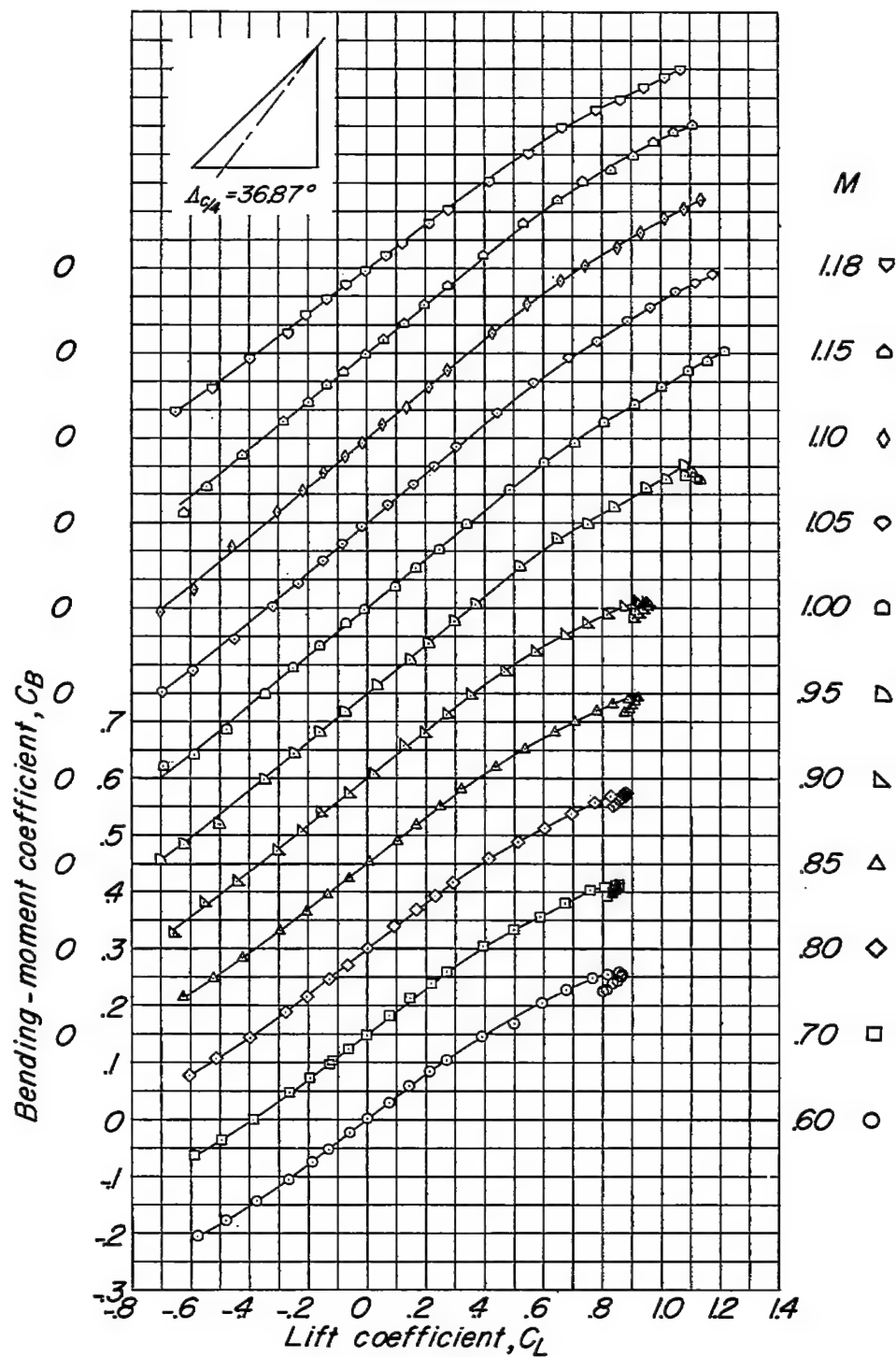
(d) Variation of C_B with C_L.

Figure 9.- Concluded.
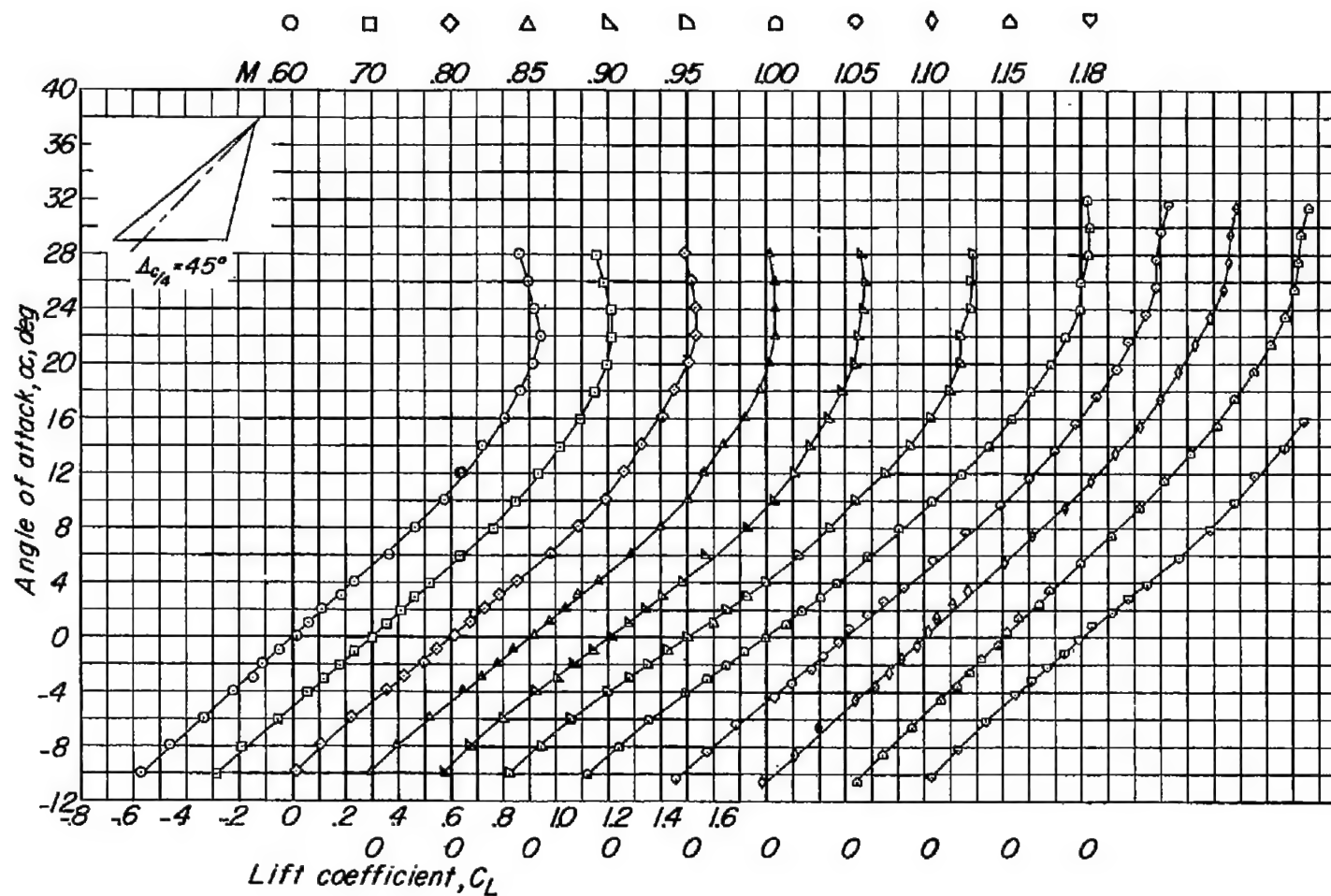
(a) Variation of α with C_L.

Figure 10.- Aerodynamic characteristics of a wing with 45° quarter-chord sweep; aspect ratio 4; taper ratio 0; and an NACA 65A003 airfoil section.
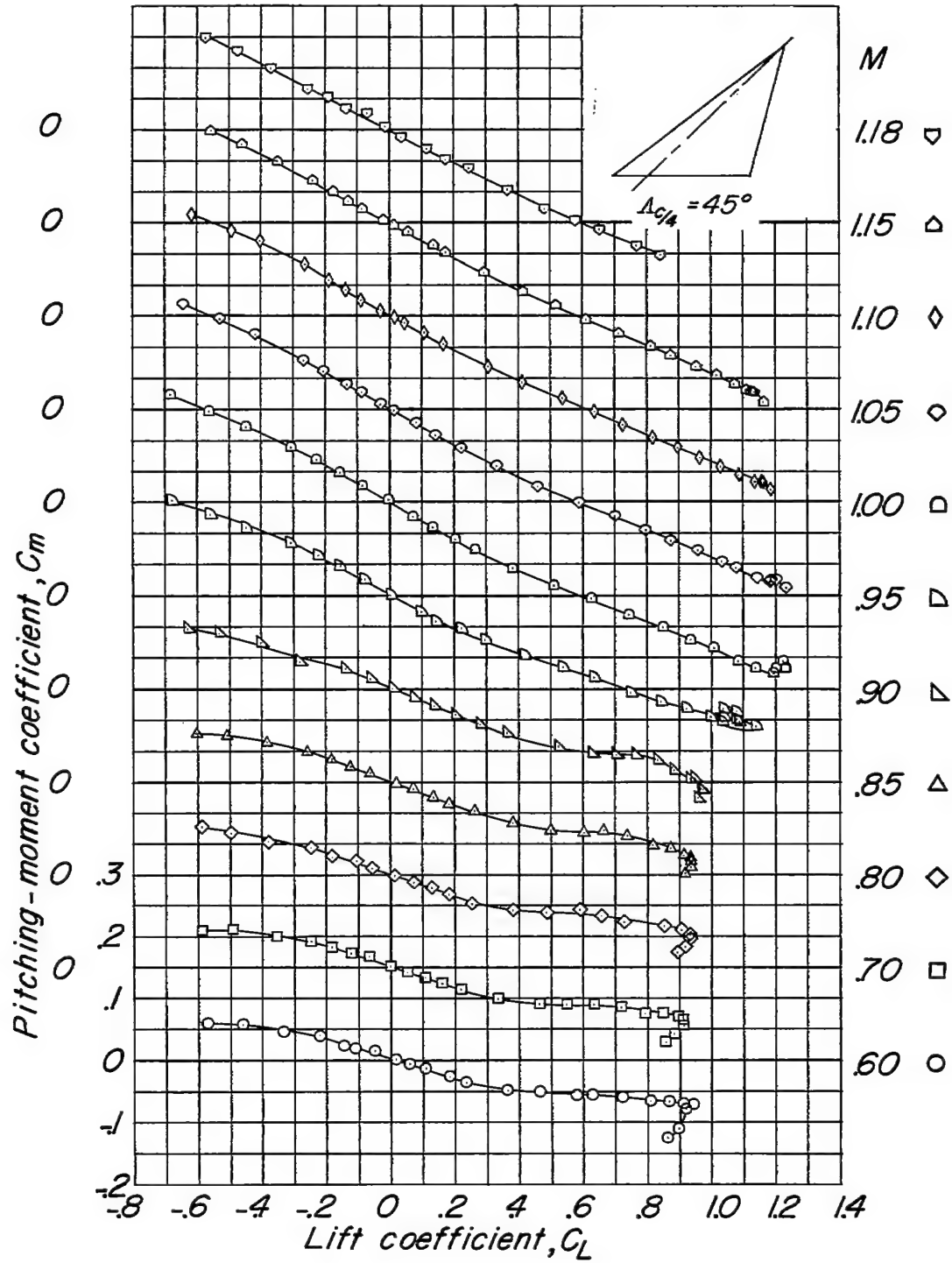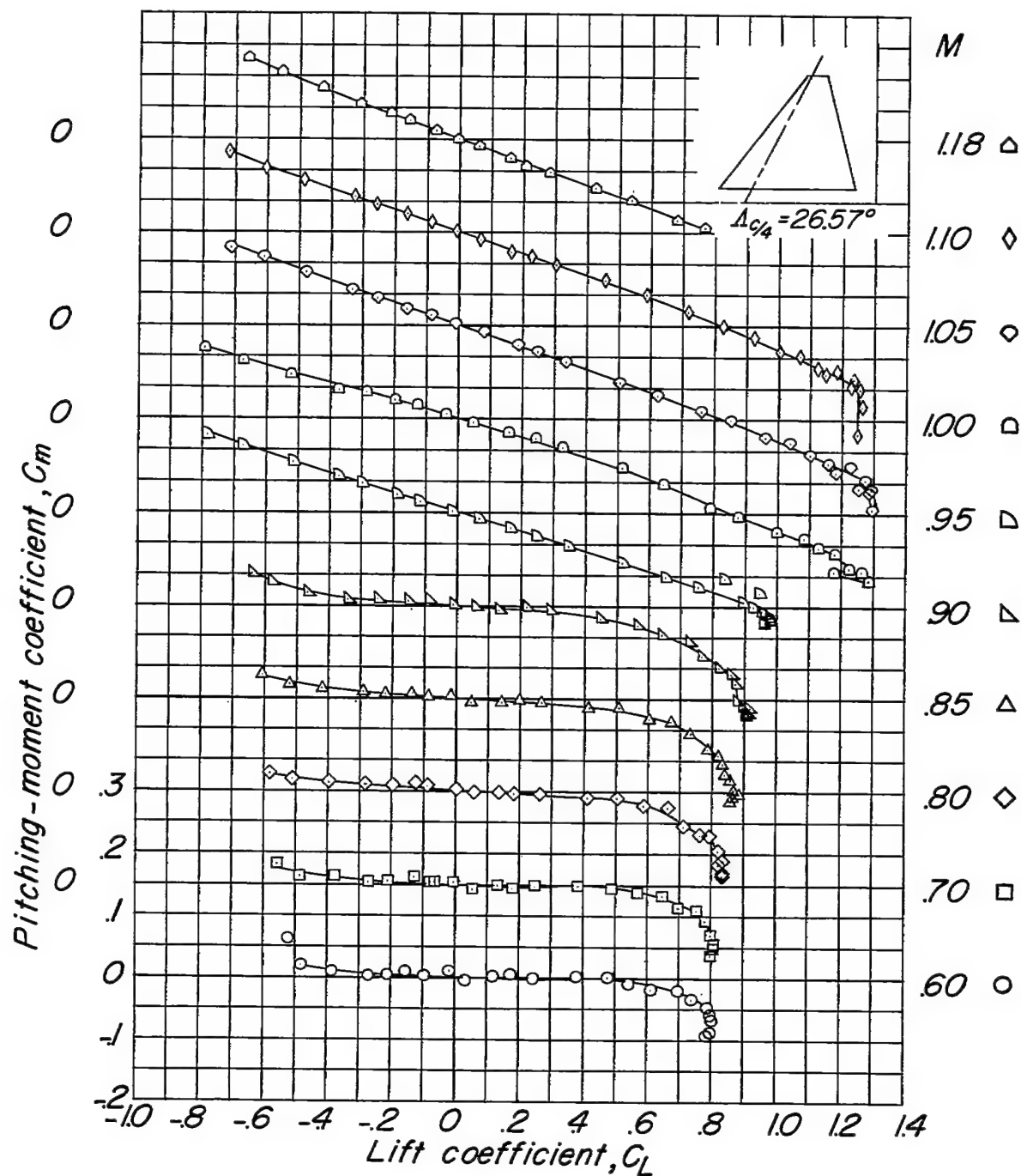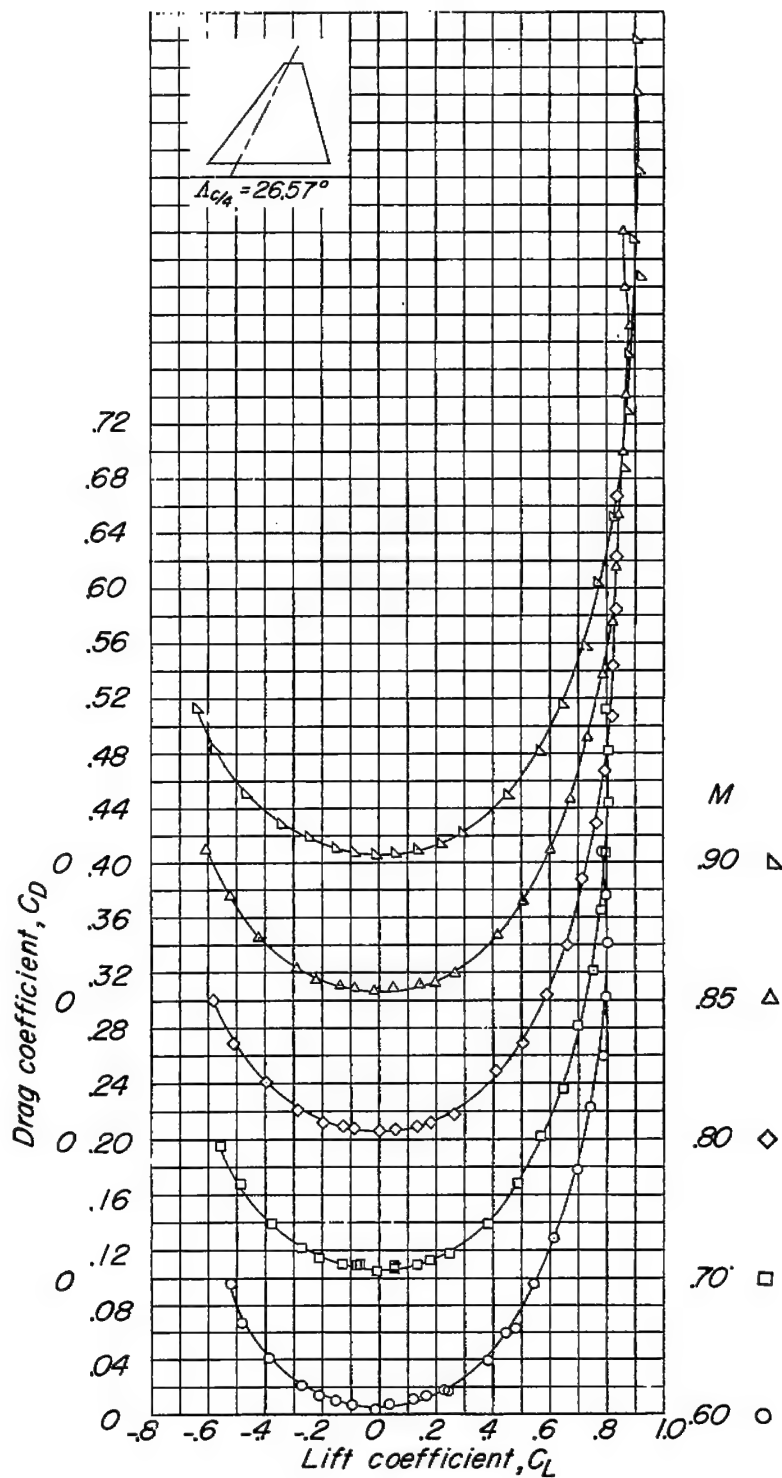
(b) Variation of C_m with C_L.

Figure 10.- Continued.
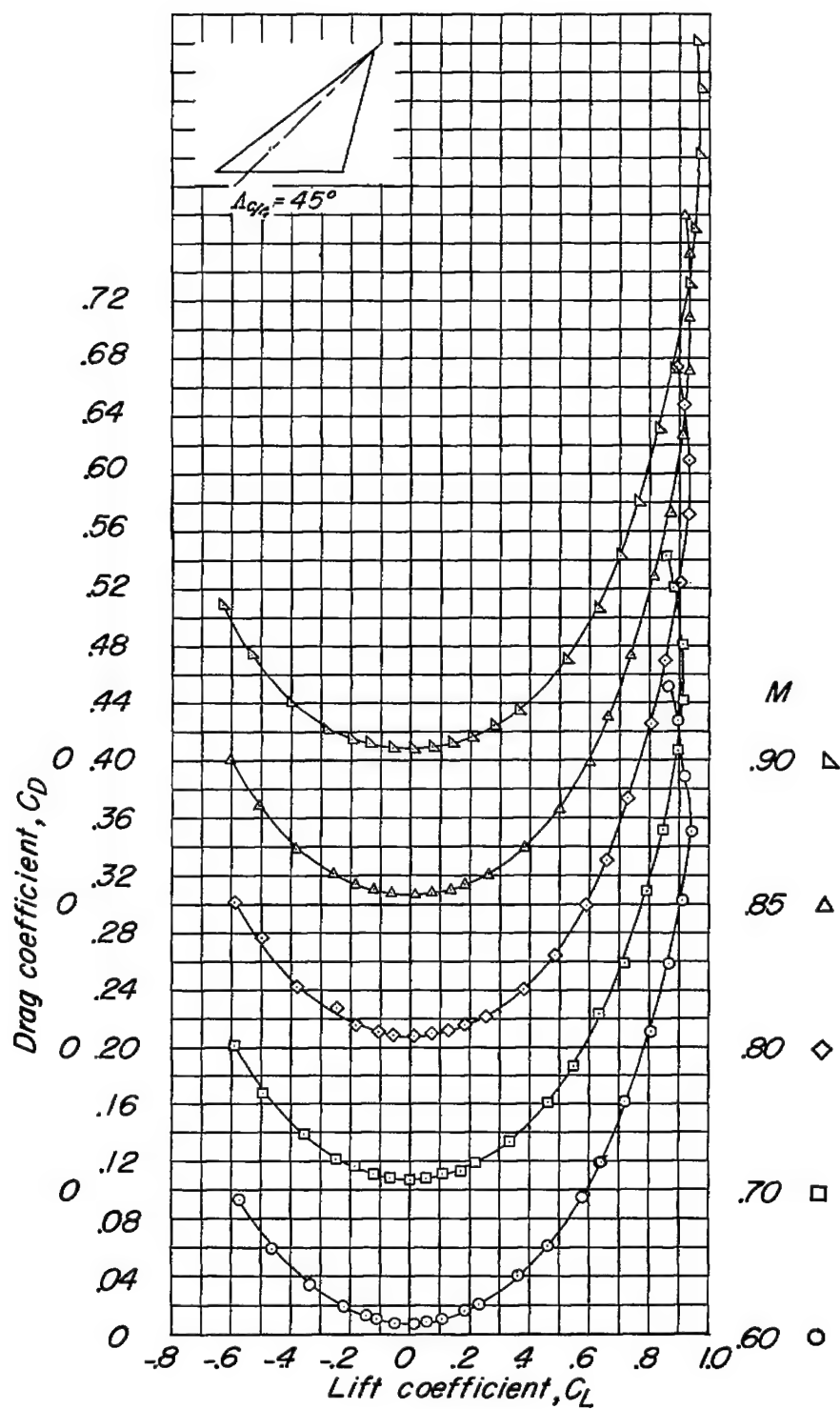
(c) Variation of C_D with C_L.

Figure 10.- Continued.
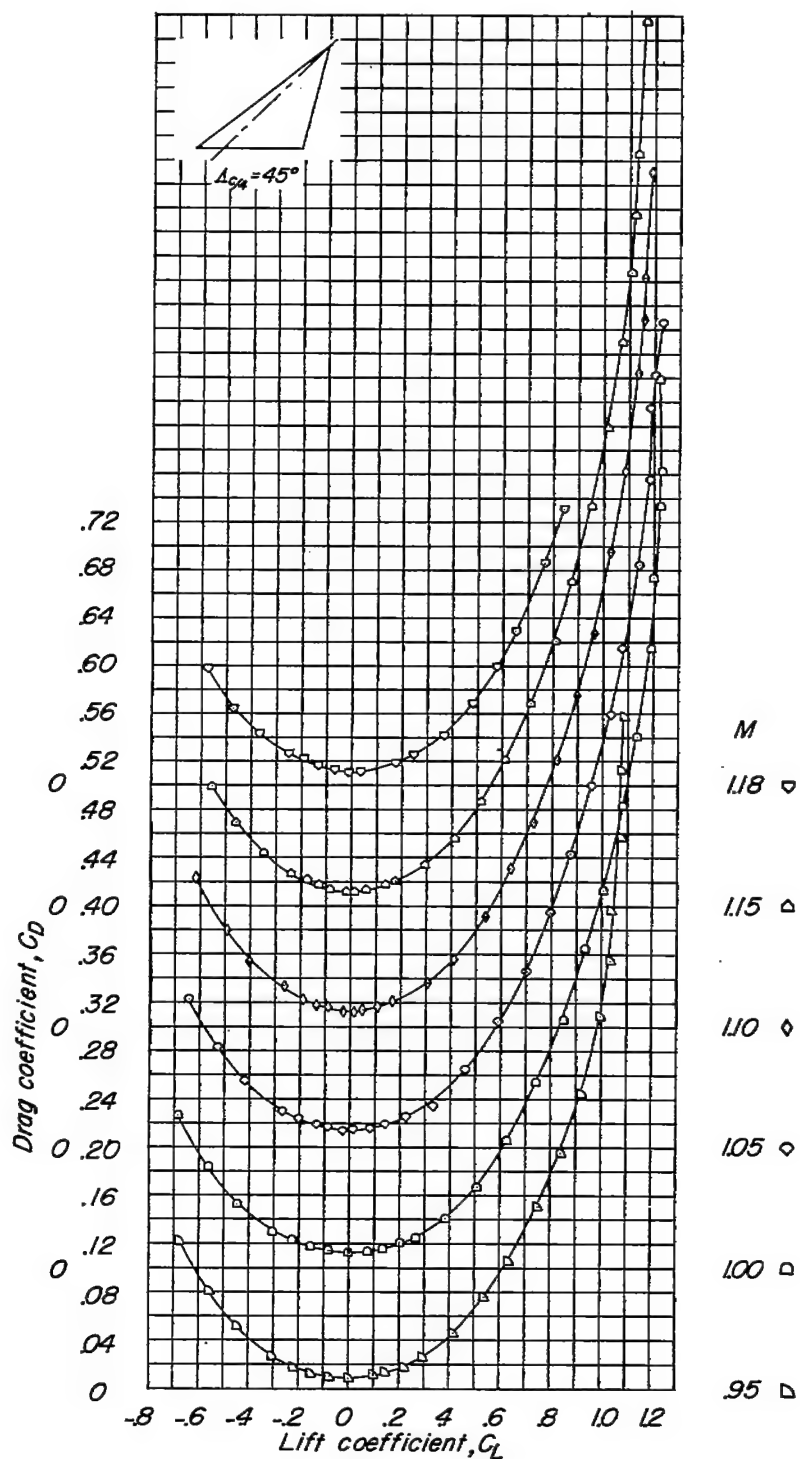
(c) Concluded.

Figure 10.- Continued.
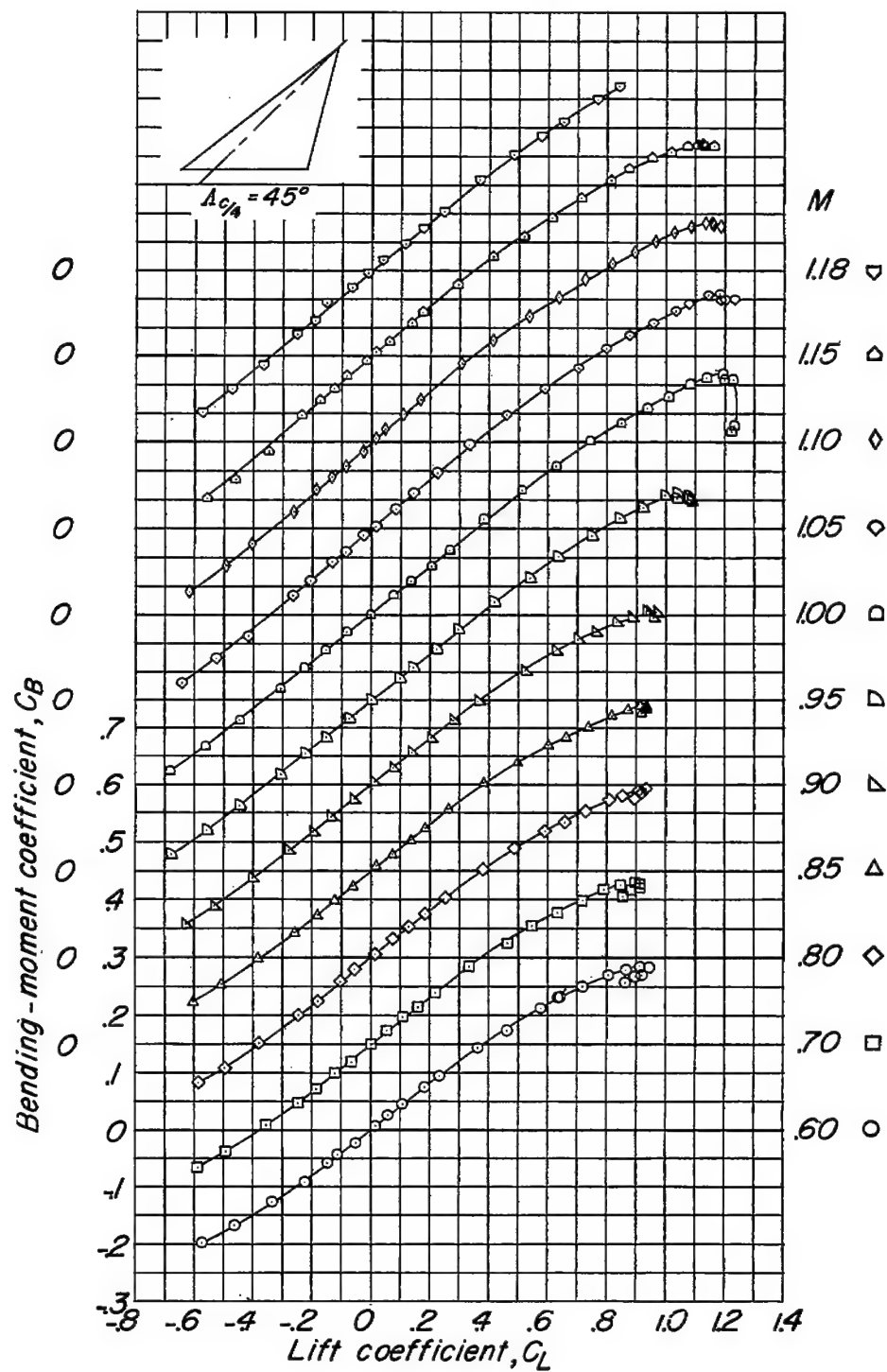
(d) Variation of C_B with C_L.

Figure 10.- Concluded.
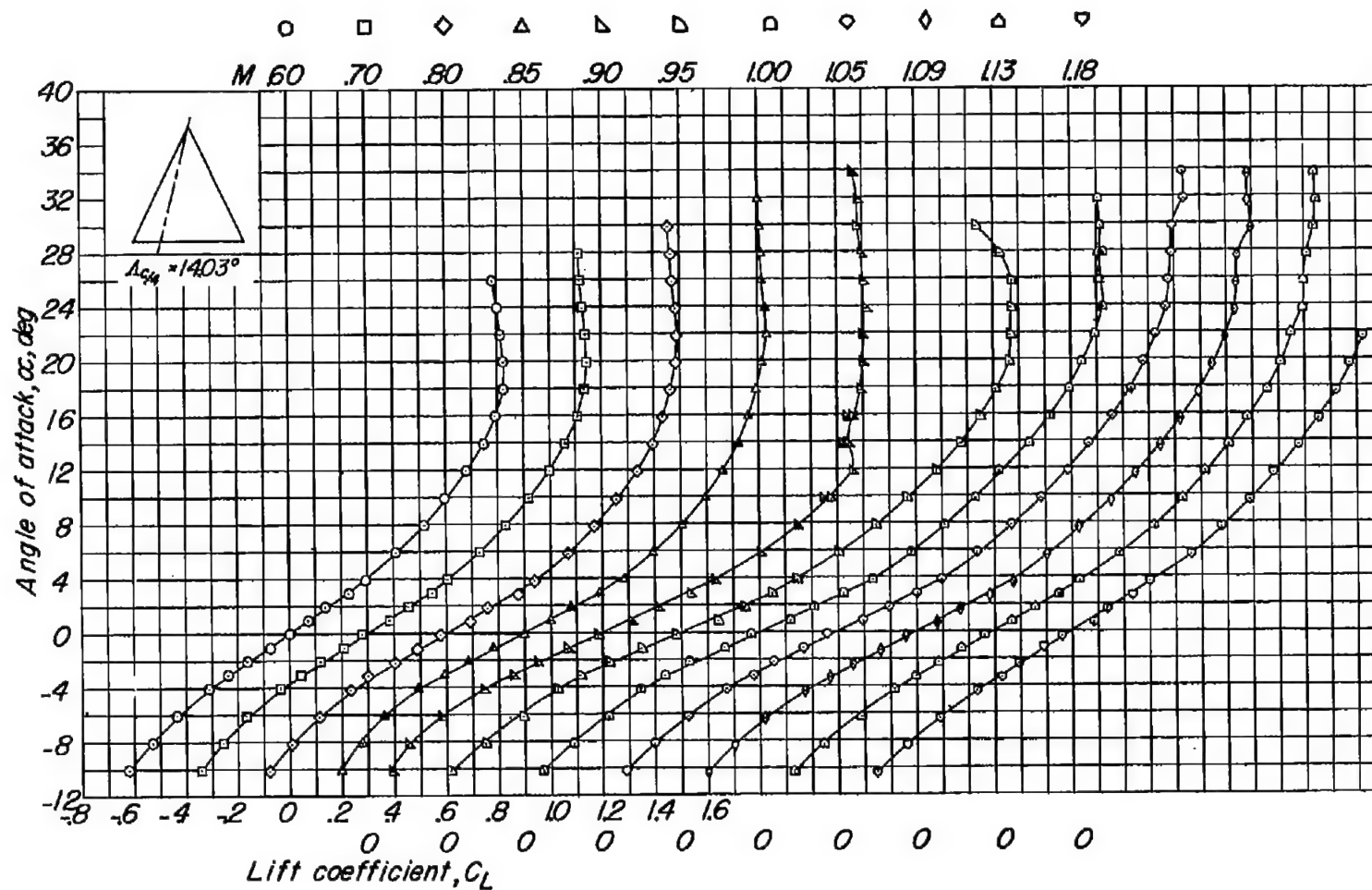
(a) Variation of α with C_L.

Figure 11.- Aerodynamic characteristics of a wing with 14.03° quarter-chord sweep; aspect ratio 4; taper ratio 0; and an NACA 65A002 airfoil section.
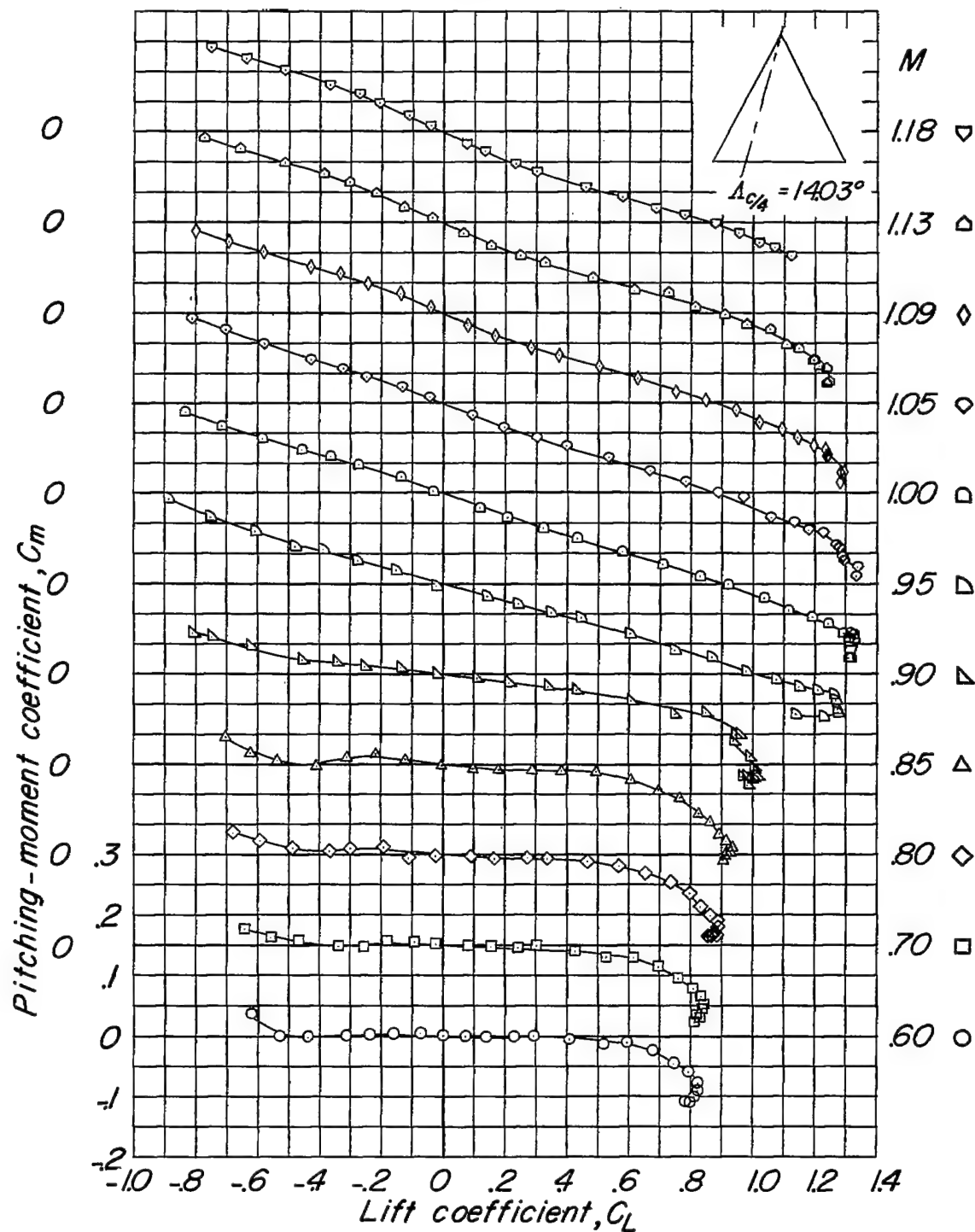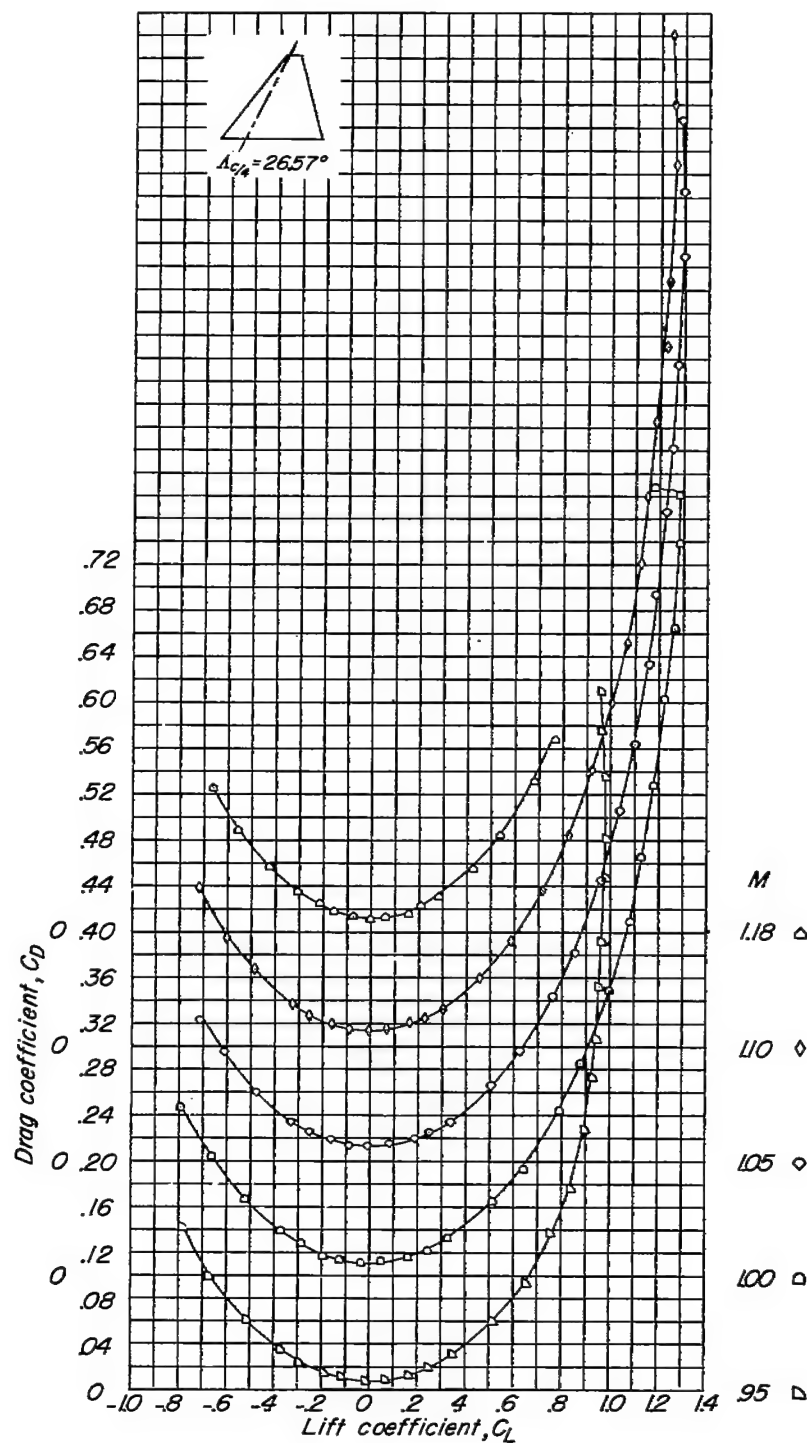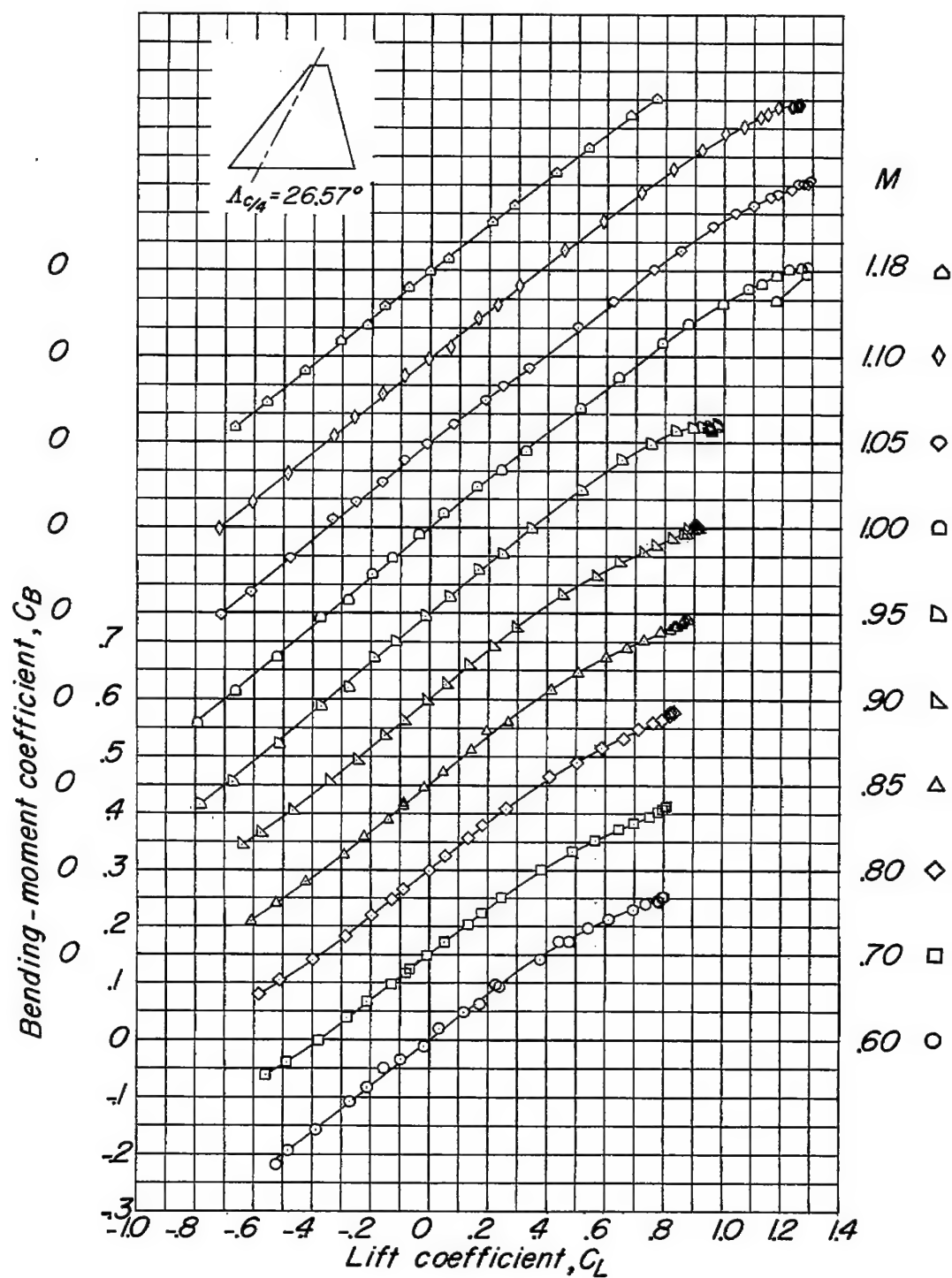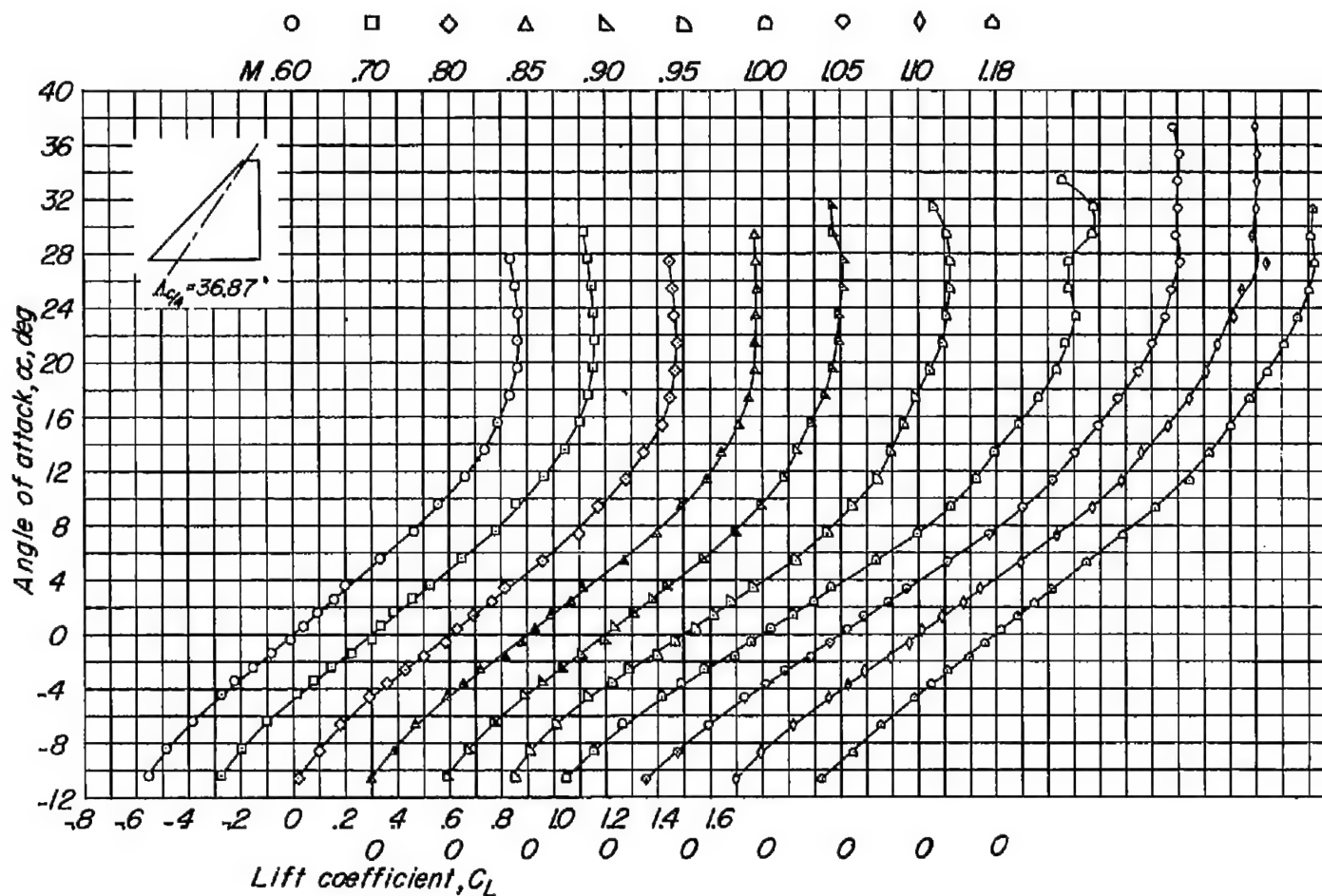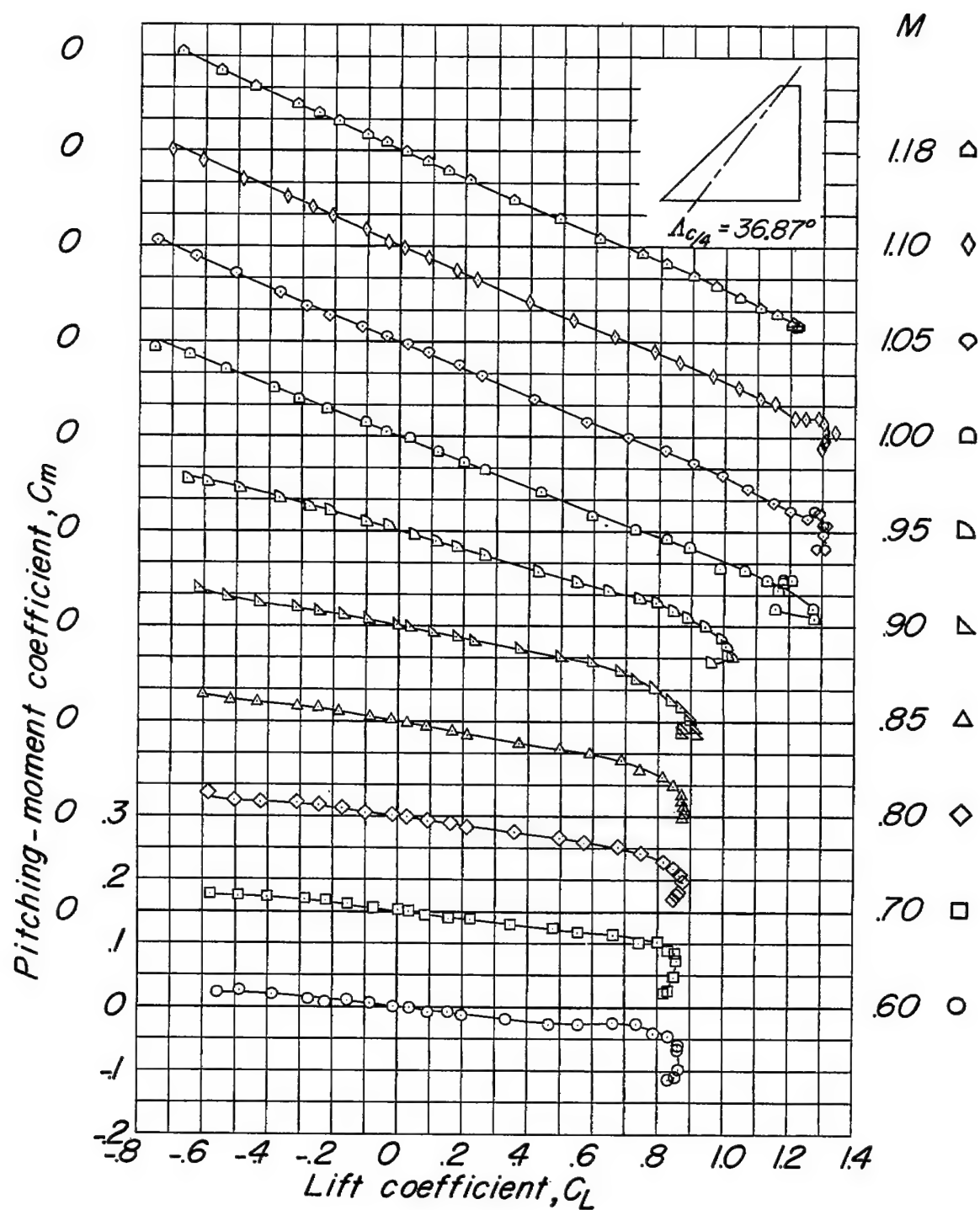
(b) Variation of C_m with C_L.

Figure 11.- Continued.
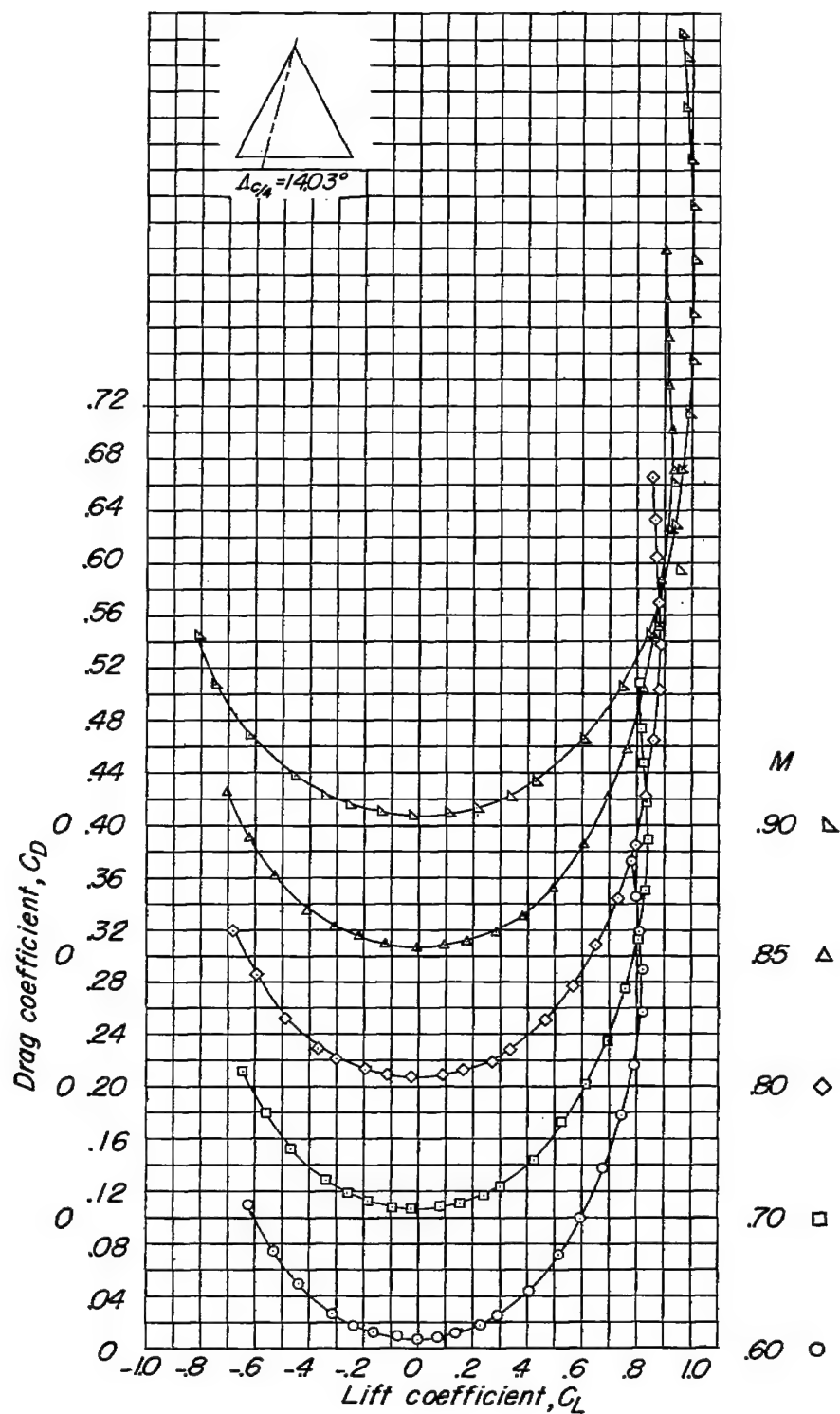
(c) Variation of C_D with C_L.

Figure 11.- Continued.
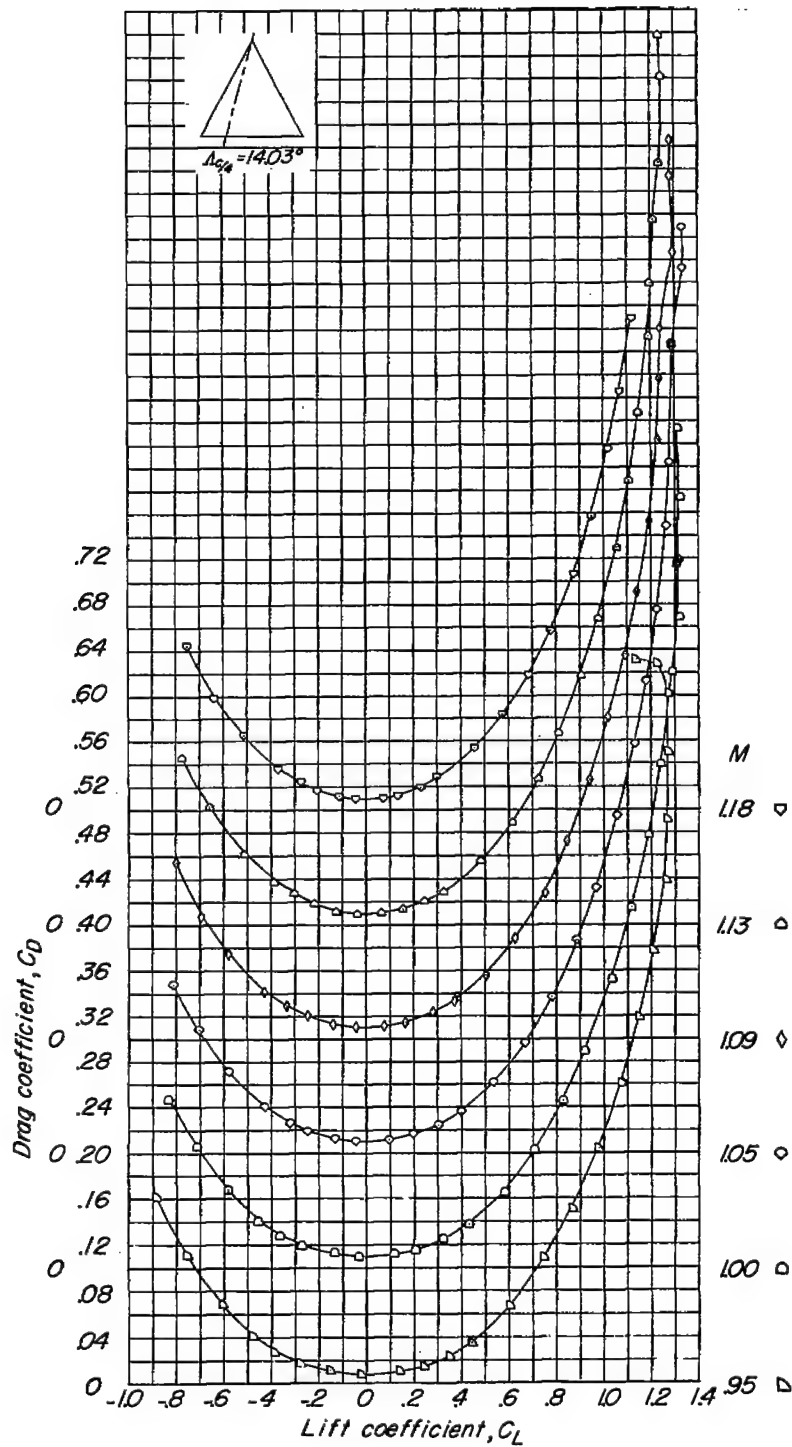
(c) Concluded.

Figure 11.- Continued.

$\Lambda_{c/4} = 14.03°$

M

1.18 ▽

1.13 △

1.09 ◊

1.05 ◇

1.00 ◻

.95 ◁

.90 ◁

.85 △

.80 ◇

.70 ◻

.60 ○

Bending-moment coefficient, C_B

Lift coefficient, C_L
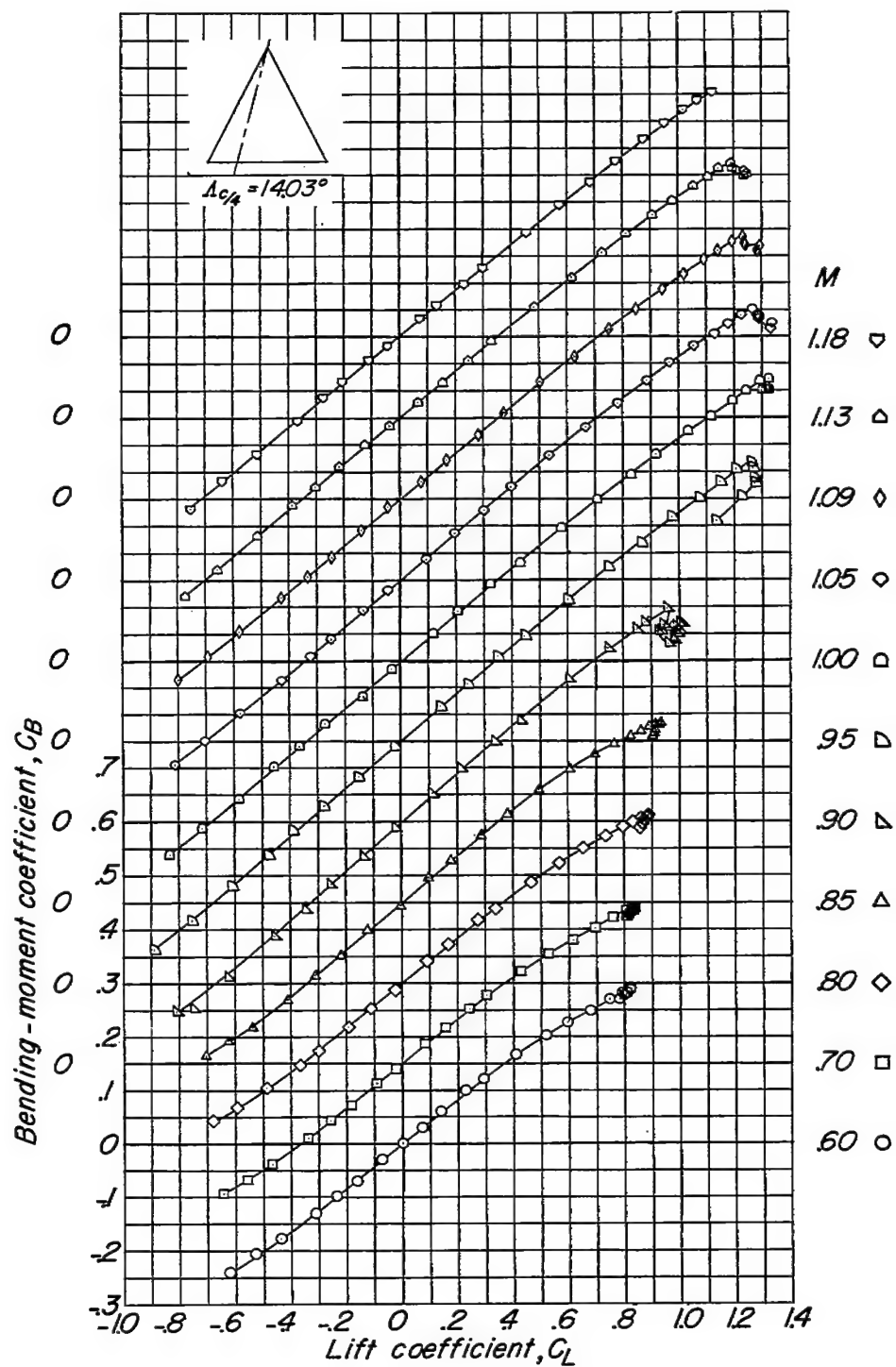
(d) Variation of C_B with C_L.

Figure 11.- Concluded.
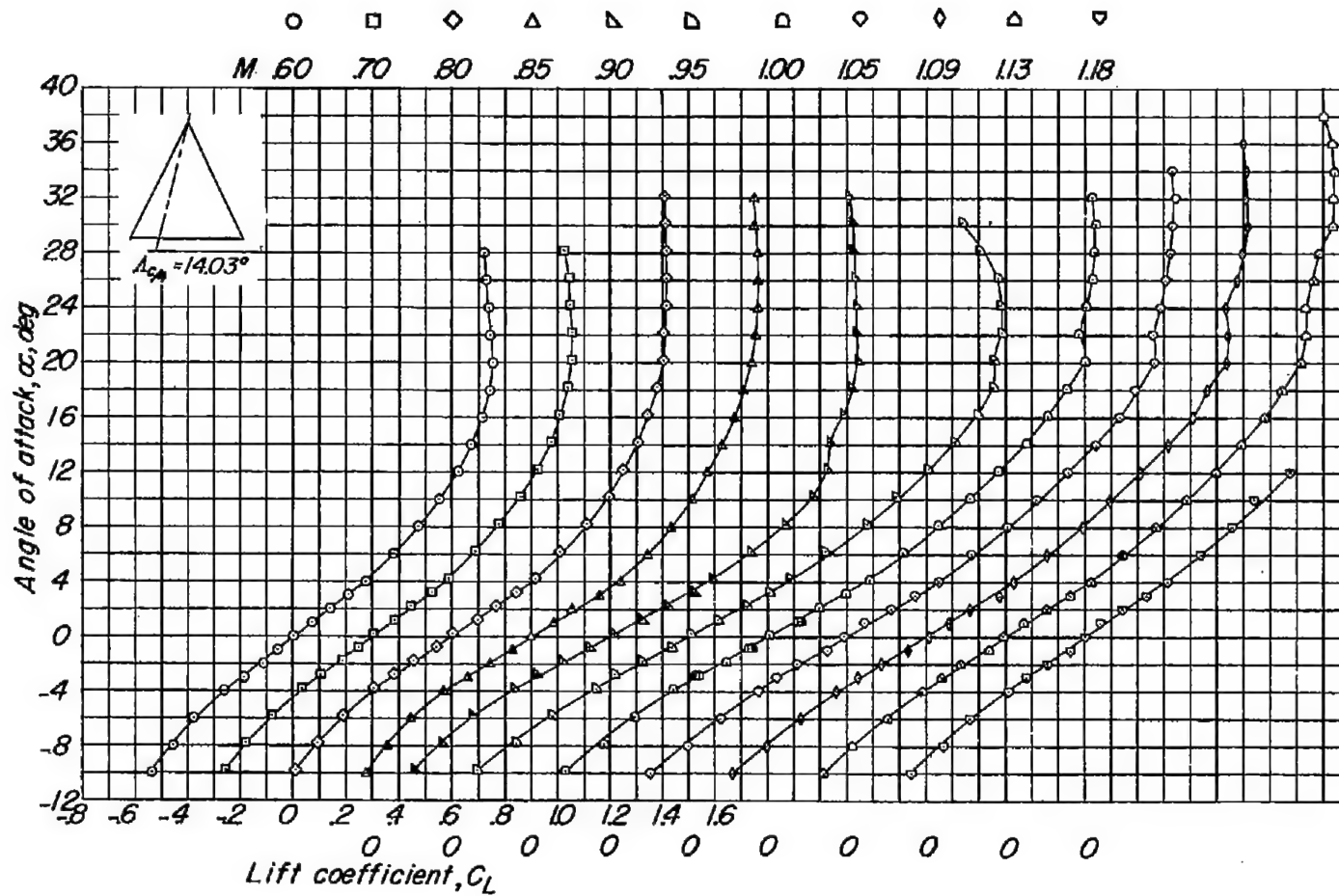
(a) Variation of α with C_L.

Figure 12.- Aerodynamic characteristics of a wing with 14.03° quarter-
chord sweep; aspect ratio 4; taper ratio 0; and an NACA 65A004.5 air-
foil section.
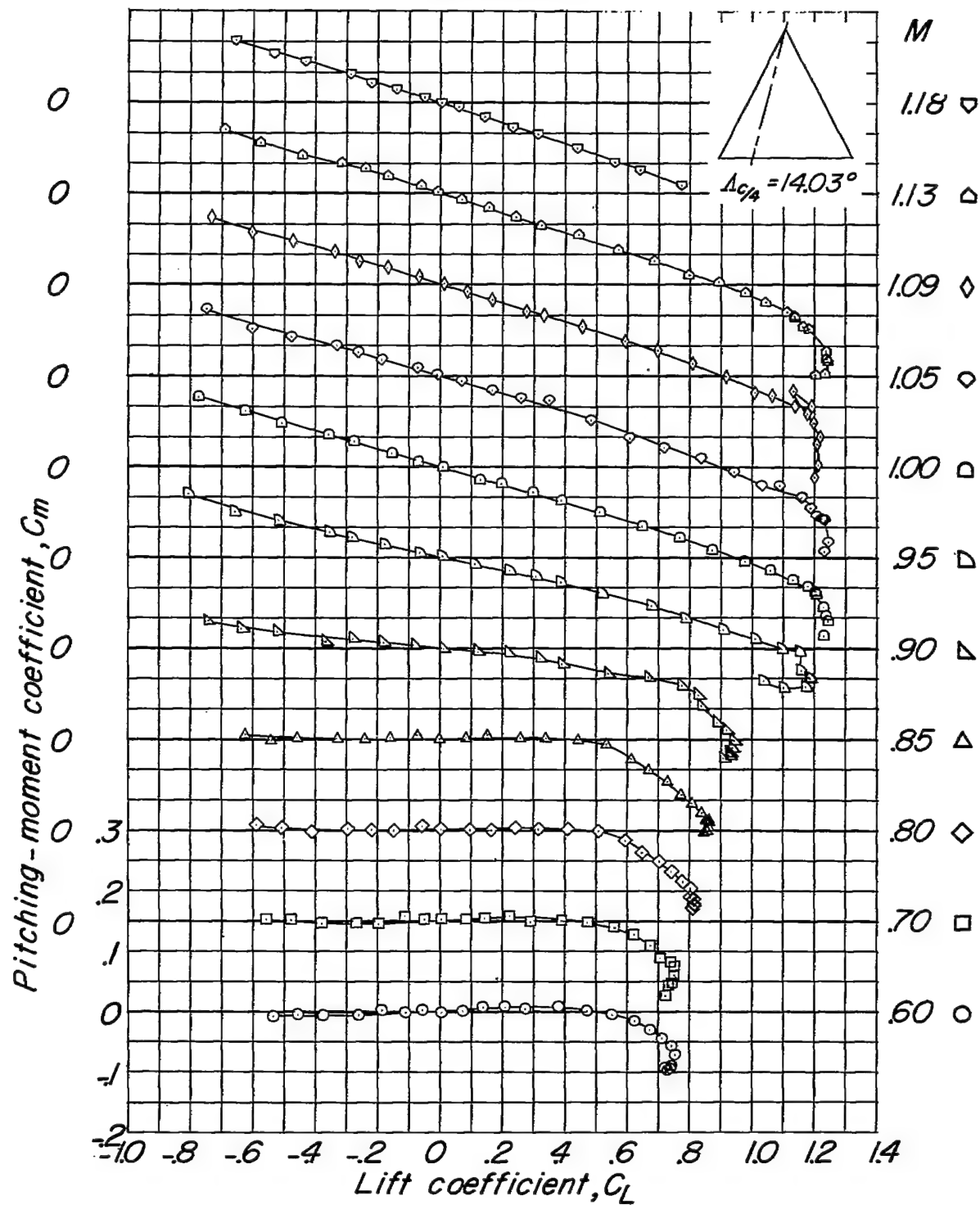
(b) Variation of C_m with C_L.
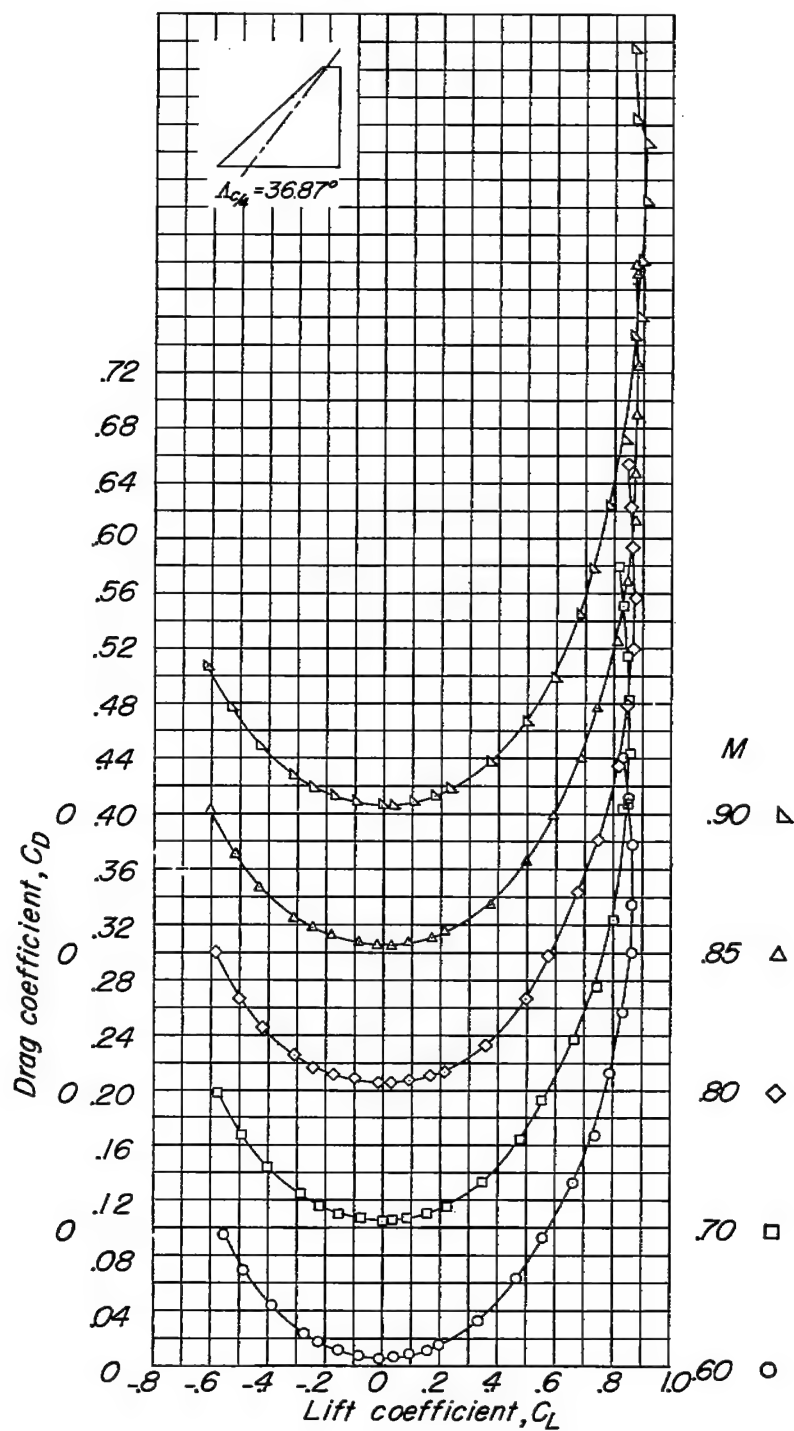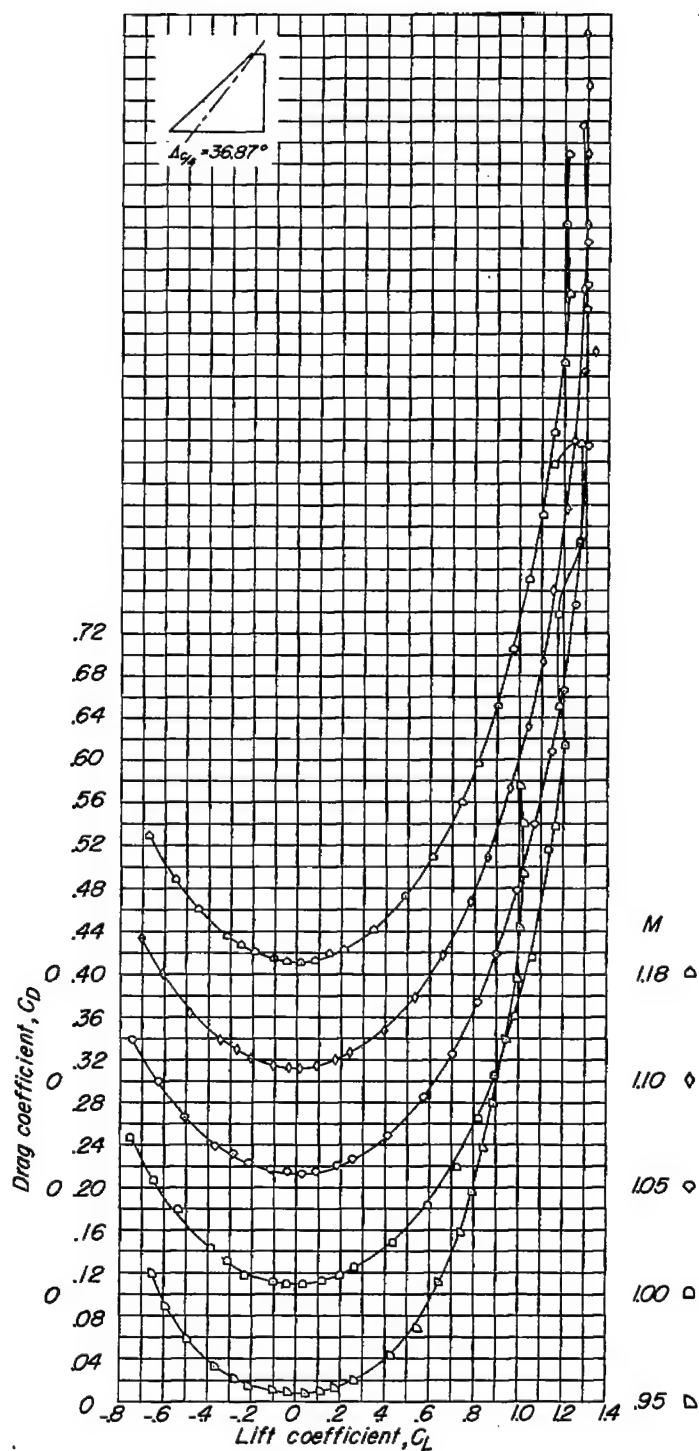
Figure 12.- Continued.
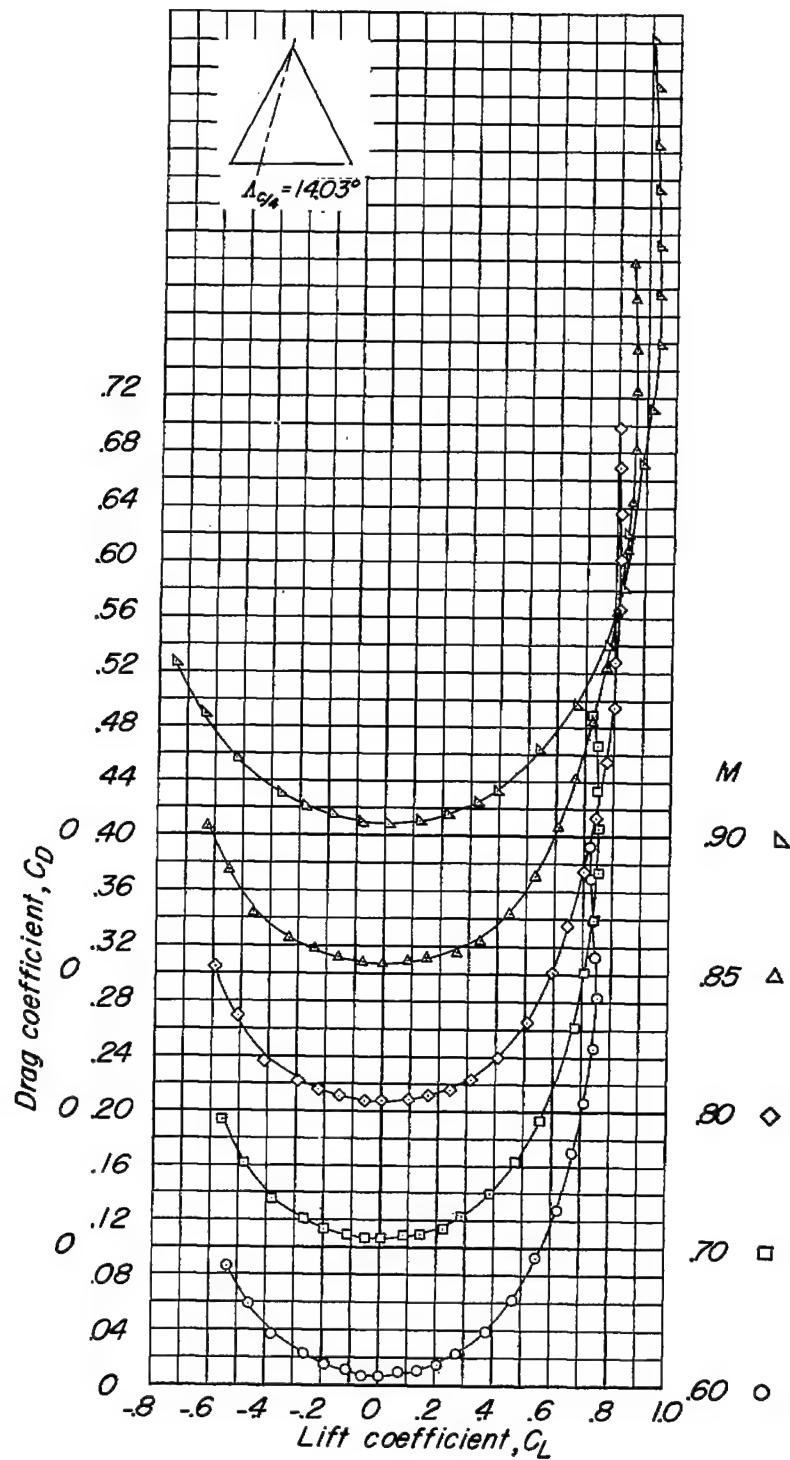
(c) Variation of C_D with C_L.

Figure 12.- Continued.
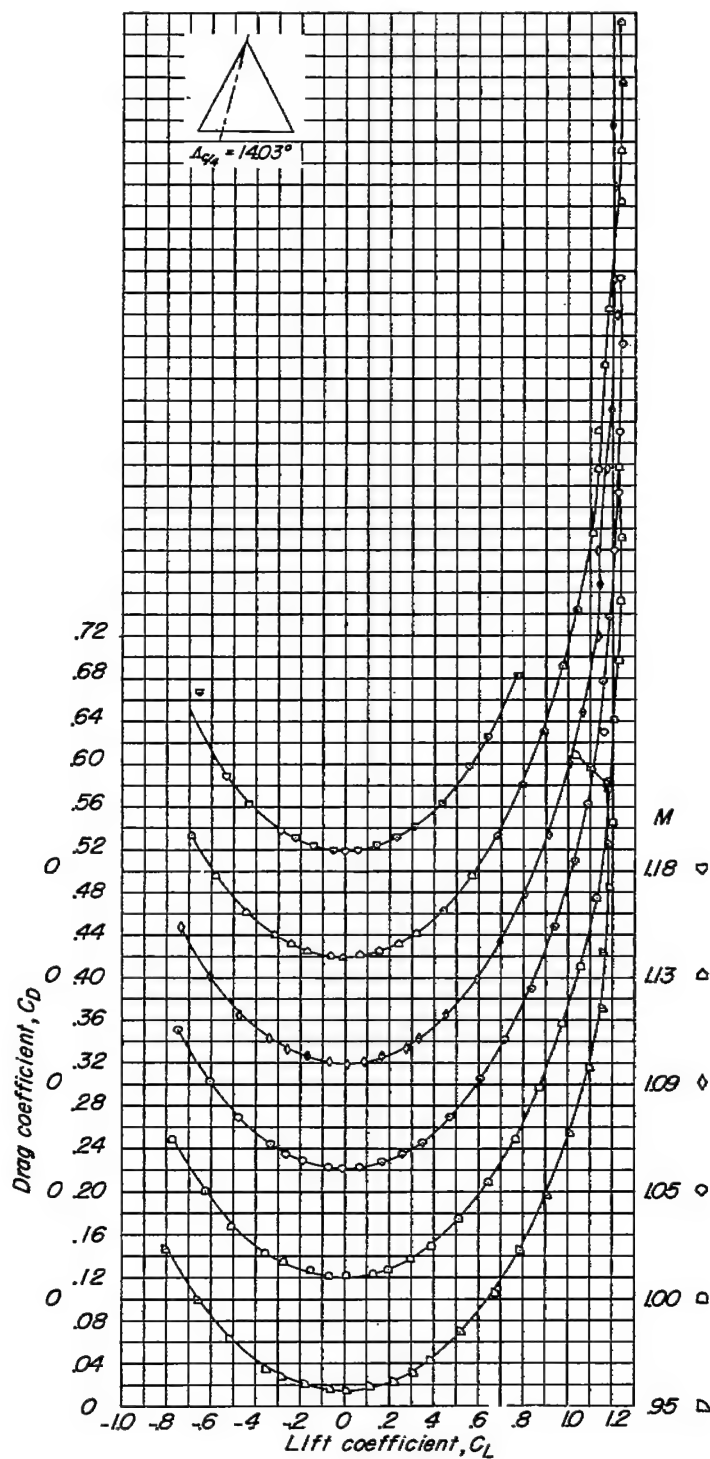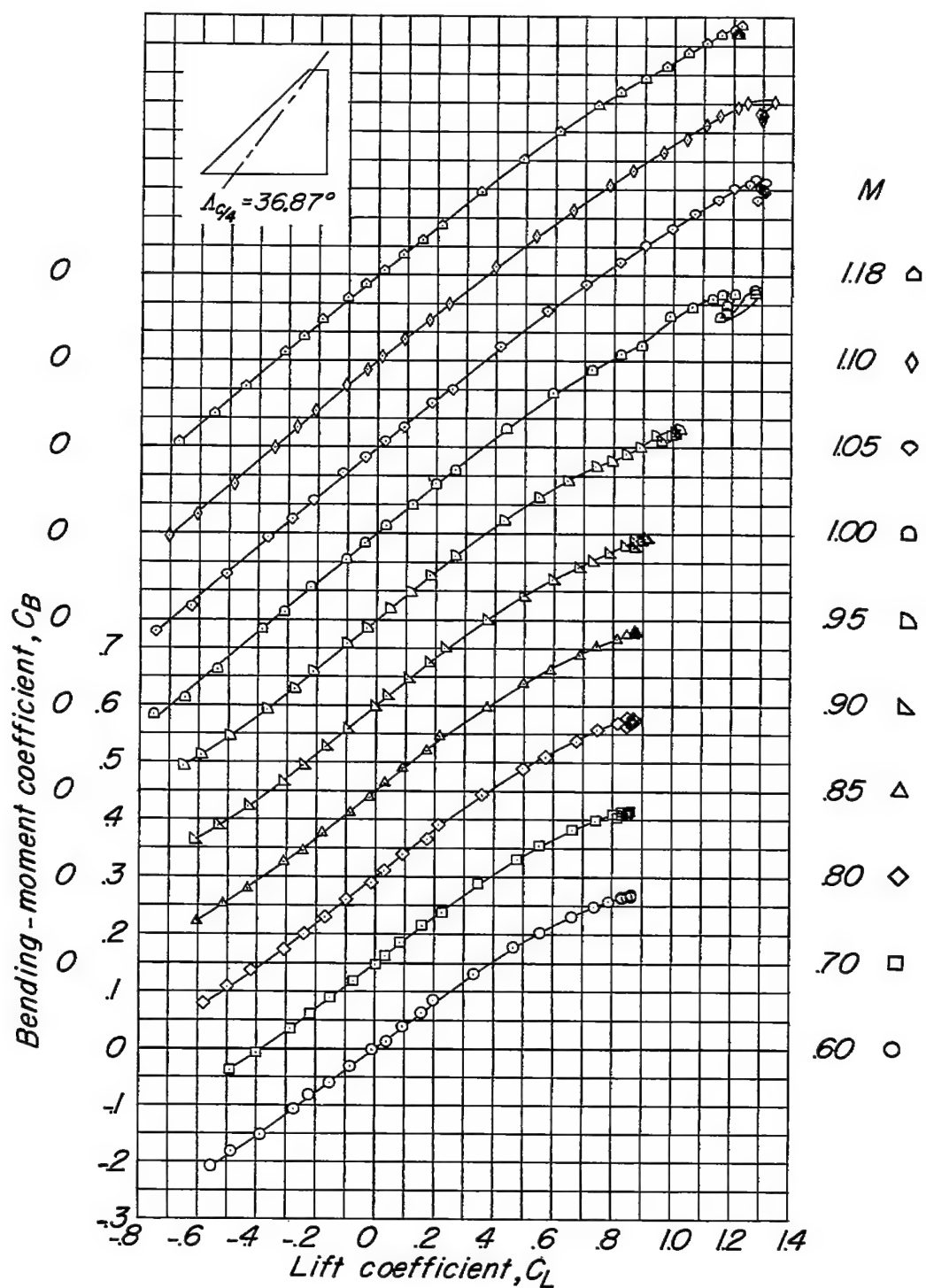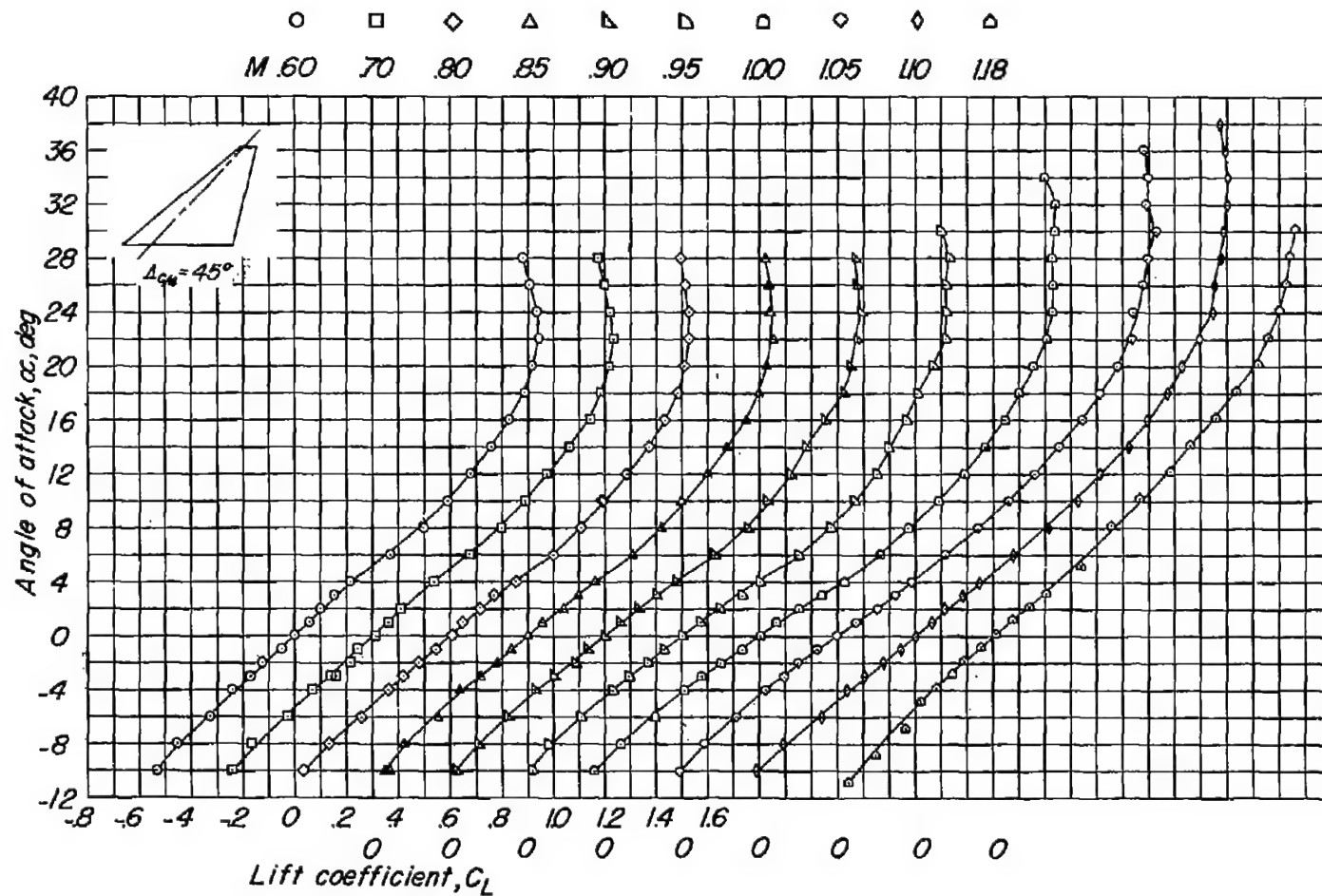
(c) Concluded.

Figure 12.- Continued.
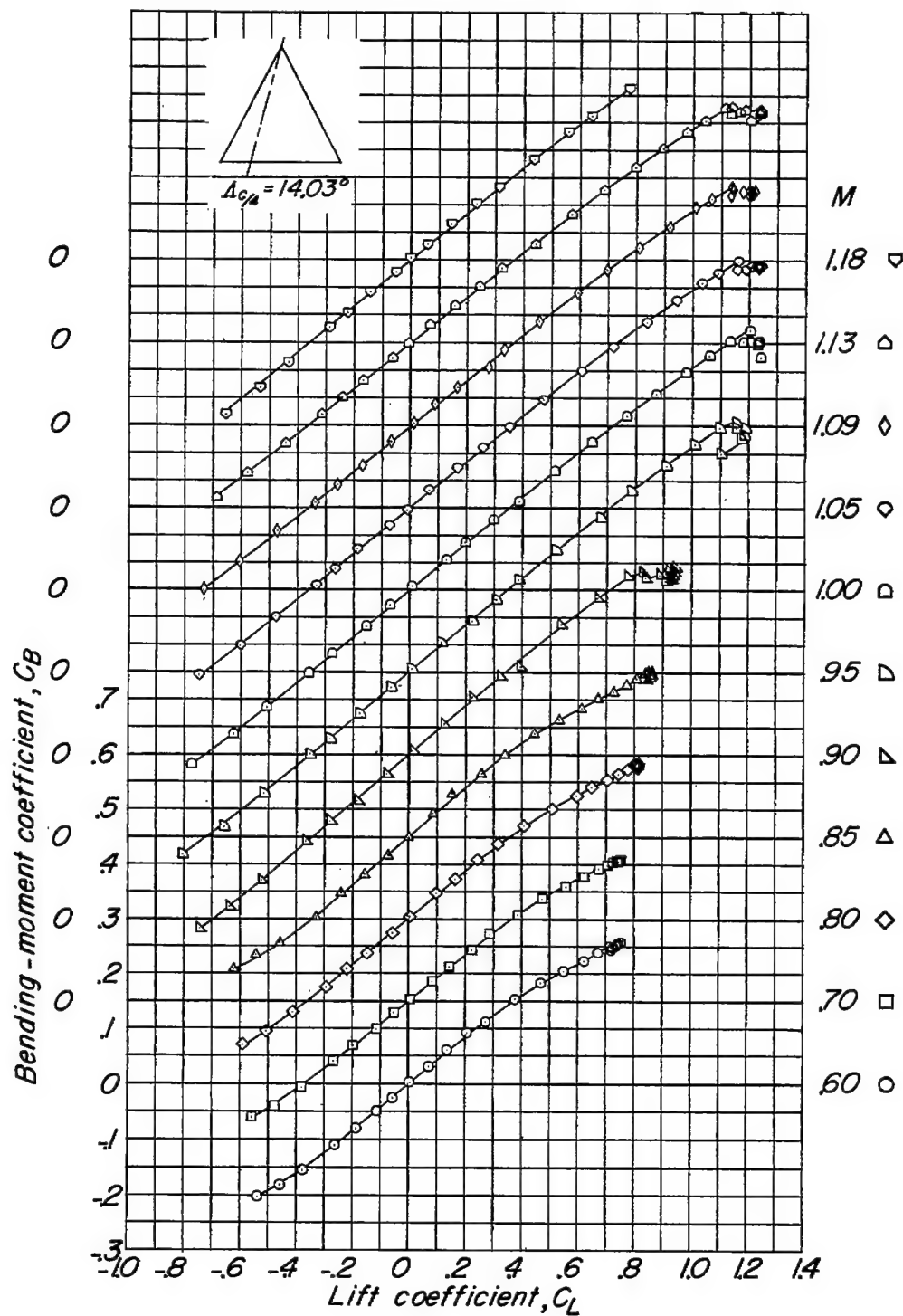
(d) Variation of C_B with C_L.

Figure 12.- Concluded.
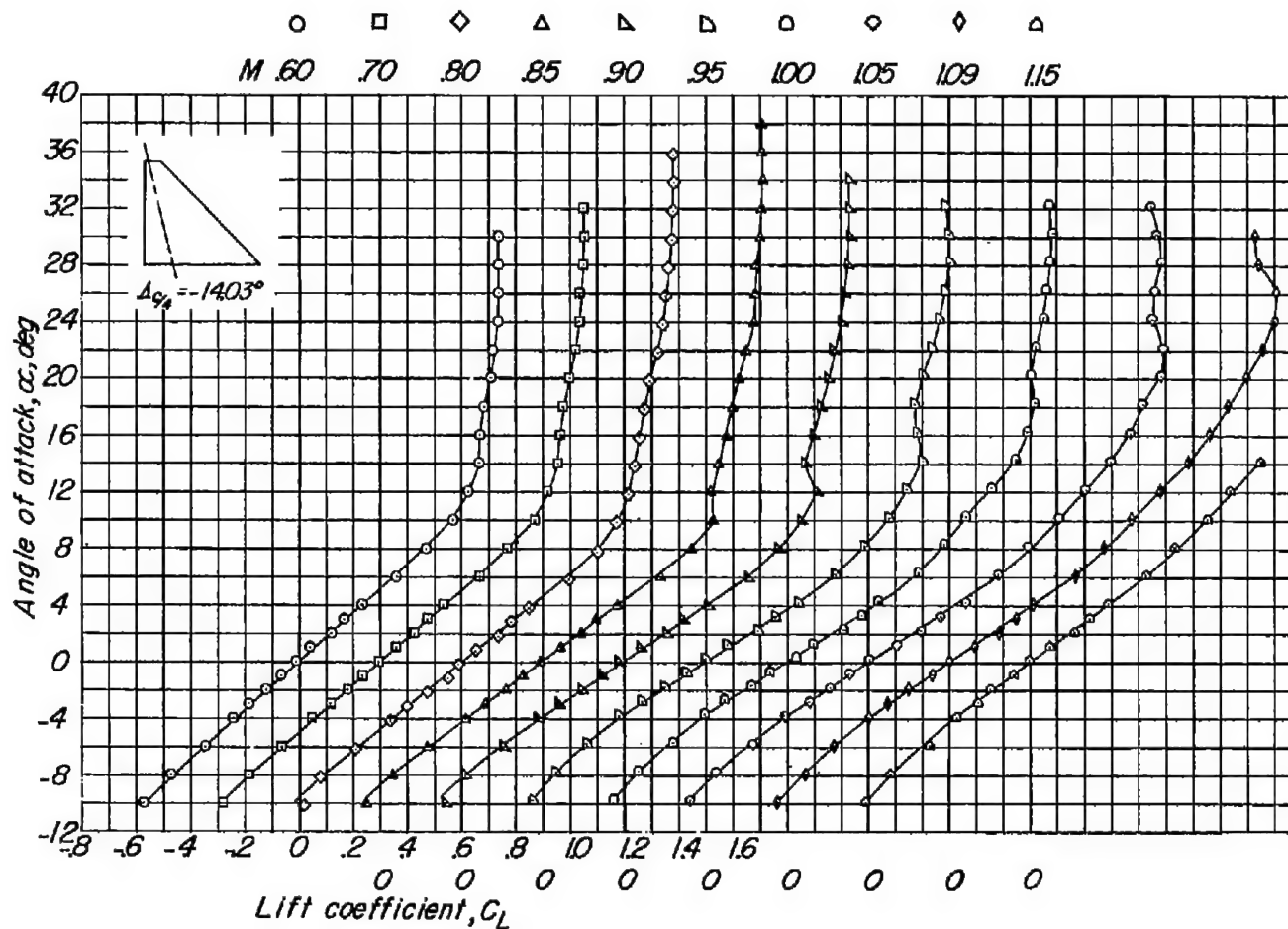
(a) Variation of α with C_L.

Figure 13.- Aerodynamic characteristics of a wing with -14.03° quarter-chord sweep; aspect ratio 3; taper ratio 0.143; and an NACA 65A003 airfoil section.
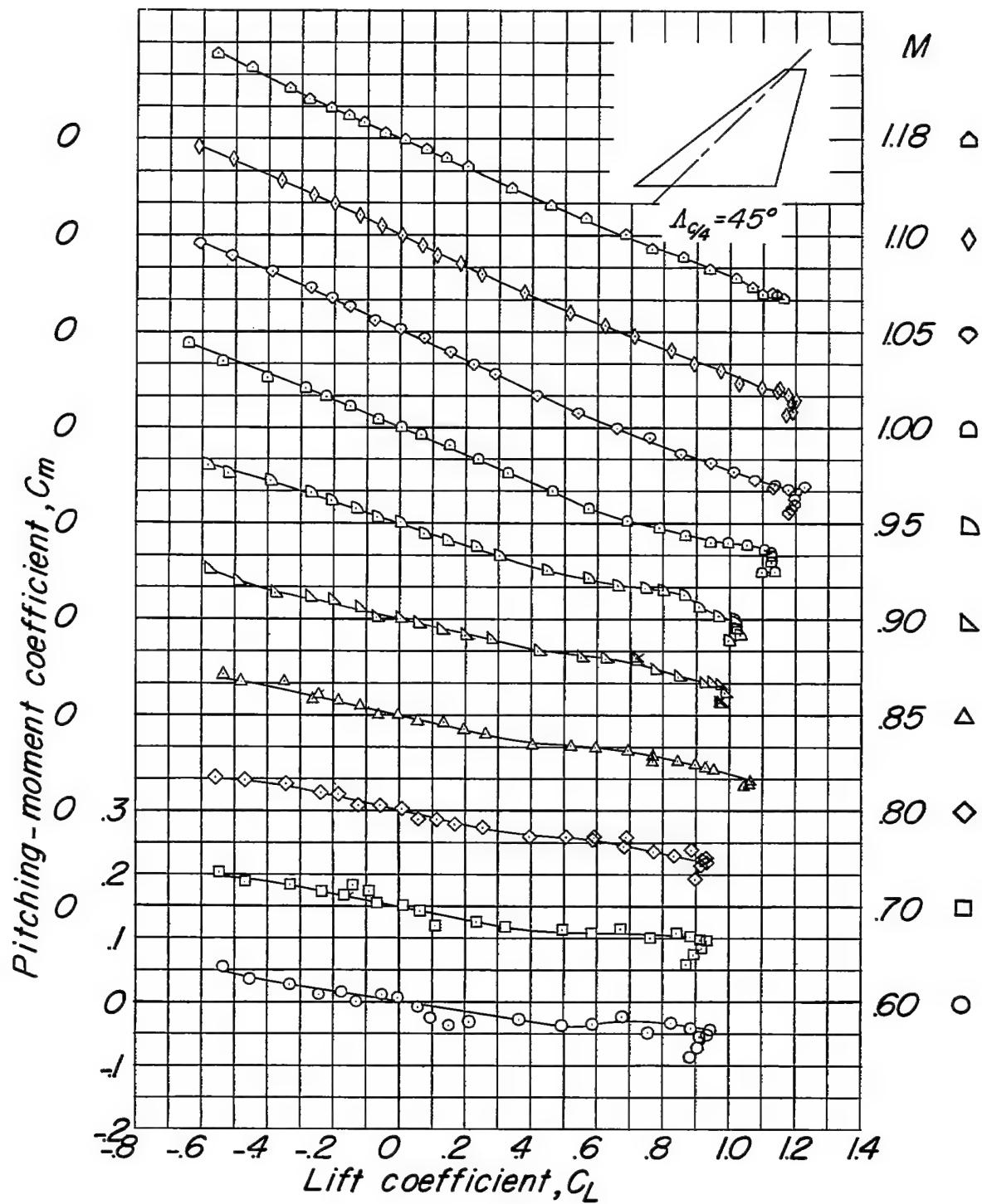
(b) Variation of C_m with C_L.

Figure 13.- Continued.

$\Lambda_{c/4} = -14.03°$

M

.90 ▷

.85 △

.80 ◇

.70 □

.60 ○

(c) Variation of C_D with C_L.

Figure 13.- Continued.

(c) Concluded.

Figure 13.- Continued.

(d) Variation of C_B with C_L.

Figure 13.- Concluded.

(a) Variation of α with C_L.

Figure 14.— Aerodynamic characteristics of a wing with 0° quarter-chord sweep; aspect ratio 3; taper ratio 0.143; and an NACA 65A003 airfoil section.

(b) Variation of C_m with C_L.
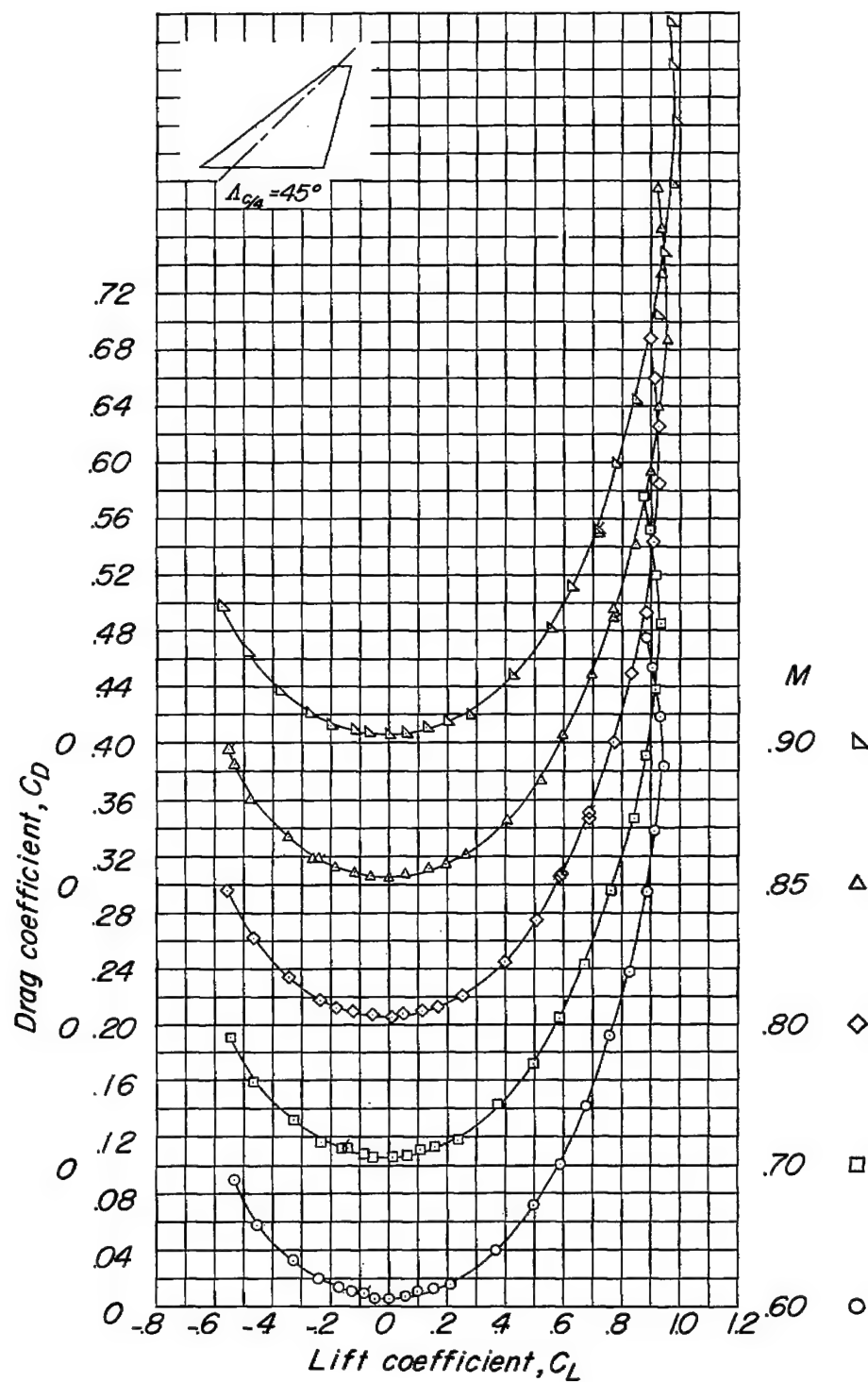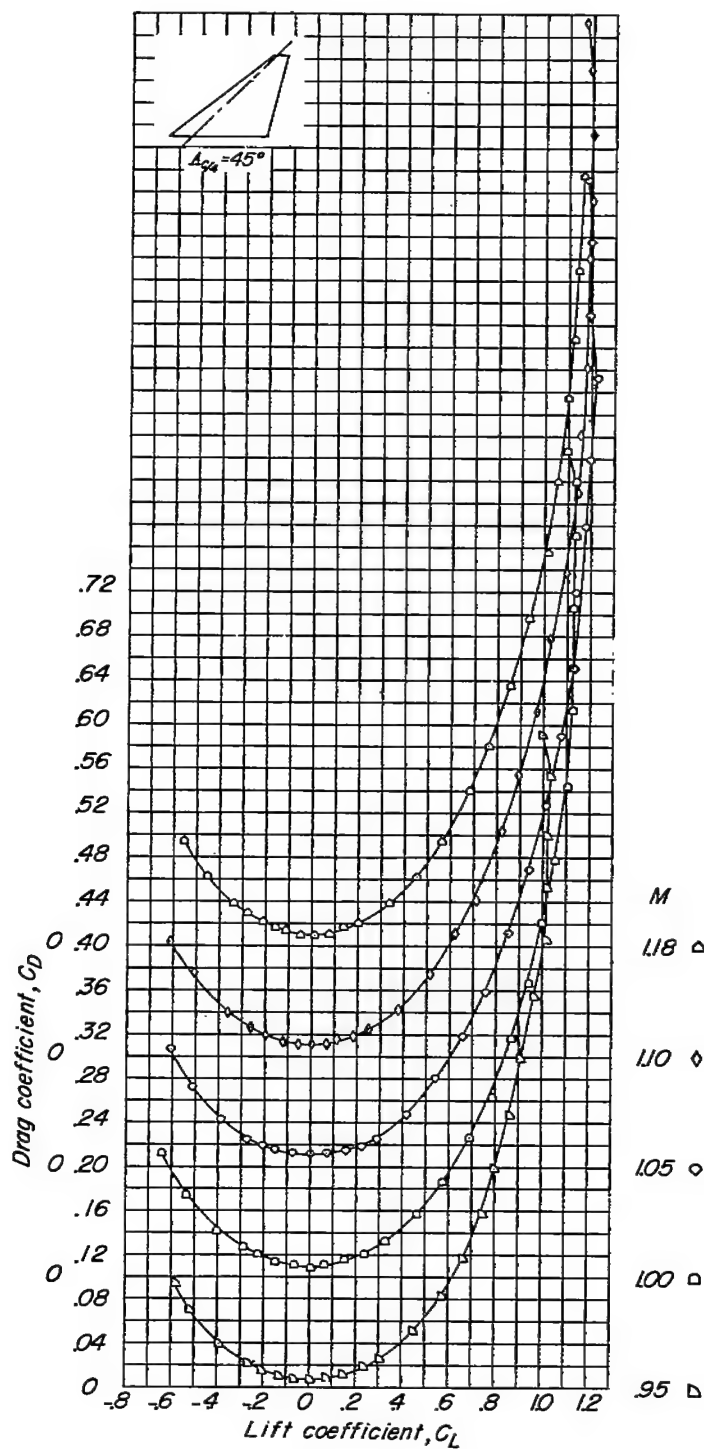
Figure 14.- Continued.

(c) Variation of C_D with C_L.

Figure 14.- Continued.

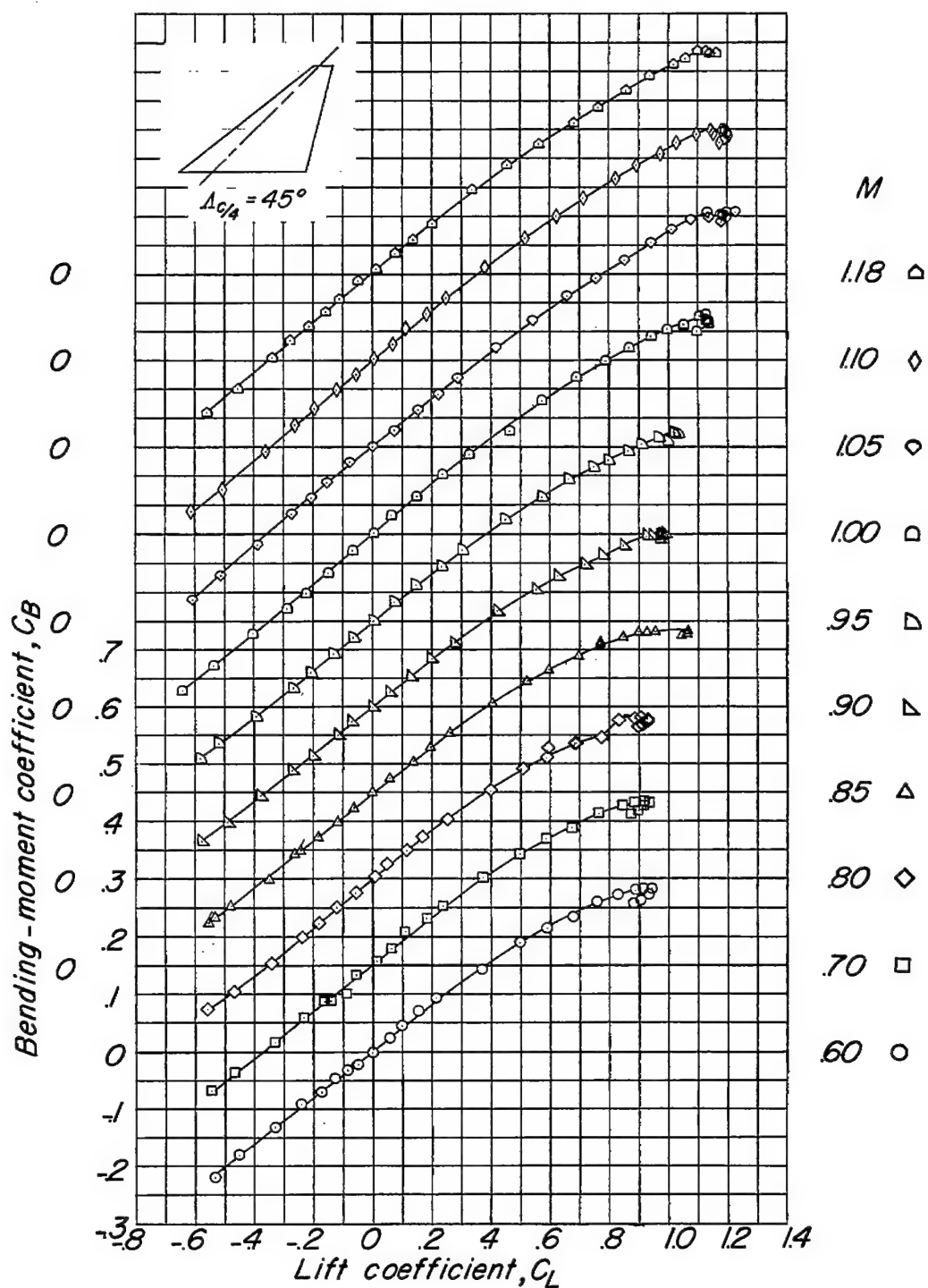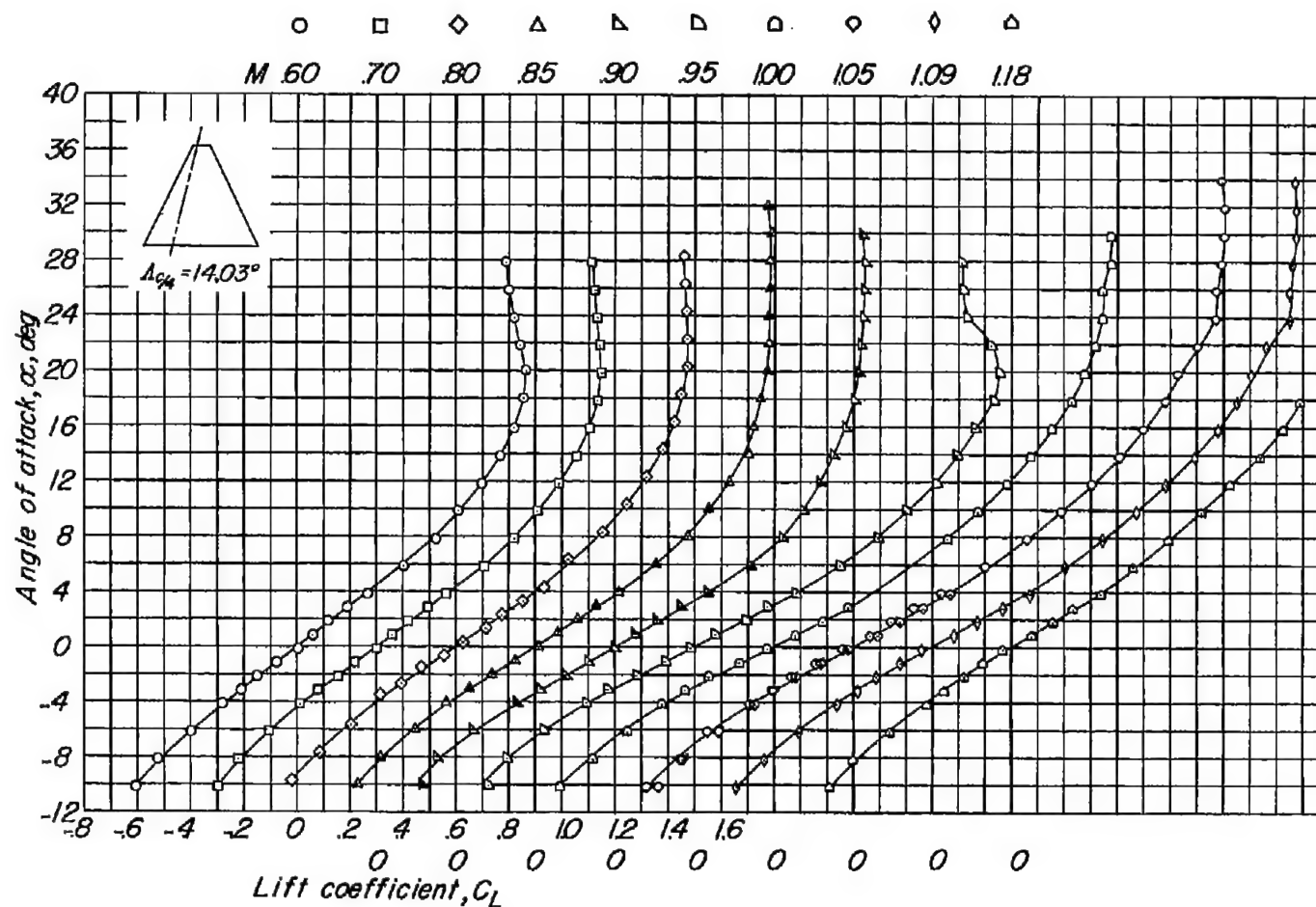(c) Concluded.

Figure 14.- Continued.

(d) Variation of C_B with C_L.

Figure 14.- Concluded.

(a) Variation of α with C_L.

Figure 15.- Aerodynamic characteristics of a wing with 14.03° quarter-chord sweep; aspect ratio 3; taper ratio 0.143; and an NACA 65A003 airfoil section.
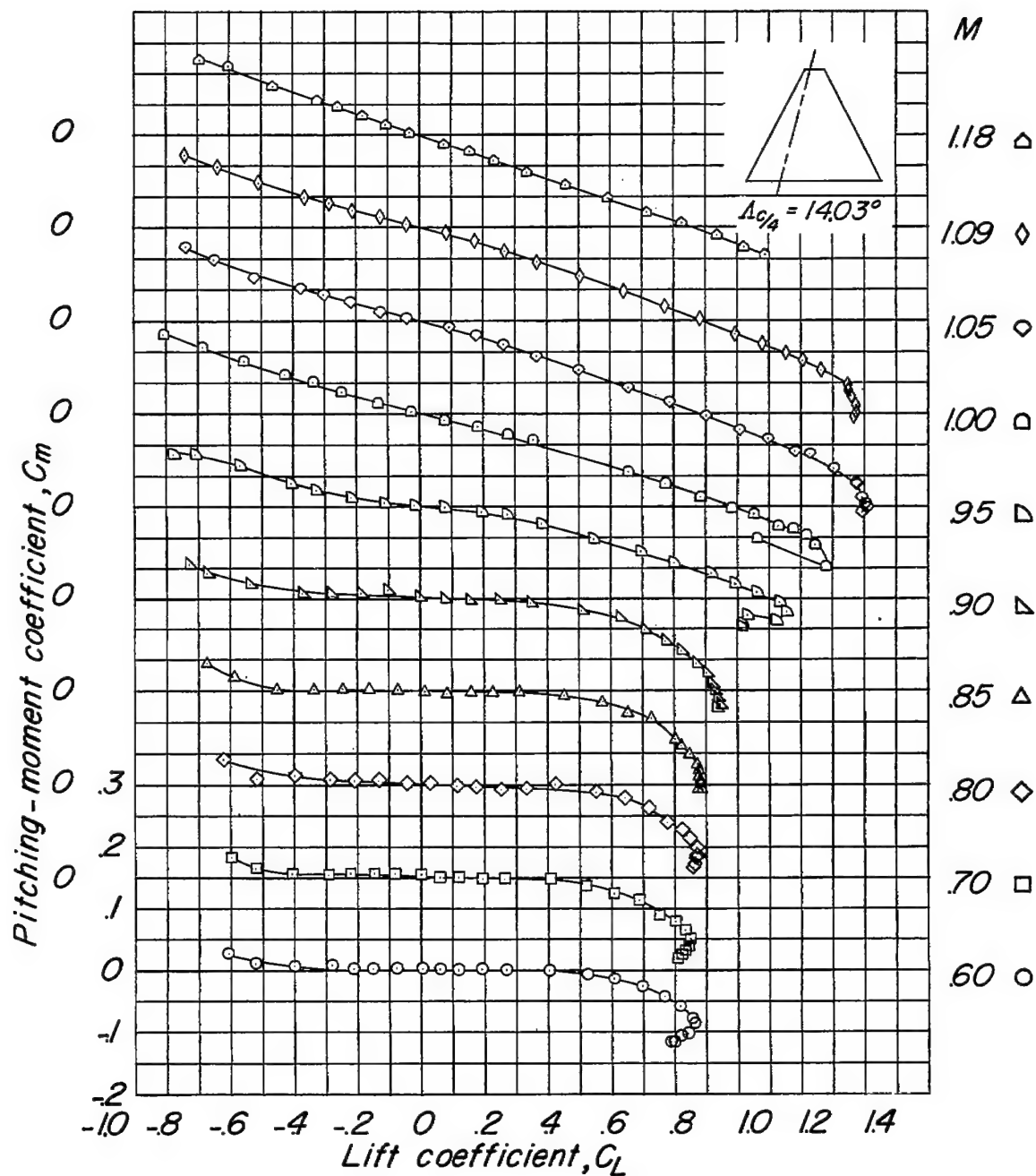
(b) Variation of C_m with C_L.
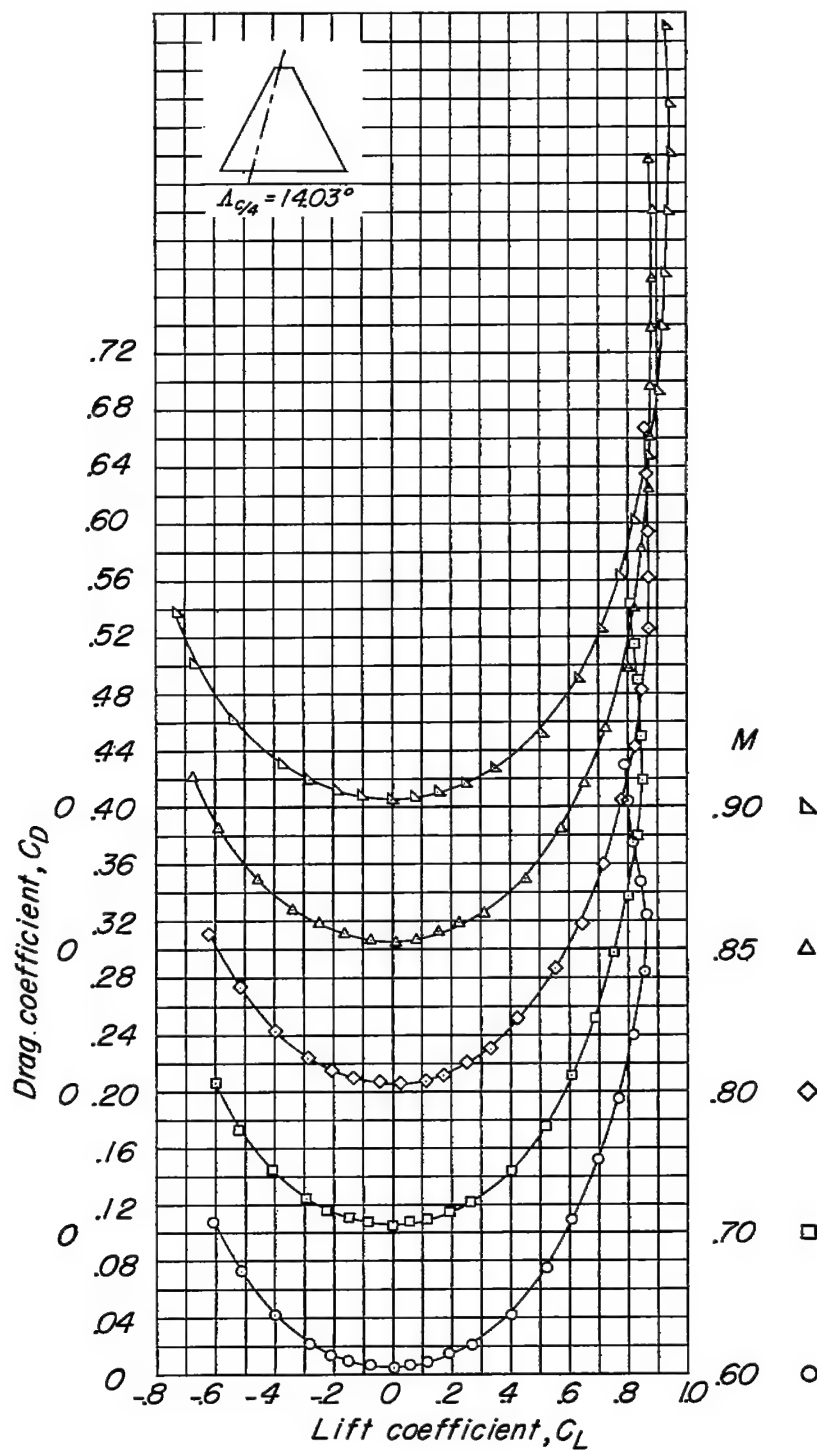
Figure 15.- Continued.

$\Lambda_{c/4} = 14.03°$

M

.90 ◁

.85 △

.80 ◇

.70 □

.60 ○

(c) Variation of C_D with C_L.

Figure 15.- Continued.

(c) Concluded.

Figure 15.- Continued.

(d) Variation of C_B with C_L.

Figure 15.- Concluded.

(a) Variation of α with C_L.

Figure 16.-- Aerodynamic characteristics of a wing with 26.57° quarter-chord sweep; aspect ratio 3; taper ratio 0.143; and an NACA 65A003 air-foil section.

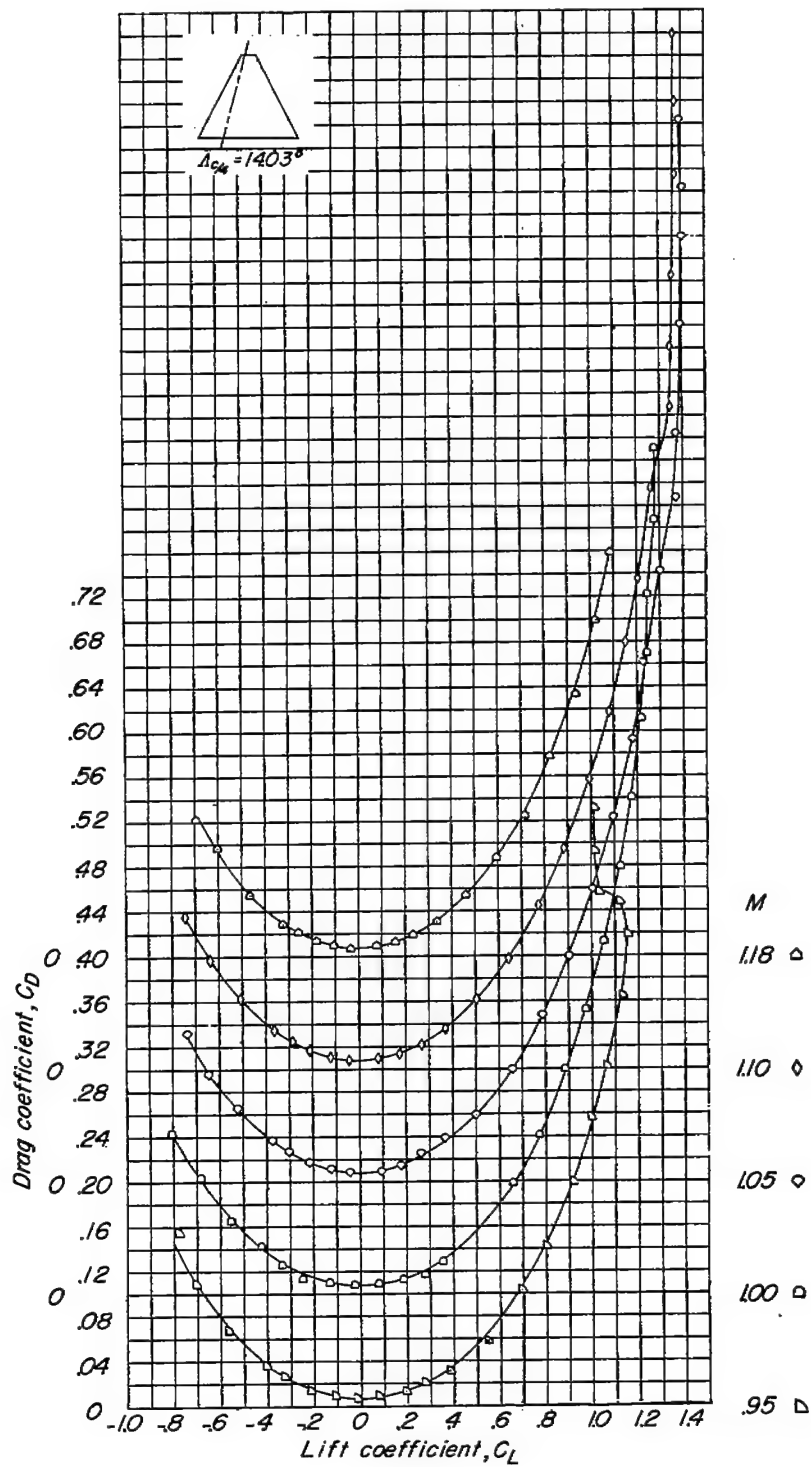(b) Variation of C_m with C_L.

Figure 16.- Continued.

(c) Variation of C_D with C_L.
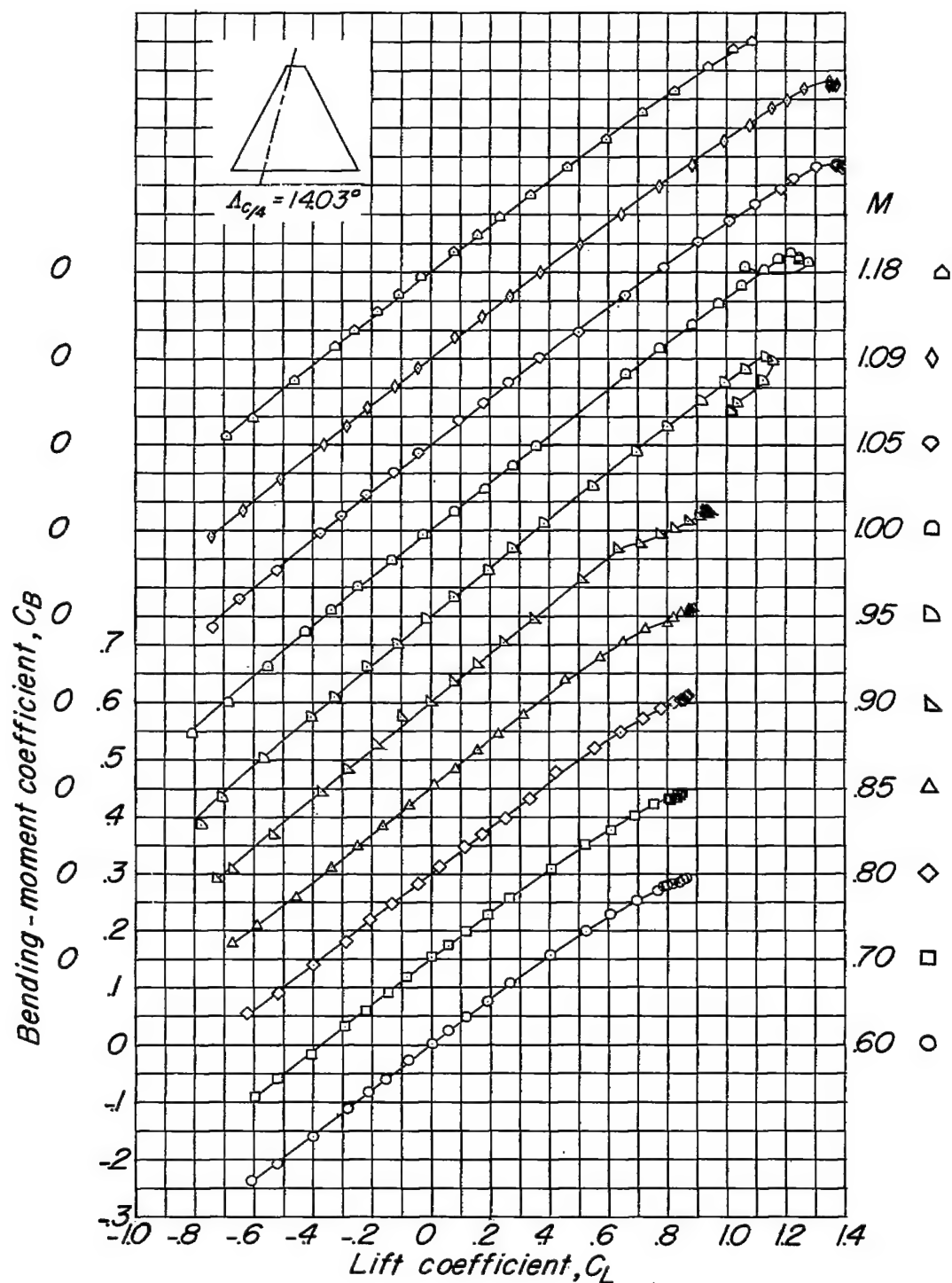
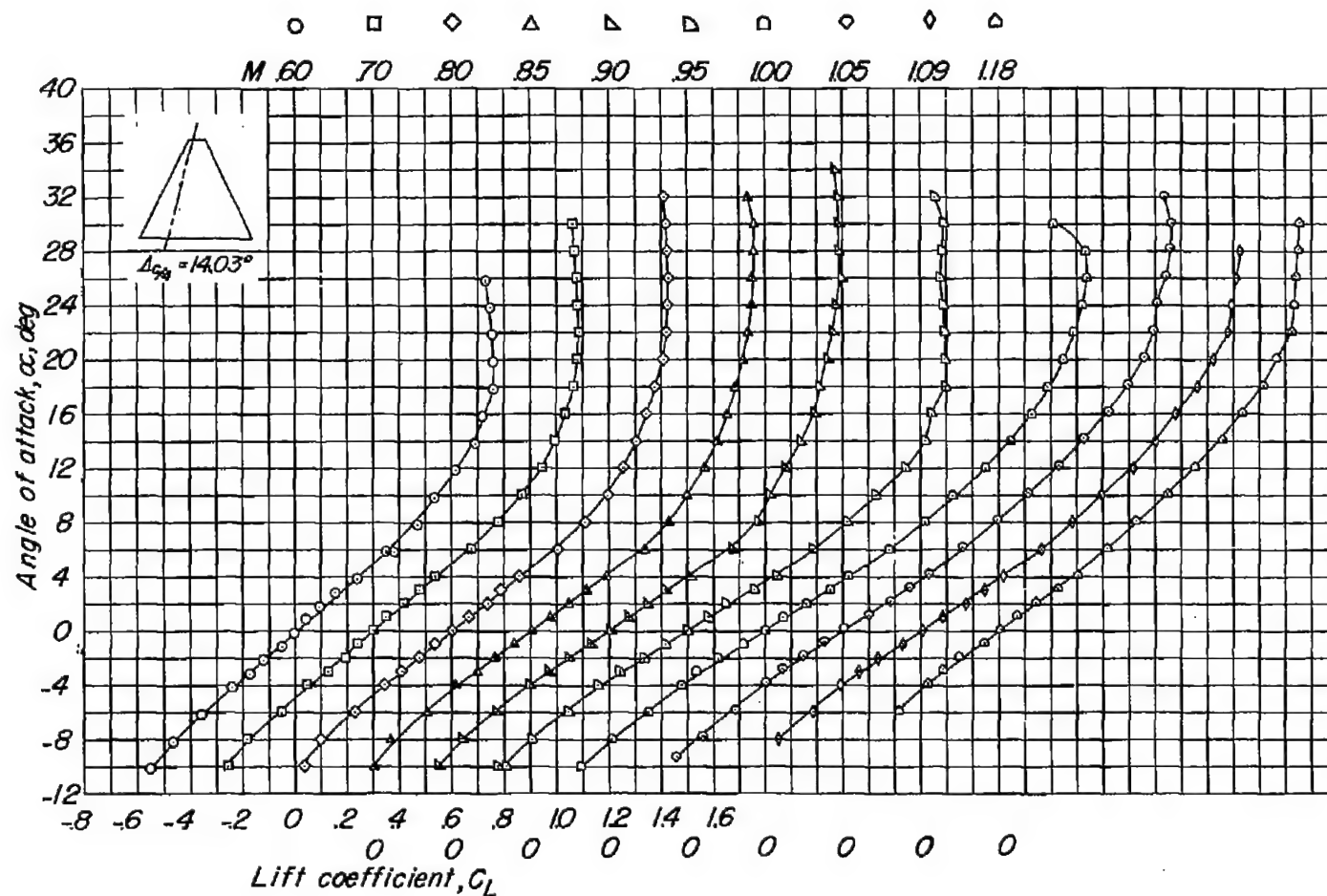Figure 16.- Continued.

(c) Concluded.

Figure 16.- Continued.

(d) Variation of C_B with C_L.

Figure 16.- Concluded.

(a) Variation of α with C_L.

Figure 17.- Aerodynamic characteristics of a wing with 36.87° quarter-
chord sweep; aspect ratio 3; taper ratio 0.143; and an NACA 65A003 air-
foil section.

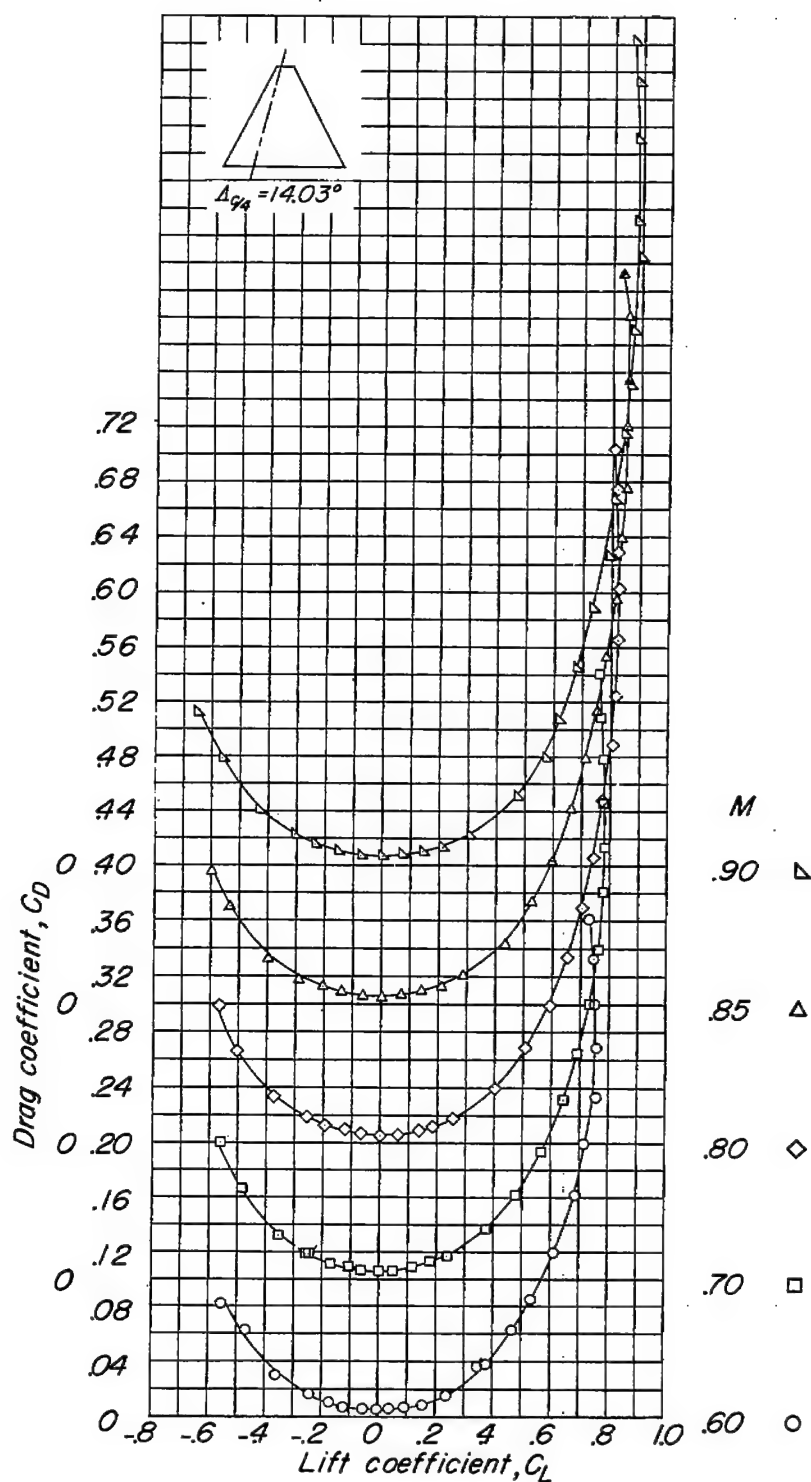(b) Variation of C_m with C_L.
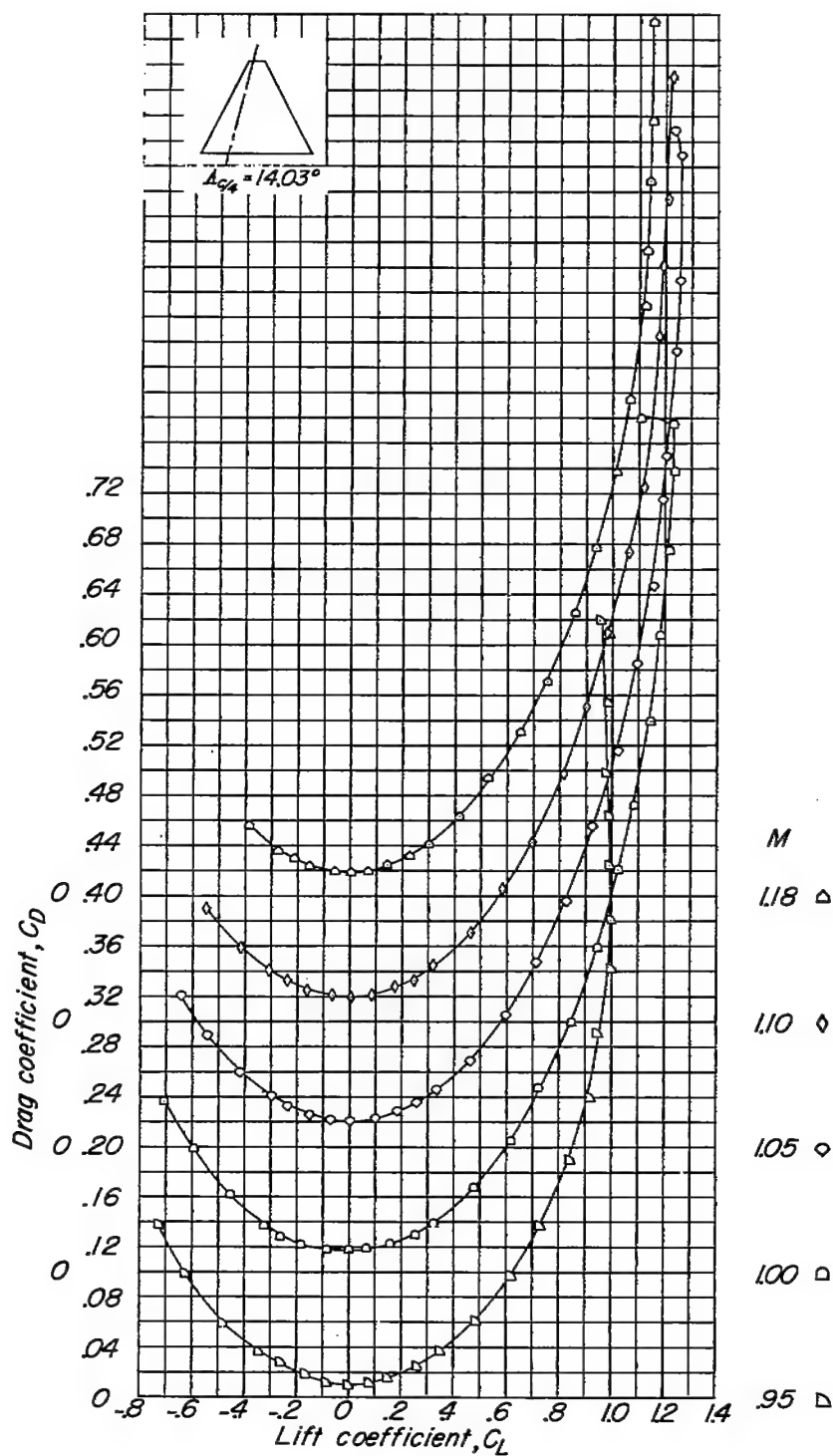
Figure 17.- Continued.

(c) Variation of C_D with C_L.

Figure 17.- Continued.

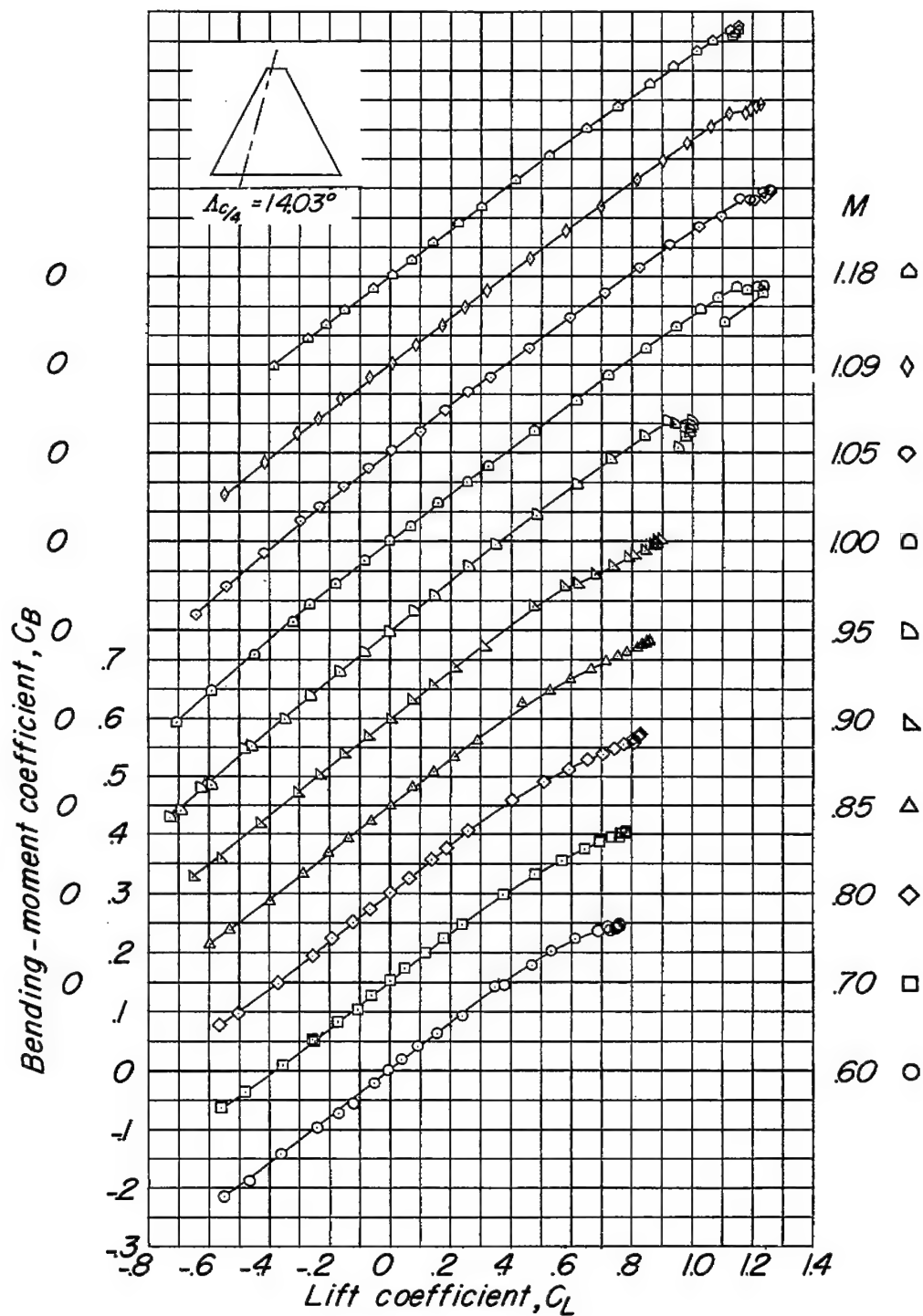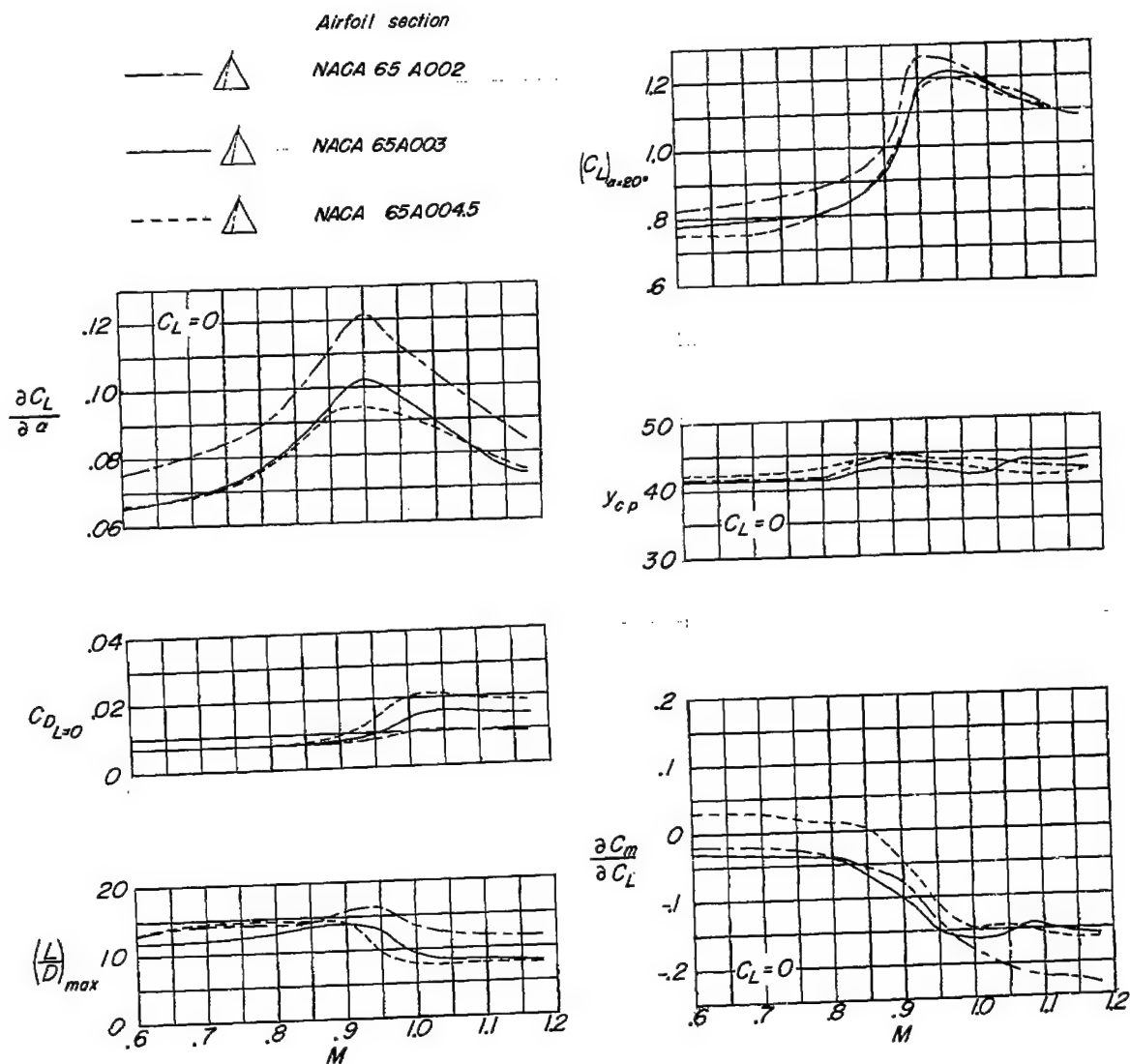(c) Concluded.

Figure 17.- Continued.

(d) Variation of C_B with C_L.

Figure 17.- Concluded.

(a) Variation of α with C_L.

Figure 18.- Aerodynamic characteristics of a wing with 45° quarter-chord sweep; aspect ratio 3; taper ratio, 0.143; and an NACA 65A003 airfoil section.

(b) Variation of C_m with C_L.

Figure 18.- Continued.

(c) Variation of C_D with C_L.

Figure 18.- Continued.

$\Lambda_{c/4} = 45°$

M

1.18 △

1.10 ◇

1.05 ◇

1.00 □

.95 □

Drag coefficient, C_D

Lift coefficient, C_L

(c) Concluded.

Figure 18.- Continued.

(d) Variation of C_B with C_L.

Figure 18.- Concluded.

(a) Variation of α with C_L.

Figure 19.- Aerodynamic characteristics of a wing with 14.03° quarter-chord sweep; aspect ratio 3; taper ratio 0.143; and an NACA 65A002 airfoil section.

(b) Variation of C_m with C_L.

Figure 19.- Continued.

$\Lambda_{c/4} = 14.03°$

(c) Variation of C_D with C_L.

Figure 19.- Continued.

(c) Concluded.

Figure 19.- Continued.

(d) Variation of C_B with C_L.

Figure 19.- Concluded.

(a) Variation of α with C_L.

Figure 20.- Aerodynamic characteristics of a wing with 14.03° quarter-chord sweep; aspect ratio 3; taper ratio 0.143; and an NACA 65A004.5 airfoil section.
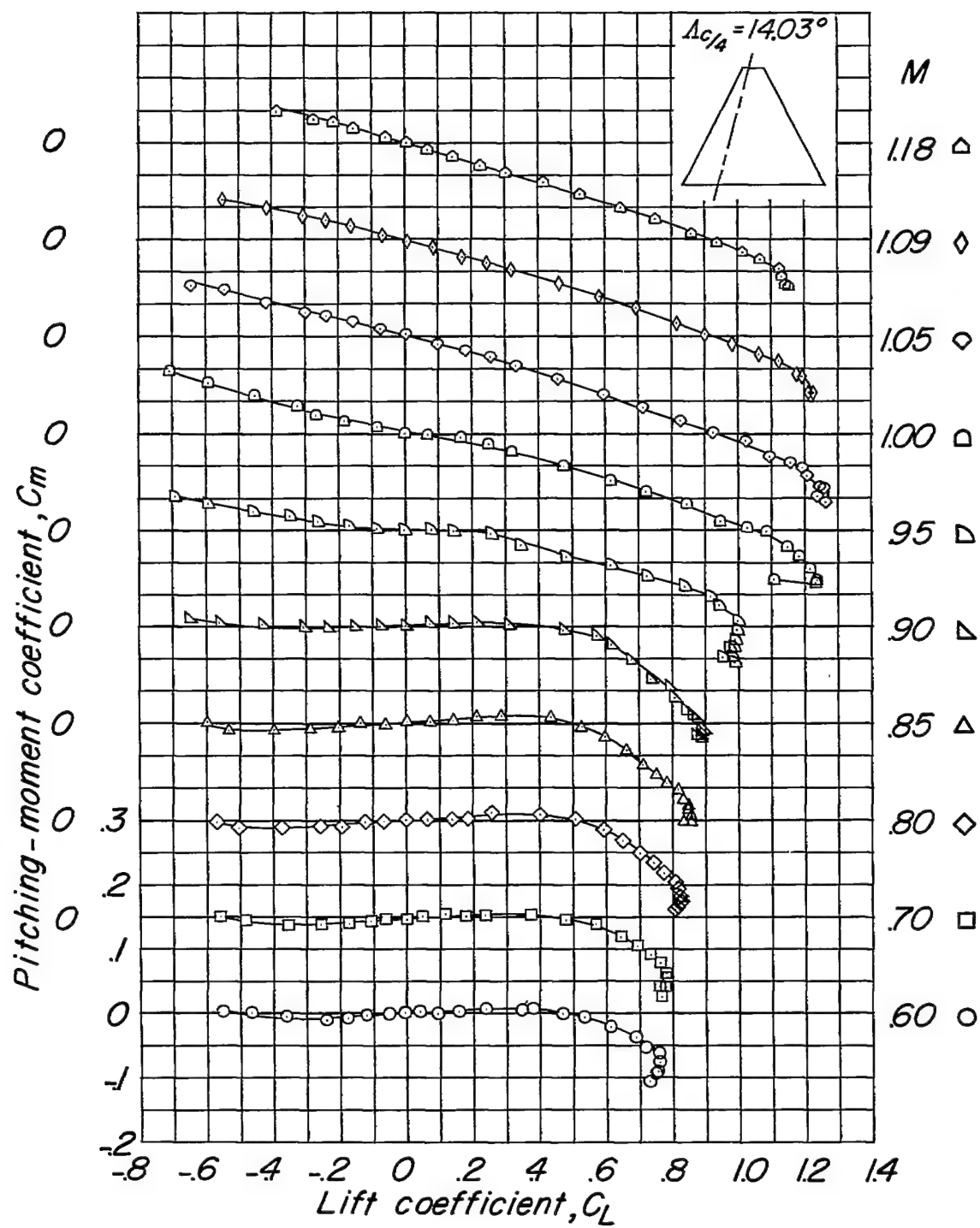
(b) Variation of C_m with C_L.

Figure 20.- Continued.

(c) Variation of C_D with C_L.

Figure 20.- Continued.

(c) Concluded.

Figure 20.- Continued.

(d) Variation of C_B with C_L.

Figure 20.- Concluded.
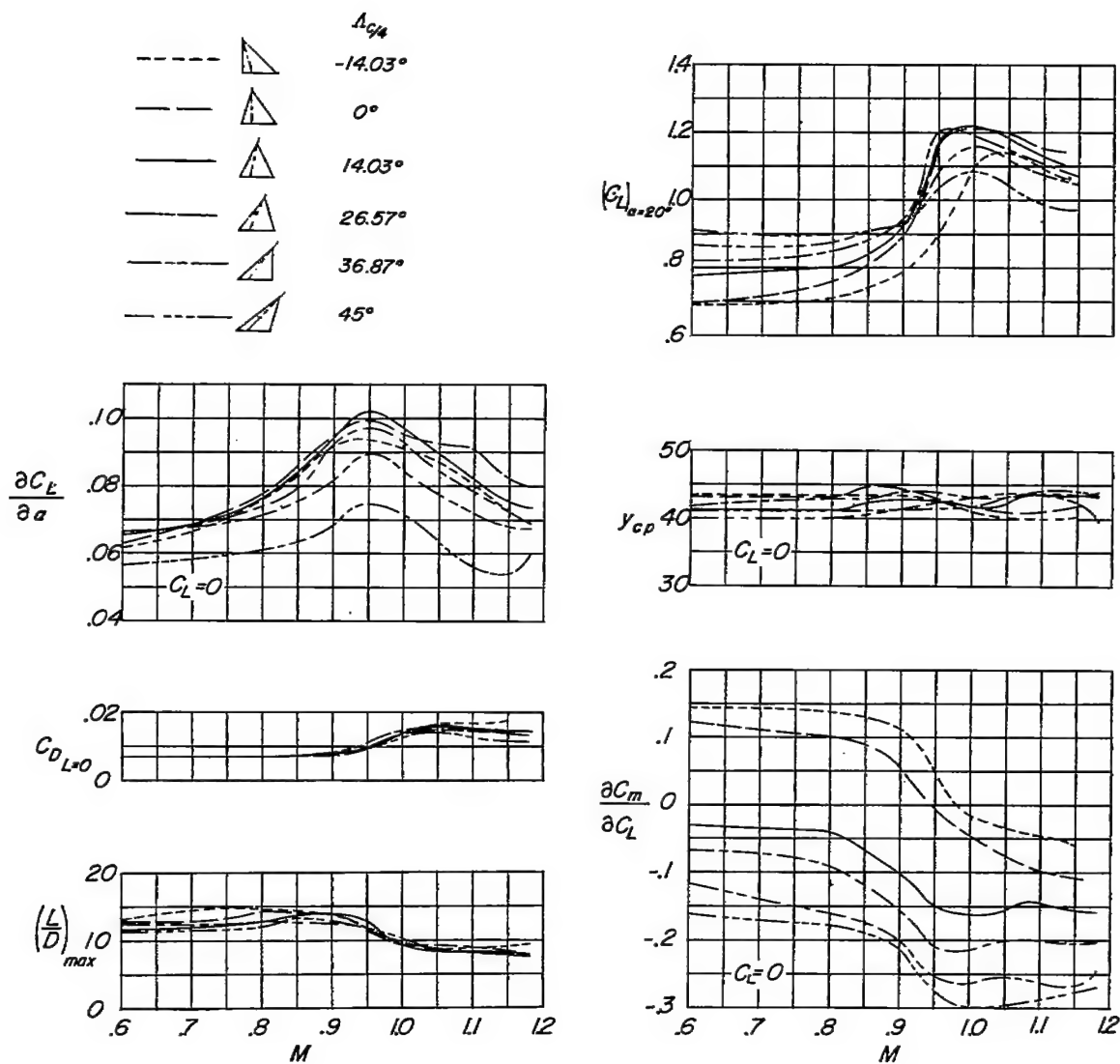
(a) Aspect ratio 4, effect of sweep,
t/c = 0.03.

Figure 21.- Effect of Mach number on aerodynamic characteristics.

(b) Aspect ratio 4, effect of thickness $\Lambda_c/4 = 14.03^\circ$.

Figure 21.- Continued.

(c) Aspect ratio 3, effect of sweep, t/c = 0.03.
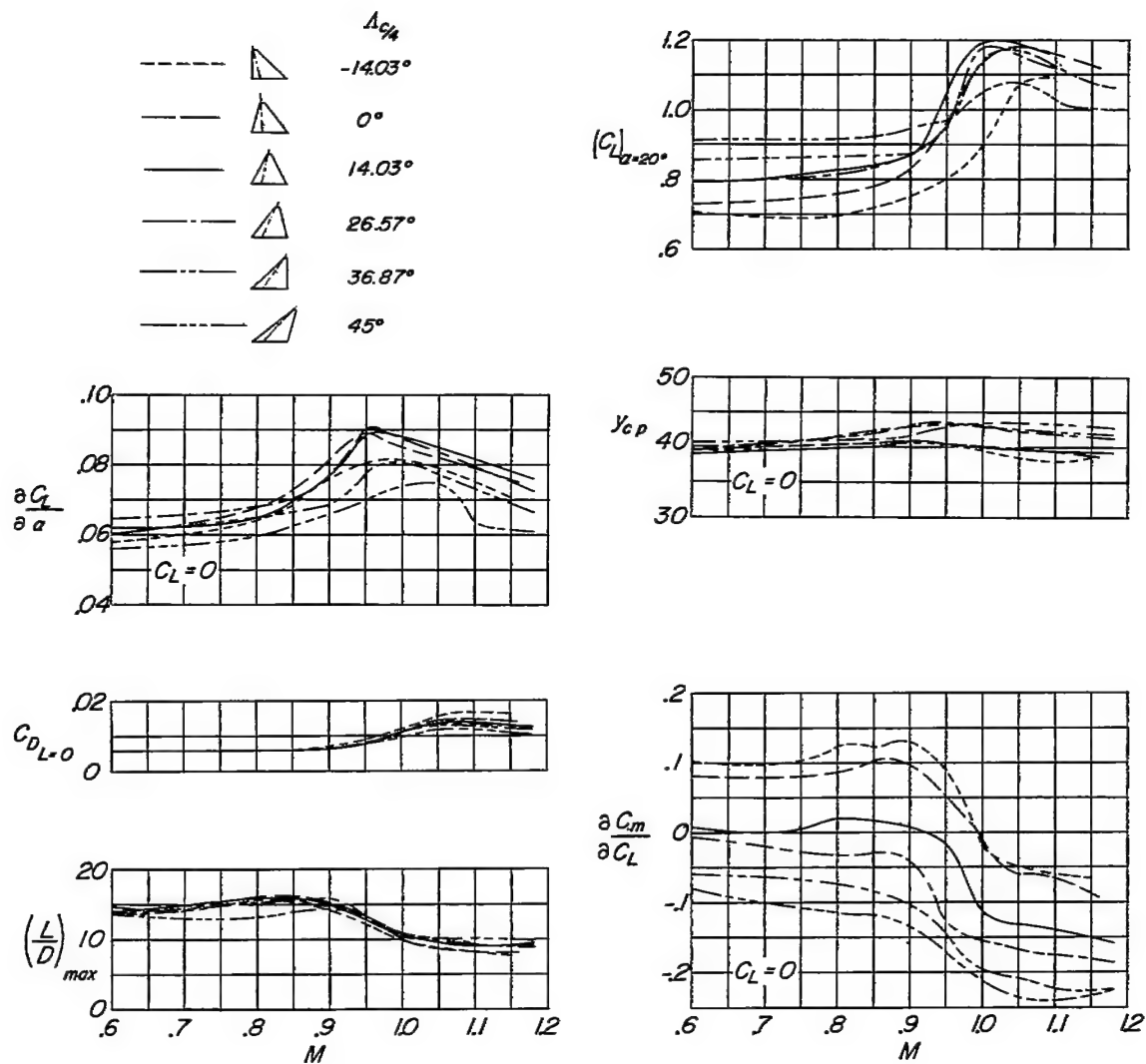
Figure 21.- Continued.
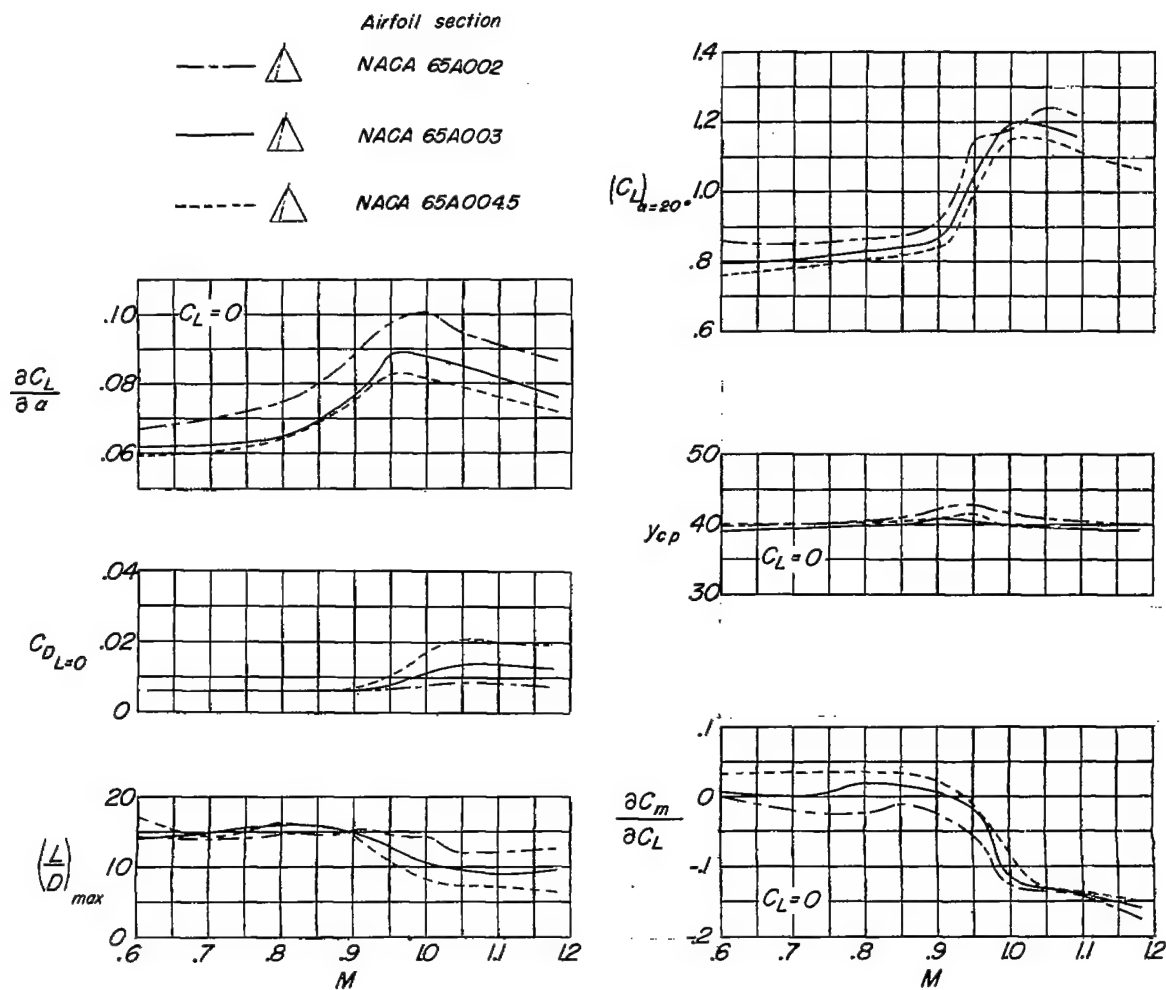
(d) Aspect ratio 3, effect of thickness $\Lambda_{c/4} = 14.03°$.
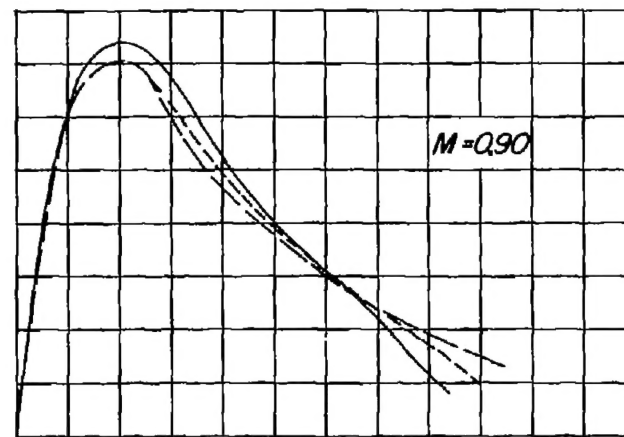
Figure 21.- Concluded.
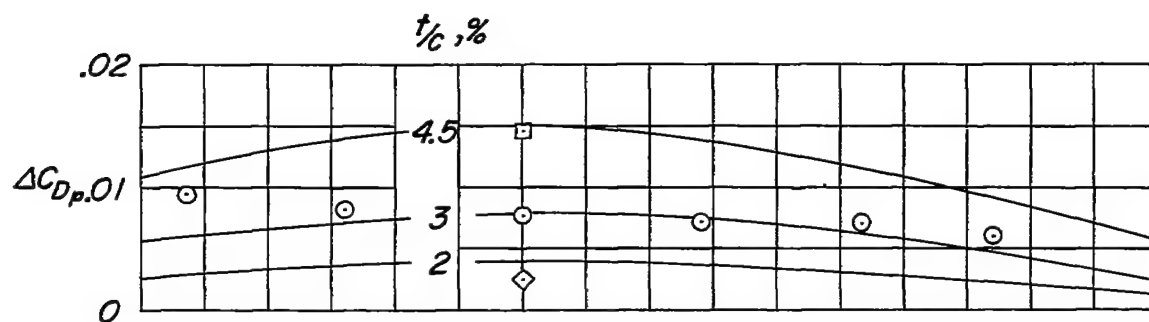
(b) Modified series, A = 3.
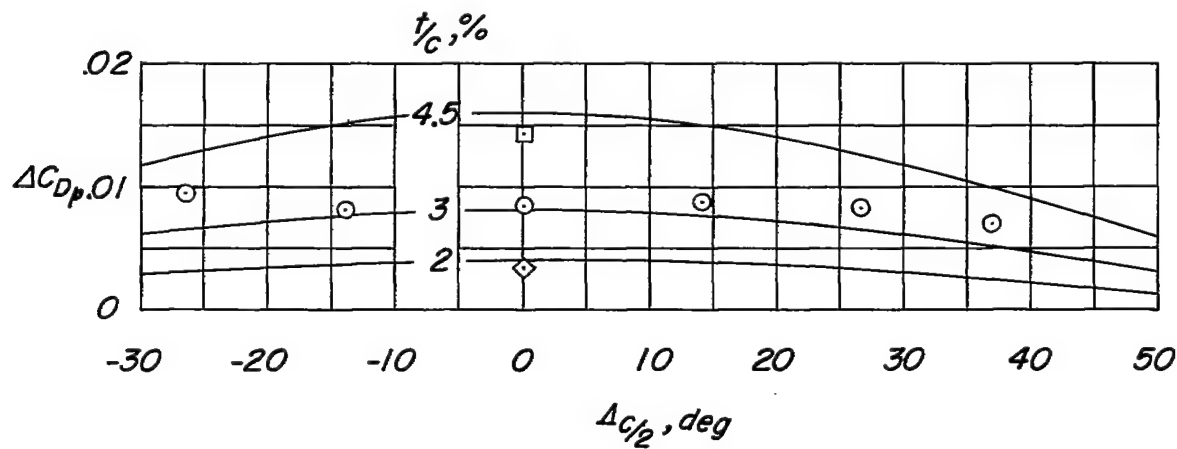
(a) Basic series, A = 4.

Figure 22.- Effect of sweep and thickness on the pressure-drag rise.

——— Basic series, A = 4
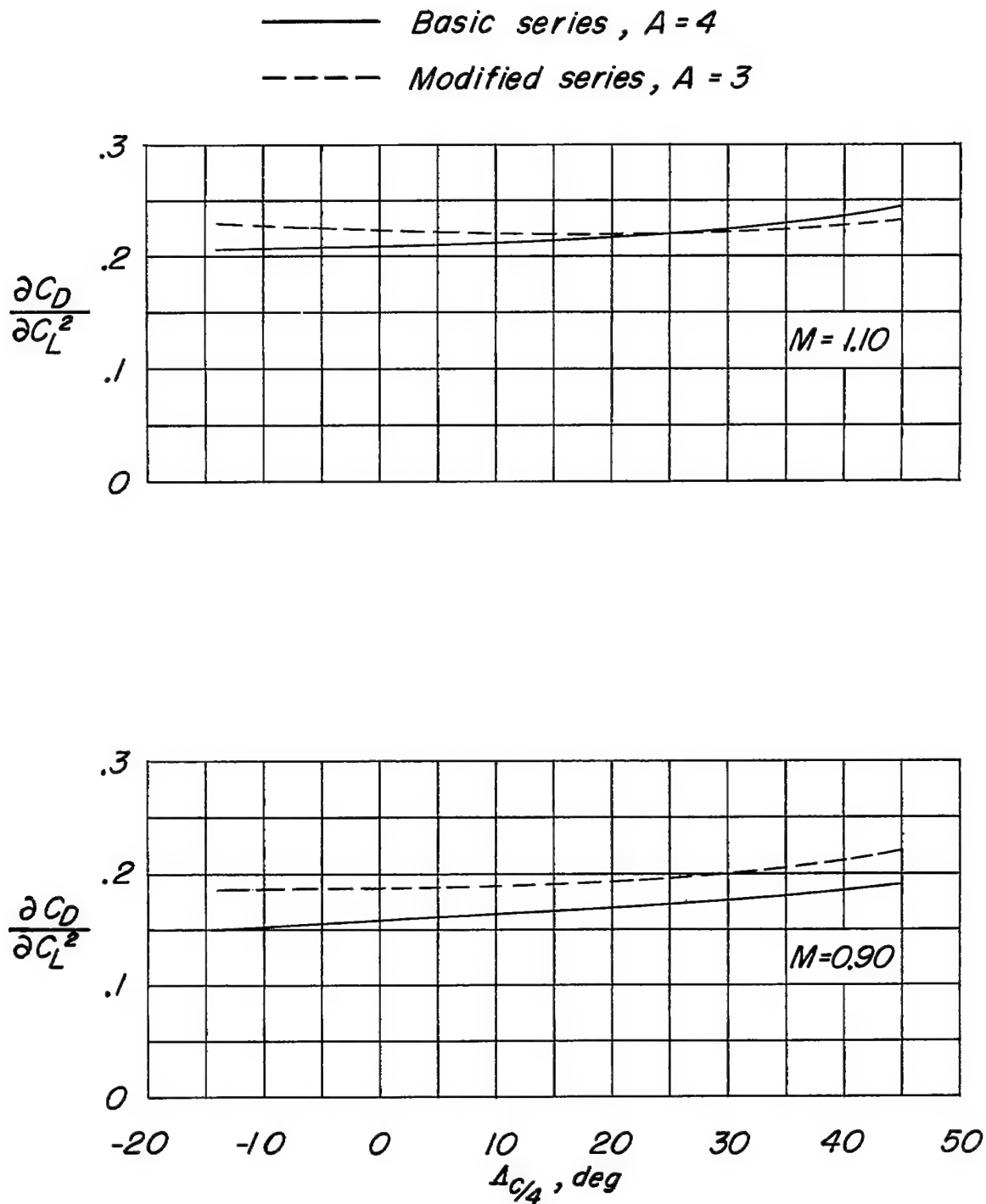
– – – – Modified series, A = 3

Figure 23.- Effect of sweep on the drag due to lift.   t/c = 0.03.
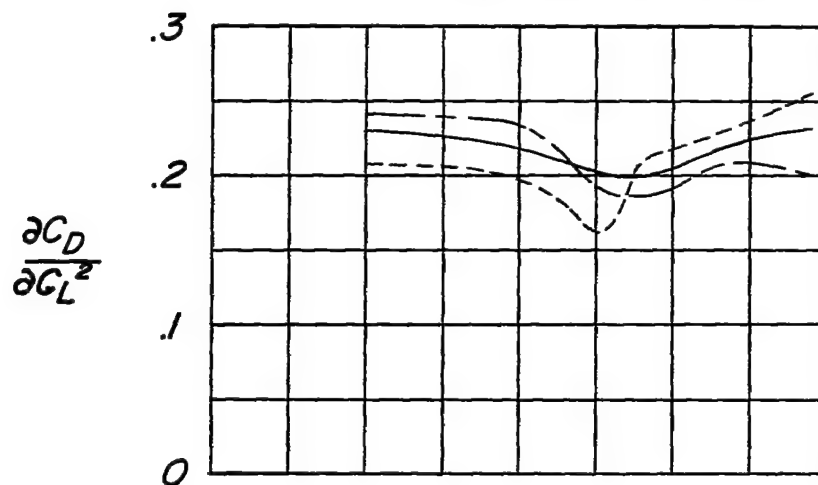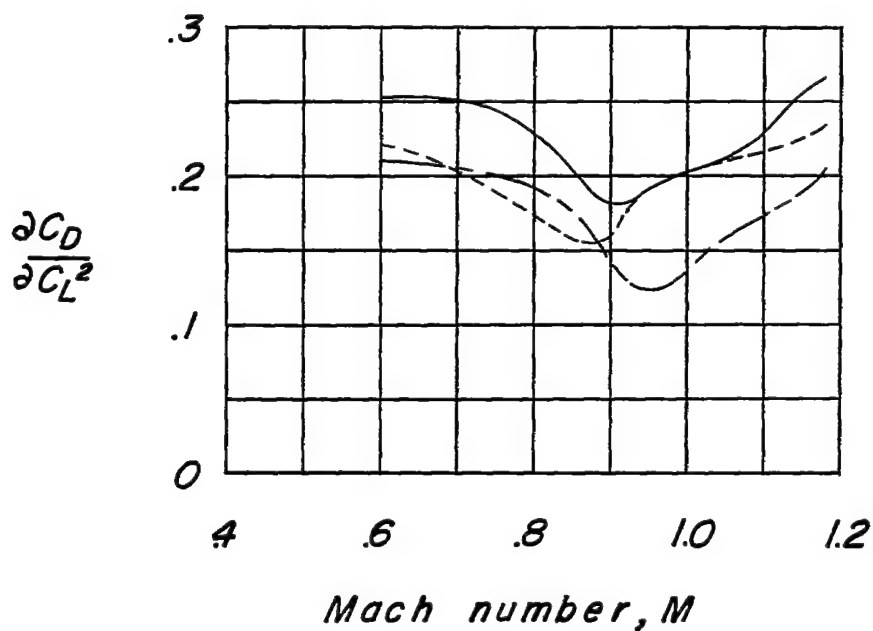
Figure 24.- Effect of thickness on the drag due to lift. $\Lambda_{c/4} = 14.03^{\circ}$.
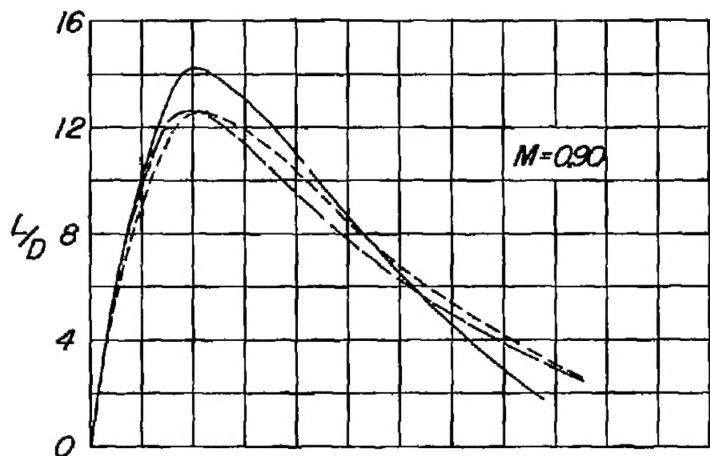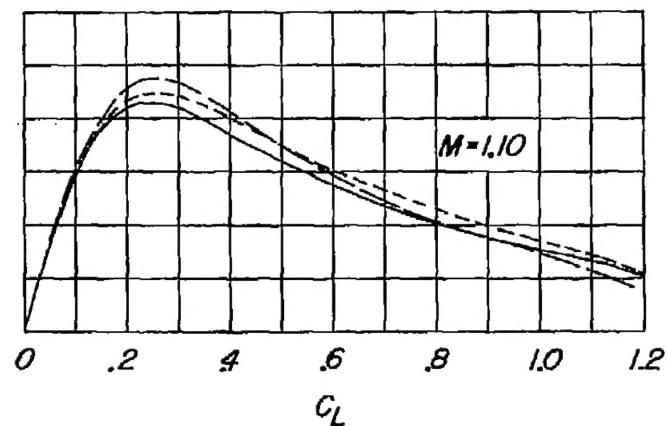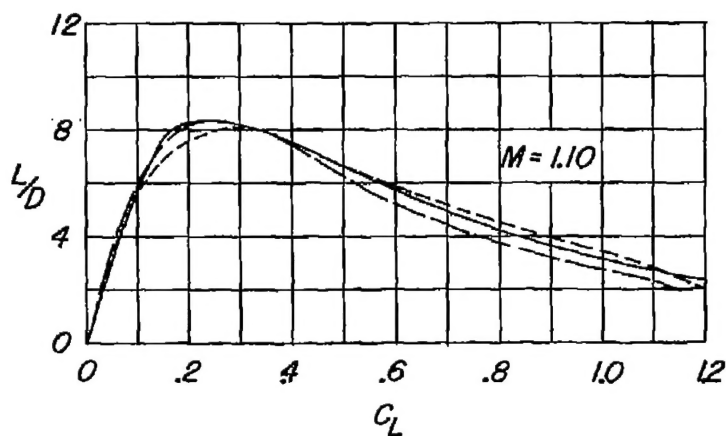
(a) Basic series, A = 4.   (b) Modified series, A = 3.

Figure 25.- Effect of sweep on the lift-drag ratios.   t/c = 0.03.

Experiment ————————
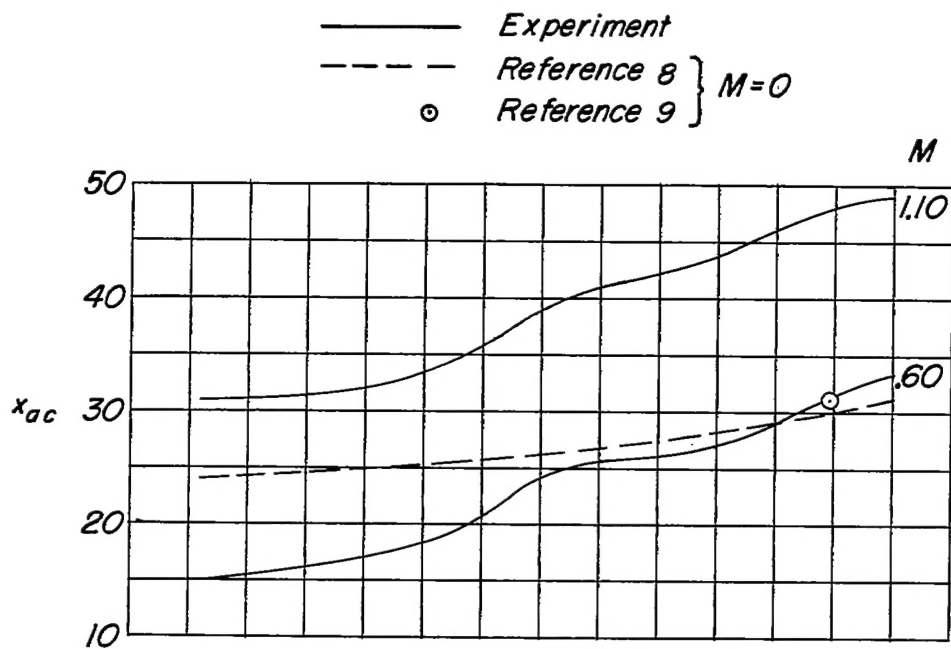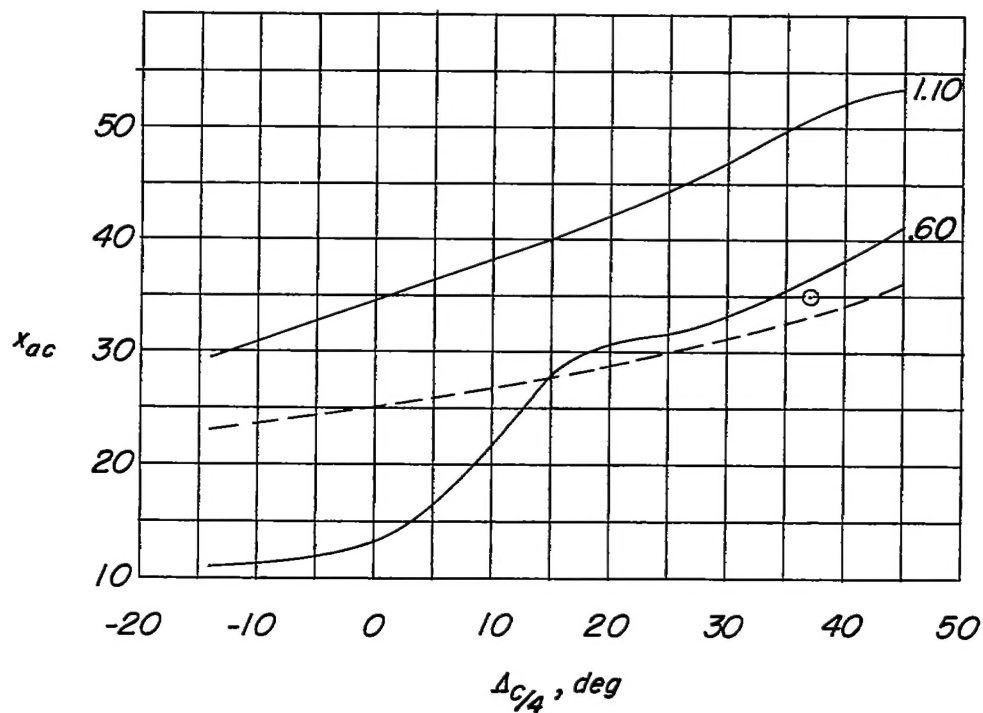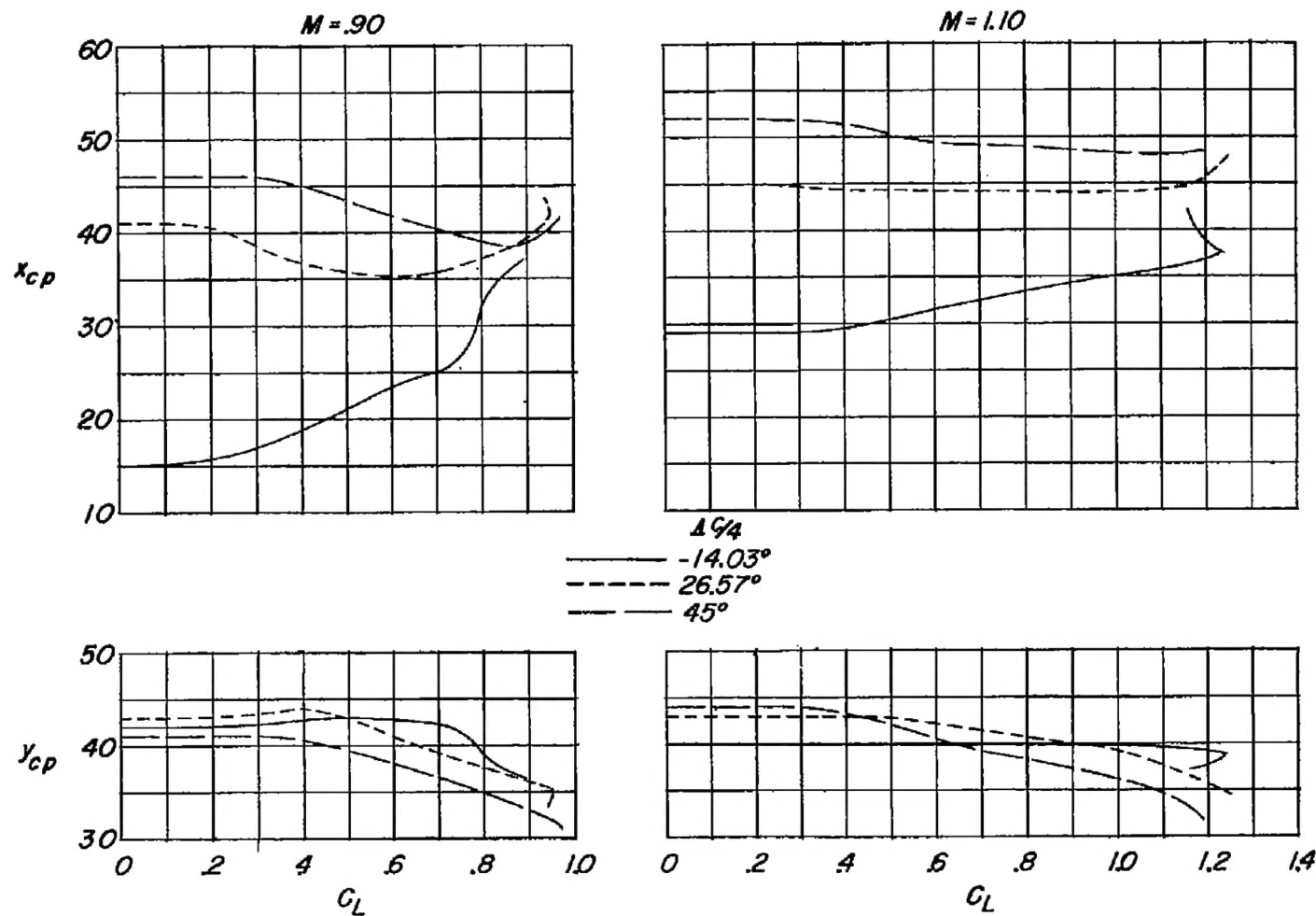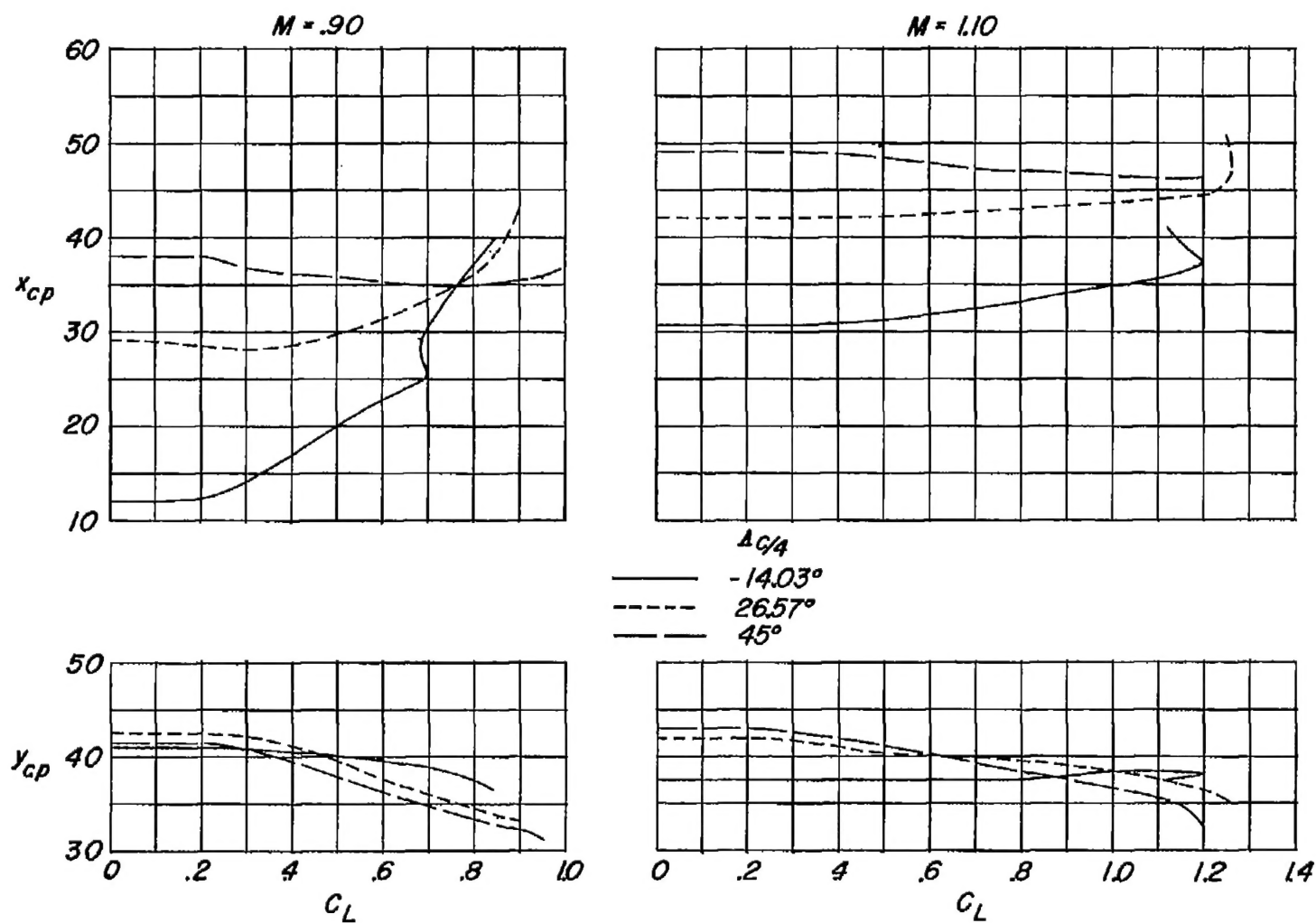
Reference 8 — — — —

Reference 9 ⊙ $\Big\}$ $M=0$

(b) Modified series, A = 3.

(a) Basic series, A = 4.

Figure 26.- Effect of sweep on the aerodynamic-center location.

M = .90

M = 1.10

x_{cp}

y_{cp}

$\Lambda \frac{c}{4}$

—————— -14.03°
– – – – – – 26.57°
— — — — 45°

C_L

C_L

(a) Basic series, A = 4.

Figure 27.- Effect of sweep on the longitudinal and lateral center-of-pressure location. t/c = 0.03.

(b) Modified series, A = 3.

Figure 27.- Concluded.